2015

Accelerated Degradation of Chlorinated Solvents By Nanoscale Zero-Valent Iron Coated with Iron Monosulfide and Stabilized with Carboxymethyl Cellulose

Shirin Ghahghaei Nezamabadi
Wright State University

ACCELERATED DEGRADATION OF CHLORINATED SOLVENTS BY NANOSCALE ZERO VALENT IRON COATED WITH IRON MONOSOLFIDE AND STABILIZED WITH CARBOXYMETHYL CELLULOSE

A thesis prepared in partial fulfillment of the
requirements for the degree of
Master of Science

By

SHIRIN GHAHGHAEI NEZAMABADI
B.S., Amirkabir University of Technology (Tehran Polytechnic), 2008

2016
Wright State University

A thesis prepared in partial fulfillment of the
requirements for the degree of
Master of Science

WRIGHT STATE UNIVERSITY

GRADUATE SCHOOL

January, 2016

I HEREBY RECOMMEND THAT THE THESIS PREPARED UNDER MY SUPERVISION BY Shirin Ghahghaei Nezamabadi ENTITLED Accelerated Degradation of Chlorinated Solvents by Nanoscale Zero-Valent Iron Coated with Iron Monosulfide and Stabilized with Carboxymethyl Cellulose BE ACCEPTED IN PARTIAL FULLFILLMENT OF THE REQUIREMENTS FOR THE DEGREE OF Master of Science.

Abinash Agrawal, Ph. D.
Thesis Director

David Dominic, Ph. D.
Chair, Department of Earth and Environmental Sciences

Committee on
Final Examination

Abinash Agrawal, Ph. D.

David Dominic, Ph. D

Sushil Kanel, Ph. D.

Robert E. W. Fyffe, Ph. D.
Vice President for Research and
Dean of the Graduate School

ABSTRACT

Ghahghaei Nezamabadi, Shirin. M.S. Department of Earth and Environmental Sciences, Wright State University, 2015. Accelerated Degradation of Chlorinated Solvents by Nanoscale Zero-Valent Iron Coated with Iron Monosulfide and Stabilized with Carboxymethyl Cellulose.

Nanoscale zero-valent iron (nZVI) injections have proven to be a promising approach for the remediation of aquifers contaminated by chlorinated organic pollutants. This study compares the efficacy of nZVI in sulfidated and unamended forms in degrading selected chlorinated hyrocarbons (CHCs). Results show that nZVI amended with iron monosulfide (FeS) increases the rate of dechlorination of CT, CF and 1,1,1-TCA compared to that by unamended nZVI.

The focus of this research was to characterize degradation kinetics and degradation byproduct distributions of CT, CF and 1,1,1-TCA by nZVI coated by iron monosulfide, which is represented as nZVI/FeS. To prevent nZVI particles from agglomerating, carboxymethylcellulose (CMC) was used as a stabilizer in all experiments. Results indicated that the nZVI/FeS system was faster and produced less toxic byproducts than nZVI for all CHCs studied. α-elimination in nZVI/FeS system was an important degradation pathway for CF and 1,l,1-TCA: it produces reactive carbene intermediates capable of degrading into benign products such as methane, ethane, and ethene.

The effect of sulfide loading on degradation was evaluated with all CHCs studied. Regardless of CHC type, the rate constant (k_{obs}) increased with increasing sulfide loading,

reaching the highest amount at 1 wt% sulfide, and then decreased with higher sulfide loading. An additional study focused on the effects of varying of the concentration of nZVI and CMC, and particle longevity on the degradation of 1,1,1-TCA in the nZVI/FeS system with 1 wt.% sulfide. Particle longevity experiments showed that reactivity with 1,1,1-TCA decreases as particles age. nZVI/FeS particles showed a rapid power function decline in reactivity with time. Increasing the amount of iron-reducing chemical during nZVI/FeS synthesis improved reactivity by 43%. The addition of a polyelectrolyte stabilizer at an optimized concentration of 4.0 g/L further increased nZVI/FeS reactivity by 350%. nZVI/FeS shows great potential for treating certain CHCs.

TABLE OF CONTENTS

LIST OF FIGURES

LIST OF TABLES

Chapter 1

BACKGROUND

1.1 CHCs Pollution in Groundwater

Chlorinated hydrocarbons (CHCs), including chlorinated methanes, ethanes, and ethenes are significant environmental contaminants due to their adverse toxicological effect at low concentrations and their presence in soil and groundwater at sites where they are produced, used or disposed (Barbee, 1994). CHCs including carbon tetrachloride (CT), perchloroethene (PCE), trichloroethene (TCE) and 1,1,1-trichloroethane (TCA) were commonly used cleaning and degreasing solvents in the United States (Doherty, 2000). They also have been used in a variety of other applications such as adhesives, pharmaceuticals, textile processing, paints and as feedstock for other chemicals. However, through general dispersal, during normal usage and also as a result of indiscriminate disposal, chlorinated solvents have caused a variety of environmental problems. One such problem of great concern is the contamination of groundwater (Mackay and Cherry, 1991).

A survey of groundwater quality at 479 waste disposal sites, including 178 CERCLA and 173 RCRA sites, and 128 sanitary/municipal landfills, showed that CHCs were detected in groundwater due to improper disposal from all 10 U.S. EPA Regions (Plumb, 1991). The mobility of CHCs in the subsurface environment is strongly influenced by their physicochemical properties. In the vadose zone, their high vapor pressures and relatively low water solubility may

cause certain CHCs them to partition into the gaseous phase and migrate as volatilized constituents. That fraction of CHC chemicals that dissolves in soil pore water or groundwater can be readily transported with the water if CHC interaction with, and adsorption by, soil and aquifer solids is not a significant factor. As immiscible DNAPLs, CHCs will migrate in the subsurface under gravitational forces until they disperse, dissolve, degrade, or are removed through remedial operations (Barbee, 1994).

1.2 Degradation of CHCs

Since 1980, when the widespread contamination with chlorinated solvents become apparent, much has been learned about their movement and fate in the environment, and many different technical approaches to addressing their contamination of soil, air and groundwater have been developed (Stroo and Ward, 2010). Because of the cost, the magnitude and difficulties of remediation of sites contaminated with chlorinated solvents, the search for and implementation of new and cost-effective physical, chemical and biological site remediation approaches still continues.

Two remediation approaches were commonly employed in 1980s and 1990s. The first was the excavation and safe disposal of contaminated soil. The second involved pumping groundwater to the surface for treatment (pump-and-treat). Complete remediation by pump-and-treat processes has proven difficult to achieve (Mackay and Cherry, 1989). Of the 77 sites reviewed by an NRC panel, 69 could not meet cleanup goals after 20 years of pump and treat (NRC, 1994). Because of geological complexities and slow rates of contaminant desorption/diffusion from the low permeability matrix in aquifers, many pore volumes of water must often be extracted/pumped in order to flush out the contaminants from a given area,

requiring treatment times on the order of decades, (Mackay and Cherry, 1989). Alternative treatment approaches have been developed to surmount some of these difficulties. These technologies include monitored natural attenuation, physical extraction/removal (e.g. soil vapor extraction, air sparging) and *in situ* destruction (e.g., bioremediation, chemical oxidation and reduction, including by permeable reactive barriers or PRBs).

PRBs involve the placement of a permeable barrier down-gradient of the contaminant source to treat the plume of contaminated groundwater. PRBs can degrade or sequester the contaminants within the reactive treatment zone and release treated water down-gradient. The reactive treatment zone of PRBs can be created by injecting/placing a mixture of reactive material and sand into the subsurface. Numerous studies have investigated various reactive reagents/materials that can be used in PRBs (Richardson and Nicklow, 2002; Henderson and Demond, 2007). The most common type of PRB is constructed using a zero-valent metal as the reactive media (Sale et al., 2008). Zero-valent iron (ZVI) became the metal of choice in early studies since it is generally non-toxic and relatively inexpensive (Matheson and Tratnyek, 1994). Iron filings from scrap metals and coarse iron particles are typically used in PRBs due to their availability and low cost. However, PRB is a passive remediation technology and does not eliminate the DNAPL source in the subsurface, necessitating continued site monitoring and, in some cases, periodic replacement of the reactive media (Roehl et al., 2005). In 1997, the development of nanoscale zero-valent iron (nZVI) that was more reactive due to smaller particle size brought with it the promise of more rapid and complete remediation of contaminants (Wang and Zhang 1997). Because of their small size, nZVI particles could potentially be injected into the subsurface and subsequently be transported to and mixed with the target contaminants. This possibility transformed zero-valent iron from an immobile, passive technology to one capable of

remediation with greater flexibility of both contaminant plumes and source zones (Nyer and Vance, 2001). *In situ* remediation by nZVI became more desirable because it may more completely degrade contamination at a lower cost. As an *in situ* technology, nZVI injection is attractive because it avoids the high cost of extracting and treating large volumes of water above ground (pump-and-treat) (Nyer and Vance, 2001), or constructing a PRB. The high reactivity of nZVI is a result of its high ratio of surface area to mass,expressed as specific surface area.. nZVI is normally injected as a slurry into the subsurface via a well. Some applications utilize single wells (direct push), while other applications may utilize pairs of wells (recirculation) (Gavaskar et al., 2005). Because no excavation is needed, nZVI can be applied at greater depths than PRBs and at sites where buildings or ongoing operations prohibit more invasive methods.

Recently, multicomponent nanoparticles have received considerable attention (e.g., Fe/FeS) (kim et al., 2011) because they provide novel functions not available in single-component nanoparticles, such as nZVI. It is expected that the improved catalytic properties can be achieved by a combination of iron sulfide and nanoscale zero-valent iron (Kim et al., 2011).

1.3 Degradation Processes Affecting Chlorinated Hydrocarbons

Highly chlorinated compounds are generally considered recalcitrant to oxidative microbial degradation (Vogel et al., 1994) which may be due primarily to the oxidized state of carbon in the molecules. The greater the number of chlorines on the hydrocarbon molecule, the more oxidized is the carbon in the compound. The oxidation state of the carbon in the hydrocarbon compound determines the range of chemical and biological transformations that the compound is likely to undergo (Vogel et al., 1994). For instance, perchloroethene (PCE) is already a highly oxidized molecule that will not naturally undergo further microbial oxidation in groundwater, but

can be dechlorinated under a reducing geochemical condition. Vinyl chloride, with just one chlorine atom substitution, may be subject to microbial oxidation using molecular oxygen and ferric iron as electron acceptors (Bradley and Chapelle, 1997).

It is often difficult to determine the exact mechanisms by which CHCs are transformed in the field. However, it is possible to discern the likely degradation processes from an understanding of the geochemical environment and the daughter products at a contaminated field site. A major concern associated with reductive degradation of CHCs is the production of toxic byproducts (Song and Carraway, 2005). For all these reasons, it is important to understand the kinetics and reaction pathways of byproducts for zero-valent metal systems (Arnold et al., 1999).

The common reaction pathways of CHC degradation are hydrogenolysis, hydrolysis, dehydrochlorination, and dichloroelimination. Hydrogenolysis (reductive dechlorination) of CHCs is a reductive process in which a halogen is substituted by a hydrogen atom, with the simultaneous addition of two electrons to the molecule as shown in Eq. 1 (Mohn and Tiedje, 1992); it is the principal microbial degradation pathway for highly chlorinated ethene derivatives under reducing condition (Nobre and Nobre, 2004).

$$RCl + 2H^+ + 2e^- \rightarrow RH + Cl^- + H^+ \quad [1]$$

Hydrolysis in natural waters is an extremely slow process, though slightly faster in basic conditions. The reaction can be represented by the following equation (Tobiszewski and Namiesnik, 2012):

$$RCl + H_2O \rightarrow R\text{–}OH + Cl^- + H^+ \quad [2]$$

CHCs may undergo dehydrochlorination, in which HCl is eliminated from the molecule as shown in Eq. 3 below (Tobiszewski and Namiesnik, 2012). The reaction results in the formation of less saturated and less halogenated compounds. It is not a redox reaction.

$$RHCCl - CRH_2 \rightarrow RHC{=}CHR + Cl^- + H^+ \quad [3]$$

Dichloroelimination (by vicinal reduction/β-elimination or α-elimination) is a process involving transfer of two electrons to the molecule and the elimination of two chlorine atoms. The reaction products can be less saturated aliphatic hydrocarbons and two chloride ions (e.g., Eq. 4 below). β elimination occurs when chlorine atoms are removed from two different carbons, whereas α elimination is the elimination of chlorine atoms from one carbon atom. Dichloroelimination typically occurs under methanogenic conditions but may also take place under partially aerobic conditions (Chen et al. 1996).

$$RCCl - CClR + 2e^- \rightarrow RC{=}CR + 2Cl^- \quad [4]$$

1.4 Mechanism of Reductive Dechlorination by Zero-Valent Iron

Zero-valent iron (Fe^0) is used in engineered remediation systems and may contribute to natural attenuation (Cundy et al. 2008). Fe^0 is capable of degrading chlorinated ethanes and ethenes through reductive dechlorination. The breakdown of carbon-chlorine bonds of CHC molecules by reductive dechlorination requires an electron donor (reductant), such as zero-valent metals. In such systems, CHCs are electron acceptors. Half-reactions for Iron in this system are shown below as Eq. 5 (Nyer and Vance, 2001):

$$Fe^0 \rightarrow Fe^{2+} + 2e^- \quad [5]$$

Song and Carraway (2006) described two parallel reaction pathways from carbon tetrachloride (CT) and chloroform (CF) to dichloromethane (DCM) and methane. Song and Carraway (2006) also suggested a direct pathway from CF to methane using short-lived carbene and radical intermediate species. There are additional reactions that can occur when more than one carbon atom is present in the CHC molecule, as in chlorinated ethenes, ethanes and propanes. Reductive dechlorination by β-elimination can occur with multi-carbon CHCs. Further, Fennelly and Roberts (1998) suggested that hydrogenoloysis, dehydrochlorination, and to a lesser extent, coupling of radical intermediates, are significant degradation processes for 1,1,1-TCA.

1.5 Degradation Kinetics of CHCs

In addition to characterizing byproducts and the degradation pathways, it is also important to understand degradation kinetics. When characterizing degradation of CHCs, investigations have argued that contaminant destruction may generally occur by reaction kinetics that are pseudo first-order with respect to the concentration of the contaminant (Johnson et al., 1996). The pseudo first-order degradation rate constant, termed k_{obs} ($time^{-1}$), is the slope of the regression line found by plotting the natural logarithm of the contaminant concentration on the ordinate (y-axis) and time on the abscissa (x-axis) (Matheson and Tratnyek, 1994). It has been observed that k_{obs} values can differ between batch and column studies (Johnson et al, 1996). The surface area concentration of metal (m^2 L^{-1} of solution) is expressed as ρ_a in Eqs. 7 and 8 below; the k_{obs} may depend on the variations in ρ_a of the metal particles (Johnson et al, 1996). The larger the surface area the faster the degradation kinetics is expected to be (Boronina et al., 1995). In order to obtain a better representation of the degradation kinetics, normalizing k_{obs} values to the

concentration of metal surface area (Johnson et al., 1996) can be done per the following equations (Salter-Blanc et al., 2012):

$$k_{SA} = k_{obs}/\rho_a \quad [6]$$

where: k_{SA} = pseudo first-order rate constant normalized by surface area (L m^{-2} hr^{-1})

k_{obs} = pseudo first-order rate constant (hr^{-1})

ρ_a = surface area concentration (m^2 L^{-1}) found by the following equation:

$$\rho_a = \alpha_s * \rho_m \quad [7]$$

where: α_s = Specific surface area (SSA) (m^2 g^{-1})

ρ_m = mass concentration (g L^{-1})

Rate constants can also be normalized with respect to the amount of reductant mass concentration used according to Eq. 8 below (Salter-Blanc et al., 2012). However, it may be best to compare mass normalized kinetics only when similar particle sizes are used due to the importance of surface area.

$$k_M = k_{obs}/\rho_m \quad [8]$$

where: k_M = pseudo first-order rate constant normalized by mass (L g^{-1} hr^{-1})

1.6 CHC Degradation with Multicomponent Nanoparticles

Multicomponent nanoparticles have received considerable attention because they provide novel functions not available in single-component nanoparticles. The multicomponent nanoparticles can possess unique physical and chemical properties due to complementary or synergistic effects created by interactions between the different components. They have great potential for a wide range of applications including biological separation, controlled release of drugs, catalysis, and

contaminant removal (Ajayan et al., 2006). In recent years, various methods have been established to enhance the reactivity of iron nanoparticles (nZVI) for degradation of contaminants. Recently, Kim et al. (2011) reported a strategy for enhancement in iron nanoparticle reactivity involving iron (core) / iron sulfide (shell) nanoparticles (nZVI/FeS), which exhibit better reactivity compared to nZVI alone. Iron sulfide minerals commonly found in reduced, sulfidic groundwater and sediment have been shown to remove some contaminants due to reduction and/or adsorption (Butler et al., 2011). nZVI particles coated with FeS have advantages of both components. Kim et al. (2011) showed that the inherent properties of pure nZVI, such as electrical conductivity, magnetic susceptibility, and specific surface area, were greatly affected by the presence of FeS. In another study, Kim et al. (2014) examined the feasibility of using nZVI/FeS for the removal of pollutants from aqueous solutions, where the optimal composition between nZVI and FeS phases was apparently responsible for an enhanced reactivity of the nZVI/FeS composite toward the contaminants. The nZVI/FeS was significantly more efficient in TCE removal than previously reported techniques (Kim et al., 2014).

1.7 nZVI Agglomeration

Perhaps the most significant challenge to applying nZVI for subsurface remediation is the rapid agglomeration of individual particles into discrete micro-scale aggregates or larger chain aggregates (Phenrat et al., 2008). Due to interparticle, magnetic, and van der Waals forces, nZVI can rapidly agglomerate (He and Zhao, 2007). As a result, the available reactive surface area of the nZVI aggregates is significantly reduced, and the transport of the larger aggregates in porous media becomes severely restricted (Petosa et al., 2010). Stabilizing agents are often added to nZVI in order to prevent or reduce nanoparticle agglomeration so that nanoparticles remain dispersed, suspended, and mobile in the aqueous phase (He et al., 2010).The benefits of using

polyelectrolytes to stabilize nZVI include their low cost, wide availability, ease of implementation, non-toxic nature, and its contributions towards long-term biotic degradation of CHCs (He et al., 2010). Several polyelectrolytes, such as carboxymethyl cellulose (CMC) and xanthan gum, are food-grade additives (He et al., 2005). Polyelectrolytes are long chain molecules that can bind with the nZVI particle and provide a negative surface charge (He et al., 2007). If steric and repulsive forces of the polyelectrolyte layer exceed the magnetic and van der Waals attraction, nZVI particles will not agglomerate (Hotze et al., 2010). In addition to the stabilization effect of polyelectrolytes on nZVI, the presence of polyelectrolytes during the precipitation-synthesis of nanoparticles affects particle nucleation and, subsequently, particle size (Shimmin et al., 2004). When nanoparticles are precipitated in aqueous solution, many small crystallites initially form which act as nuclei for further growth. Polyelectrolytes mediate faster nucleation, more numerous crystallites, and slow particle growth, all of which yields more numerous particles with smaller diameter (Shimmin et al., 2004).

Surface modification of nZVI by polymers has been achieved through two different approaches: (i) post-grafting where bare nZVI in suspension is mixed with polymer solutions to allow adsorption of the polymers onto the surface of already made particles (Phenrat et al., 2008) and (ii) pre-grafting or synthesis of nZVI by reduction of mixtures of Fe salt solutions in the presence of polymers where polymers may impact nucleation and growth of the nanoparticles (Sakulchaicharoen et al., 2010). Cirtiu et al. (2011) investigated the differences between pre- and post-synthesis stabilization of nZVI by CMC (Carboxymethyl Cellulose), PAM (Polyacrylamide), PSS (Polystyrene Sulfonate), and PAA (Polyacrylic Acid). They reported that although post-synthesis nZVI stabilization generally resulted in smaller particle diameters, more stable colloidal suspensions were produced when nZVI was pre-stabilized. In studies of post-

synthesis nZVI stabilization, CMC performs poorest in terms of colloidal stability, with either PSS or PAP performing better (Kim et al., 2009). However, pre-synthesis stabilized studies suggest that CMC outperforms PAA, PAM, and PSS, in terms of stability (Cirtiu et al. 2011).

1.8 Research Objectives

This study examines the reactivity and longevity of zero-valent iron nanoparticles coated with FeS (nZVI/FeS) with respect to selected CAHs. The goals of the experiments are to compare the reactivity of nZVI/FeS with nZVI in degrading select groundwater pollutants and to assess the reaction pathways. Bench-scale experiments were conducted to determine the distribution of reaction products, degradation kinetics, and carbon mass balance. This research expands on previous studies to examine the reactivity of nZVI/FeS for different selected contaminants and determine nZVI lifespan. The results of this research will evaluate the efficacy of nZVI/FeS as an alternative to nZVI in groundwater remediation. The study can be divided into five objectives:

(1) Evaluate the effect of sulfide loading and nZVI loading on degradation of CHCs.

(2) Measure degradation kinetics of select CHCs using a pseudo first-order modeling to compare the performance of nZVI/FeS to nZVI.

(3) Determine the degradation byproduct distribution and assess degradation pathways/ mechanisms resulting from reactions involving nZVI/FeS and various CHCs.

(4) Evaluate the effect of stabilizer loading on nZVI/FeS system.

(5) Measure nZVI/FeS system longevity.

Chapter 2

MATERIALS AND METHODS

2.1 Materials

The following chemicals were used as received: carbon tetrachloride (CT; Fisher Scientific, purity: 99.8%), chloroform (CF; Fisher Scientific, purity: 99.8%), 1,1,2-trichloroethane (1,1,2-TCA; Sigma-Aldrich, purity: 97%), 1,1,1-trichloroethane (1,1,1-TCA, Sigma-Aldrich, purity: 99%). Other chemicals used included ferrous sulfate ($FeSO_4.7H_2O$; MP Biomedicals, purity: > 99%), sodium sulfide ($Na_2S.9H_2O$; Alfa Aesar, purity: >98%), sodium borohydride ($NaBH_4$; Sigma-Aldrich, purity: >98%), carboxymethyl-cellulose sodium salt (CMC-Na; Sigma-Aldrich, molecular weight 90,000 amu), TAPSO (N-[tris(hydroxymethyl)methyl]-3-amino-2-hydroxypropanesulfonic acid; Sigma-Aldrich, purity: 99%), sodium hydroxide (NaOH; Fisher Scientific, purity: > 99%), and high purity gases (He, N_2, H_2, air; Weiler Welding, Dayton, Ohio, purity: 99.999%).

2.2 Methods

2.2.1 Reagents

The stock solutions for CHCs were prepared by adding 20 μL of pure organic liquid to a 160 mL serum bottle containing 160 mL Milli-Q water (i.e. no headspace) and sealed using Teflon-lined rubber stopper and aluminum crimp. Stock solution bottles were wrapped in aluminum foil and

placed on an end-over-end rotator (setting at 70; 45 rpm) for two days to allow the compound to completely dissolve. Sodium sulfide (Na_2S) that was used for modifying nZVI surface was prepared by dissolving 2.47g of $Na_2S.9H_2O$ salt in 100 mL de-oxygenated water to prepare 0.1 *M* sodium sulfide reagent. Experimental reactors were filled with deoxygenated 30 mM (typically 96 mL; 2.88 mmoles) TAPSO titrated to pH 7 by 1 *M* NaOH. Carboxymethyl-cellulose sodium salt (19.2 mL of 20 g/L) was used as a polyelectrolyte for stabilizing nanoparticles. Final CMC concentration in the reactors was 4 g/L or 0.4 g/L. All reagent solutions used in setting-up the batch reactors were de-oxygenated in advance by sparging with high purity nitrogen gas for at least 40 minutes prior to their placement in the anaerobic chamber.

Appendix A provides the calculations for determining the amounts of CHC aqueous in reactor (μmoles) after partitioning.

2.2.2 nZVI and nZVI /FeS Synthesis

nZVI were synthesized using ferrous sulfate heptahydrate, sodium borohydride, and CMC. TAPSO buffer was used to achieve pH 7. The source of sulfide for the experiments was sodium sulfide. Reactors were prepared in an anaerobic chamber in a nitrogen gas atmosphere with 1-2% hydrogen. The synthesis of nZVI was accomplished through the borohydride reduction method, in which deoxygenated aqueous solution of ferrous sulfate heptahydrate ($FeSO_4.7H_2O$) was reacted with sodium borohydride ($NaBH_4$) in an anaerobic chamber at room temperature (20-22 ºC) (Song and Carraway, 2005). Experiments were performed at 0.05 or 0.1 g/L of nZVI modified with 4 g/L CMC. CMC-nZVI was synthesized in the anaerobic chamber starting with (0.320 mL - 0.860 mL) of 200 mM $FeSO_4.7H_2O$ deoxygenated solution in a 160 mL serum bottles, followed by adding(0-19.2 mL) of 20 g/L CMC stock solution. The bottle was swirled gently three times for 5 seconds each at 15 second intervals and then Fe^{2+} was

allowed to complex with CMC solution for 15 minutes without mixing. Afterwards, 25 mL of deoxygenated 30 mM TAPSO buffer was added to achieve an initial pH of 7. (0.262mL - 0.525 mL) of 1M $NaBH_4$ solution was added to the bottle to reduce the Fe^{2+} to Fe^0. The reaction is described by Equation [9] (Song and Carraway, 2005):

$$Fe\ (H_2O)_6^{2+} + 2BH_4^- \rightarrow \quad Fe^0 + 2B(OH)_3 + 7H_2 \qquad [9]$$

This was followed by adding deoxygenated, deionized water in the batch reactors to make the total aqueous volume equal to 96 mL. Control reactors were prepared for each experiment with 96 mL Milli-Q water. After removing from the anaerobic chamber, the calculated amount of 0.01 M deoxygenated Na_2S solution was added to the reactors containing freshly-prepared CMC-nZVI in the fume hood to achieve the desired concentration of sulfide in solution. The solution will be equilibrated for 15 minutes on a rotator for homogenized mixing of the reactants.

Equations (10-12) present key reactions (Poltun, 2003; Rickard and Luther, 2007) expected to occur on the surface of nZVI during treatment with Na_2S (sulfidation):

$$Fe^0 + 2H_2O \rightarrow Fe^{2+} + 2OH^- + H_2 \qquad [10]$$

$$Na_2S + H_2O \rightarrow 2Na^+ + HS^- + OH^- \qquad [11]$$

$$Fe^{2+} + 2HS^- \rightarrow FeS + H_2S \qquad [12]$$

2.2.3 Experimental Set-up

Batch reactors containing nZVI were prepared in an anaerobic chamber in order to ensure that CHC, rather than oxygen, served as the preferred electron acceptor (oxidant) for nZVI. This

prevented the oxidation of nZVI particles by O_2 during reactor preparation/set-up. Each experiment included duplicate batch reactors in order to validate results. After reactor setup, each batch reactor was injected with 50 μL of target CHC stock solution using a 250 μL syringe. Immediately after injection, each batch reactor was equilibrated on a rotator by end-over-end mixing at 45 rpm for 3 minutes. 50 μL of reactor headspace was periodically extracted using a 250 μL gas-tight syringe and analyzed by gas chromatography. Reactors were well mixed on an end-over-end rotator at 45 rpm for the duration of the experiment except when headspace of the reactor was sampled.

2.2.4 Chemical Analysis

The amount of CT and daughter products in nZVI/FeS reactor was quantified by gas chromatography (Hewlett-Packard, model 6890 system) equipped with electron capture (ECD) and flame ionization (FID) detectors. An HP-624 column (30 m x 0.32 mm x 0.25 μm, Agilent Technologies) was used with high purity helium serving as the carrier gas at constant flow of 1.8 mL min^{-1}. The GC method was as follows: front inlet = 250 ^oC, FID = 250 ^oC, ECD = 300 ^oC, and oven temperature (isothermal) = 100 ^oC. The make-up gas for GC 6890 was high purity N_2 with a flow rate of 25 mL min^{-1} for the FID and 60 mL min^{-1} for the ECD. The flow rate for high purity H_2 was 30 mL min^{-1} and for high purity air it was 450 mL min^{-1}.

2.2.5 Data Treatment

Five standards for each compound were prepared in 160 mL serum bottles with 96 mL Milli-Q water. CHC standards were injected with various amounts of stock solution, wrapped in aluminum foil, and allowed to equilibrate for at least 2-3 hours on an end-over-end rotator (45

rpm). Calibration curves for each compound were created by placing GC peak area obtained for each standard on the abscissa (x-axis) and amount (μmoles) in each bottle on the ordinate (y-axis). The linear regression equation of the data points on the x-y scatter plot could then be used to transform GC peak areas into compound amounts in batch reactors.

For degradation experiments, the CHC amount (μmoles) was plotted on the ordinate (y-axis) and time on the abscissa (x-axis). First-order degradation rate constants (k_{obs}; h^{-1}) were determined from the exponential regression through the selected data points. nZVI Mass normalized degradation rate constant (k_M, L g^{-1} hr^{-1}) was calculated from dividing k_{obs} by nZVI concentration, ρ_m (g L^{-1}). Mass balance analysis of byproducts was performed from the amount (μmoles) of various products generated from the degradation of the target CHC, and their respective molar mass fraction yields (m/m_o), referred to as yields henceforth.

Chapter 3

RESULTS AND DISCUSSION

3.1: Results

The results shown here focus on selected CHCs degradation ,byproducts (mole fraction) and rate constant, however additional information on degradation and by products over sampling period are shown in Appendix B.

3.1.1 Chlorinated Methanes

3.1.1.1 Carbon Tetrachloride Degradation by nZVI

The results for CT degradation with stabilized 0.05 g/L nZVI are plotted in Fig. 3.1. Observed products are CF and methane. Degradation was notably fast (k_{obs} = 5.79 hr^{-1}; k_M = 1.15x10^2 L g^{-1} hr^{-1}) and CT was degraded below the detection limit within 1 hour. After 1.5 hours, CT remaining (m/m_0) was 0.0 while CF yield (m/m_0) was 0.67. CF appeared to be a stable product, as no further degradation was observed. A trace amount of methane was observed from the start of the experiment, but it was not quantified throughout this study.

3.1.1.2 Carbon Tetrachloride Degradation by nZVI/FeS

The results of CT degradation with 0.05 g/L stabilized nZVI with 1 wt% sulfide are shown in Fig. 3.2. CT was completely degraded in less than 1 hour (k_{obs} = 11.2 hr^{-1}; k_M = 224 L g^{-1} hr^{-1}). Observed products were CF and methane. CF formed quickly and peaked (m/m_0: 0.67) around 0.75 hour; the onset of CF decline corresponded with the complete disappearance of CT. A minor amount of methane appeared immediately after CT was added to the reactor. Any other byproduct, such as dichloromethane (DCM), remained below the detection limit. After 2 hours, CT remaining (m/m_0) was 0.0, while CF yield (m/m_0) was 0.56 (Table 3.1).

3.1.1.3 Effect of Sulfide Loading in nZVI/FeS on CT Degradation.

The degradation of CT by nZVI/FeS was evaluated with 0.05 g/L nZVI and a range of sulfide loadings (0.5-10 wt. % sulfide). CF and methane were observed as degradation products. After 1.5 hours from the start of experiments, the amounts of CT remaining (m/m_0) varied from 0.0 to 0.68, while corresponding CF yields (m/m_0) varied from 0.76 declining to 0.12. The rate constants of CT degradation (k_{obs}) increased with increasing sulfide loading up to 1 wt. % and, then, declined at higher sulfide loading.

At 0.5-2 wt. % sulfide loading, CT degradation was fast and it declined below the detection limit in less than 1 hour (k_{obs} =7.33-11.2 hr^{-1}; k_M = 146.64-224 L g^{-1} hr^{-1}) (Figs. 3.3-3.5 and Table 3.2). At greater sulfide loadings (4-10 wt. %), however, CT degradation was progressively much slower in comparison (k_{obs} = 1.66-0.13 hr^{-1}; k_M = 33.2-2.6 L g^{-1} hr^{-1}) (Figs. 3.6-3.11; Table 3.2). R^2 values quantifying goodness-of-fit to the pseudo first-order model were greater than 0.987, with most above 0.99 (Table 3.2). In most cases, the model was fitted to four or more data

points, with a minimum of three points used in cases of rapid degradation for calculating overall k_{obs}.

3.1.1.4 Chloroform Degradation by nZVI

The results for CF degradation with stabilized 0.1 g/L nZVI are shown in Fig. 3.12. Observed products are DCM and methane. Degradation was slow (k_{obs} = 0.08 hr^{-1}; k_M = 0.82 L g^{-1} hr^{-1}). DCM and methane continued to accumulate during the 3 hours long experiment. After 3 hours, CF remaining (m/m_0) was 0.72 while DCM and methane yields (m/m_0) were 0.11 each. The carbon mass balance (m/m_0) was >0.94 during the experiment suggesting most products were identified. Any other intermediate, such as chloromethane (CH_3Cl), was below the instrument detection limit

3.1.1.5 Chloroform Degradation by nZVI/FeS

CF degradation with nZVI/FeS (0.1 g/L stabilized nZVI and 1 wt. % sulfide) is shown in Fig. 3.13. Observed products are DCM and methane, and their yields (m/m_0) were 0.17 and 0.22 respectively at the end of experiment. Further, CF remaining and the carbon mass balance mole fractions at the end of experiment were 0.56 and 0.95, respectively. CF reduction kinetics (k_{obs} = 0.193 hr^{-1}; k_M = 1.93 L g^{-1} hr^{-1}) are faster than nZVI system (k_{obs} = 0.08 hr^{-1}; k_M = 0.8 L g^{-1} hr^{-1}); see Figs. 3.12 and 3.13, and Table 3.3.

3.1.1.6 Effect of Sulfide Loading on CF Degradation

The effect of sulfide in nZVI/FeS on CF removal was examined by varying sulfide loading (0.5-2 wt. %). For all CF degradation experiments, R^2 values quantifying goodness-of-fit to the pseudo first-order model were higher than 0.95, with most above 0.99 (Table 3.3). Total carbon

yields (m/m_0) are slightly greater than 1 in all CF experiments, which may be due to error in byproduct calibration curves. The results indicated that CF remaining (m/m_0) after 2 hours are comparable to CF reduction with nZVI (Figs. 3.13-3.16; Table 3.4). Also, small increase in DCM and methane yields with increasing sulfide loading are demonstrated. Methane yields (m/m_0) with 0.5-1 wt. % sulfide were higher than yield observed with nZVI (Table 3.4); however, at higher sulfide loading (1.5 and 2 wt. %) methane yields decreased (0.17 and 0.16). DCM yield (m/m_0) declined somewhat with 0.5 wt. % sulfide in comparison to nZVI, but at higher sulfide loading (1- 2 wt. %) methane yields were ~0.14). Most CF destruction and the highest DCM and methane yields were obtained at 1 wt. % sulfide loading. Good total carbon mass balance was observed at all sulfide loadings investigated, indicating that DCM and methane were the dominant byproducts from CF reduction by nZVI/FeS.

The reaction kinetics (k_{obs}) for CF increased with increasing sulfide loading and reached the highest value at 1 wt.% sulfide (k_{obs} = 0.193 hr^{-1}; k_M = 1.93 L g^{-1} hr^{-1}), see Figs. 3.17, 3.18.

3.1.2 CHLORINATED ETHANES

3.1.2.1 Degradation of 1,1,1 TCA by nZVI and nZVI/FeS

1, 1, 1-TCA degradation with stabilized 0.1 g/L nZVI was observed (k_{obs} = 0.086 hr^{-1}; k_M = 0.86 L g^{-1} hr^{-1}; Fig. 3.19; Table 3.5). 1,1 DCA and ethane formed as degradation products. After 3 hours, 1, 1, 1-TCA remaining (m/m_0) was 0.64, and 1,1-DCA and ethane yields (m/m_0) were 0.073 and 0.014, respectively. In comparison, the degradation of 1,1,1-TCA with nZVI/FeS (0.1 g/L stabilized nZVI and 1 wt% sulfide) (k_{obs} = 0.61 hr^{-1}; k_M = 6.1 L g^{-1} hr^{-1}) was faster than degradation of 1,1,1-TCA with nZVI (Fig. 3.20, Table 3.6). 1,1-DCA, ethane, and ethene were identified as degradation byproducts. After ~3 hours, 1,1,1-TCA remaining (m/m_0) was 0.14,

while the 1,1-DCA, ethane, and ethene yields (m/m_0) were 0.049, 0.034, and 0.033, respectively. A low carbon mass balance yield (m/m_0 = 0.25) suggests that a significant part of the original 1,1,1-TCA was degraded into unidentified products.

3.1.2.2 Effect of Sulfide Loading in nZVI/FeS on 1,1,1 TCA Degradation

1,1,1-TCA degradation by nZVI/FeS was evaluated with 0.1 g/L nZVI at various sulfide loadings (0.5, 1 and 1.5 wt.%); see Figs. 3.20 – 3.22. After 3 hours from the start of experiments, 1,1,1-TCA remaining (m/m_0) varied from 0.13-0.33, while 1,1-DCA yields (m/m_0) varied from 0.049 to 0.063 (Table 3.6); further, ethane and ethene yields (m/m_0) did not vary much. The degradation kinetics of 1,1,1-TCA reached its maximum at 1 wt.% sulfide loading (Fig 3.23 and 3.24). The carbon mass balance yields were generally poor for all sulfide loadings; m/m_0 were 0.36, 0.25 and 0.45 for 0.5, 1 and 1.5 wt. % sulfide, respectively. Other possible byproducts, like 1,1-DCE, were below detection limits and likely account for remaining carbon mass balance. Increase in sulfide loading to 1 wt. % caused a faster 1,1,1-TCA degradation kinetics (k_{obs} = 0.61 hr^{-1}; k_M = 6.1 L g^{-1} hr^{-1}), and 1,1,1-TCA remaining was lowest (m/m_0: 0.26; Table 3.6). However, at 1.5 wt.% sulfide loading, 1,1,1-TCA removal was significantly less efficient in comparison to 1 wt.% sulfide; 1,1,1-TCA remaining was greater (m/m_0: 0.34), and its degradation kinetics also declined (k_{obs} = 0.32 hr^{-1}; k_M = 3.2 L g^{-1} hr^{-1}).

3.1.3 Effect of Iron Loading on 1,1,1-TCA Degradation

1,1,1-TCA degradation by nZVI/FeS was evaluated for two different nZVI concentrations (0.1 and 0.5 g/L) with 1 wt.% sulfide (k_{obs} = 0.61-1.01 hr^{-1}; k_M = 6.09-2.02 L g^{-1} hr^{-1}; Fig. 3.25, 3.26 and Table 3.7). 1,1-DCA, ethane and ethene were observed as degradation products (Figs. 3.20 and 3.25, and Table 3.8). After 2 hours from the start of experiments, 1,1,1

TCA remaining (m/m_0) varied from 0.12-0.23, with minor variations in 1,1-DCA and ethane yields (m/m_0: 0.07-0.08 and 0.03-0.05, respectively. Ethene yields (m/m_0) remained virtually unaffected at 0.03. Some evidence of 1,1-DCA degradation was noted for experiments involving nZVI/FeS.

3.1.4 nZVI/FeS Longevity

3.1.4.1 Degradation of 1,1,1-TCA by Fresh and Aged nZVI/FeS

The degradation of 1,1,1-TCA with nZVI/FeS (0.1 g/L stabilized nZVI and 1 wt.% sulfide) was observed over the course of 9 days. nZVI/FeS stabilized by 4 g/L CMC showed a power function decline in reactivity (k_m) with time**.** The k_{obs} of 1,1,1-TCA declined 2.6-fold overnight from 0.79 hr^{-1} to 0.31 hr^{-1} (k_m = 7.9 to 3.1 L g^{-1} hr^{-1}; Fig. 3.27, and Table 3.9), but it stabilized thereafter; the k_{obs} of 1,1,1-TCA on day 5 and day 9 were 0.27 hr^{-1} and 0.26 hr^{-1}, respectively. The final 1,1,1-TCA mole fraction was almost same for the last three injections (Table 3.10).

3.1.5 Effect of CMC Concentration on Reactivity

3.1.5.1. Degradation of 1,1,1-TCA by Varying CMC Concentrations

The effect of variable CMC concentration on nZVI/FeS reactivity with 1,1,1-TCA degradation (0.5 g/L nZVI and 1 wt.% sulfide) investigated at 0, 0.4 and 4.0 g/L CMC is summarized in Table 3.11. Unamended ZVI degraded 1,1,1-TCA only 7% during 2 hours sampling and no byproduct was detected (Fig.3.28). In the 0.4 g/L CMC experiment, about 74% of 1,1,1-TCA

degraded in 3 hours and ethane and ethane were observed as byproducts, however the week total carbon yield result confirmed about 60% of byproducts were under the detection limit (Fig. 3.29). nZVI stabilized with 4g/L CMC could degrade about 87% 1,1,1-TCA in 3 hours. Beside Ethene and Ethane, 1,1_DCA would observe in this experiment. As shown in Figure 3.30, the addition of CMC stabilizer significantly improved nZVI/FeS reactivity toward 1,1,1-TCA, by as much as 45 fold increase in k_{obs} between 0 and 4.0 g/L.

3.2: Discussion

3.2.1 Chlorinated Methanes

3.2.1.1 Carbon tetrachloride degradation by nZVI

As reported in the previous section, CT was degraded completely by stabilized 0.05 g/L nZVI in 1.5 hours. Lien and Zhang (1999) investigated CT degradation by nanoscale and microscale iron particles (<10 µm; commercial grade iron particles sourced from the supplier Aldrich); their results indicate that nZVI reactivity per unit surface area (k_{SA}) is about 5 times greater that of the microscale iron particles. In another study (Song and Carraway, 2006), CT degradation by 0.16 g/L unstabilized nZVI (0.02 g nZVI in 124 mL buffered water) was investigated (k_{obs} = 5.02 hr^{-1}; k_M = 31.38 L g^{-1} hr^{-1}). The k_M (reactivity) of unstabilized nZVI particles towards CT (Song and Carraway, 2006) was ~4-fold slower than k_M for stabilized nZVI reported in this study.

3.2.1.2 Carbon tetrachloride degradation by nZVI/FeS

The nZVI/FeS system showed greater effectiveness at degrading CT compared to nZVI alone. Only a few studies involving nZVI/FeS have been reported in the literature (Kim et al., 2011; 2013; 2014). Kim et al. (2011) reported that nZVI/FeS showed superior reactivity than nZVI

towards TCE degradation. In comparison to unstabilized nZVI (k_M =22 L g^{-1} hr^{-1}) (Song and Carraway, 2006); however, CT degradation with nZVI/FeS (containing 1 wt. % sulfide) in the present study was 8-fold faster (k_M = 224 L g^{-1} hr^{-1}).

The first step in CCl_4 reduction may involve removal of one chlorine to produce a trichloromethyl radical (Song and Carraway, 2006), after which the pathways branch. If hydrogenation occurs to replace the chlorine with hydrogen, CF is formed, which may further degrade to DCM (Song and Carraway, 2006, Feng and Lim, 2005), and onward possibly to chloromethane and methane by sequential dechlorination. However, in this study CH_4 evolved too early to be attributable to a hydrogenolysis product of DCM reduction. Also, experiments with chlorinated methane as the target contaminant indicate DCM degrades very slowly or not at all in the presence of CMC-stabilized nZVI (Lein and Zhang, 1999). Methane formation during CT degradation may therefore be the result of alternative pathways like direct reduction (Lein and Zhang, 1999) where multiple chlorines may be removed from CT at the same time (Table 3.12).

3.2.1.3 Effect of sulfide loading in nZVI/FeS on CT degradation

As reported in section 3.1.1.3, the rate constants of CT degradation (k_{obs}) increased with increasing sulfide loading up to 1 wt% and, then, declined at higher sulfide loading (Figs. 3.31-3.33). There could be several reasons for increase in CT k_{obs} till 1 wt% sulfide in nZVI/FeS system. The FeS surface layer can be more selective in electron transfer from Fe^0 core to the adsorbed CT than the iron oxide surface in unamended nZVI. Park et al. (2006) suggested that sulfide minerals can be less hydrophilic compared to iron oxides, which suggests that FeS layer on the sulfidated nZVI can potentially enhance CT chemisorption and efficient electron transfer

in comparison to unamended nZVI. The possible explanation for decreasing rate constant at higher sulfide loading can be due to blocking of the reactive sites by increase in FeS on the nanoparticle surface thereby inhibiting the dissolution of iron core. Similar phenomenon has also been observed in iron-based bimetallic systems (Xu and Bhattacharyya, 2005; Parshetti and Doong, 2009); for example, inadequate and excessive Ni loading on nZVI surface may lead to formation of Fe-rich area or Ni-rich area, which lowered the catalytic activity (Parshetti and Doong, 2009). Therefore, the highest reactivity of nZVI/FeS at 1% sulfide loading may be due to an optimal FeS arrangement on Fe^0 surface.

3.2.1.4 Chloroform degradation by nZVI

DCM produced from CF reduction was via hydrogenolysis pathway, as previously suggested with nZVI (Lein and Zhang, 1999). However, DCM degradation with nZVI is typically slow (Lein and Zhang, 1999). The kinetics of DCM degradation with nZVI is not fast enough for methane yields observed during CF reduction (Song and Carraway, 2006). Therefore, to account for the methane yield observed from CF degradation, it is suggested that CF transformation to methane occurred directly, and without DCM as a reaction intermediate (Song and Carraway, 2006), although small amounts of methane could also from DCM reduction via hydrogenolysis. Direct transformation of CF to methane has previously been suggested with ZVI (Song and Carraway, 2006), and with Ni-nZVI and microscale bimetallic Ni/Fe (Feng and Lim, 2005).

3.2.1.5 Chloroform degradation by nZVI/FeS.

As reported in section 3.1.1.5, CF degradation with nZVI/FeS (0.1 g/L stabilized nZVI and 1 wt% sulfide) resulted in a substantial methane yield (m/m_0: 0.22) in 2 hr, a 2-fold increase in comparison to CF degradation with nZVI. DCM yield was also higher (m/m_0: 0.14) with

nZVI/FeS in comparison to CF degradation (m/m_0: 0.11) with nZVI. This was likely due to faster CF reduction kinetics (k_{obs} = 0.193 hr^{-1}; k_M = 1.93 L g^{-1} hr^{-1}) that shows a ~2-fold increase in comparison to nZVI (k_{obs} = 0.08 hr^{-1}; k_M = 0.82 L g^{-1} hr^{-1}).

3.2.1.6 Effect of sulfide loading on CF degradation.

In the experiments of CF degradation with 0.1 g/L nZVI/FeS containing various sulfide loading (0.5-2 wt.%) described earlier in section 3.1.1.6, small increase in DCM yields and substantial methane yield with increasing sulfide loading is demonstrated. This suggests an increase in direct CF transformation to methane at higher sulfide loading. The reaction kinetics (k_{obs}) for CF increased by increasing sulfide loading and reached the highest value at 1 wt.% sulfide (k_{obs} = 0.193 hr^{-1}; k_M = 1.93 L g^{-1} hr^{-1}), a nearly 2-fold increase in comparison to nZVI (k_{obs} = 0.082 hr^{-1}; k_M = 0.82 L g^{-1} hr^{-1}). Similar to results described for CT degradation in section 3.2.1.3, the highest reactivity of nZVI/FeS with 1% sulfide loading may be attributed to an optimal FeS arrangement on the Fe^0.

3.2.2 CHLORINATED ETHANES

3.2.2.1 Degradation of 1,1,1-TCA by nZVI and nZVI/FeS

Song and Carraway (2005) studied on 1,1,1-TCA degradation by 0.081 g/L unstabilized nZVI (0.01 g nZVI in 124 mL buffered water) and the degradiation kinetics (k_{obs}= 0.34 hr^{-1}; k_M= 4.2 L g^{-1} hr^{-1}) is greater than stabilized nZVI in this study. It is likely that stabilization (by CMC) causes decreased reactivity of particles in water (Phenrat et al., 2009). The daughter products of 1,1,1-TCA degradation by nZVI in this investigation are 1,1-DCA, ethane and ethane, which is similar to Song and Carraway (2005) experiment, but their yields are different. 1,1-DCA, formed

via hydrogenolysis, accounted for 69% of total carbon mass (Song and Carraway, 2005). However, in this study 1,1-DCA mole fraction yield is only 7%, which is less toxic and more desirable outcome. The nZVI/FeS system was more effective at degrading 1,1,1-TCA compared to the nZVI system (7 fold faster). Current results indicate that nZVI coated by sulfide can affect 1,1-DCA reduction rate and lead the reaction pathway to non-toxic daughter products.

Degradation of 1,1,1-TCA formed 1,1-DCA via hydrogenolysis, which degraded further to form ethane via hydrogenolysis (1,1,1-TCA→ 1,1-DCA→ chloroethane→ ethane). It is likely because during 3 hours sampling, first 1,1-DCA accumulated and then degraded to some extent. Since ethene and ethane formed quickly and simultaneously with 1,1-DCA, and not sequentially from 1,1-DCA degradation in this study, their production may have occurred by a parallel pathway. Ethane production from 1,1,1-TCA degradation by nZVI has been suggested to occur via reductive α-elimination pathway (Song and Carraway, 2005) and could be the parallel pathway for producing ethane (Table 3.12).

The formation of ethene (m/m_0 = 0.025) from 1,1,1-TCA degradation by fresh 0.1 g/L nZVI modified with 1 wt.% sulfide may suggest a pathway that forms 1,1-DCE by dehydrohalogenation followed by hydrogenolysis to ethene via vinyl chloride (1,1,1TCA→ 1,1-DCE→ VC→ ethene) (Fennelly and Roberts, 1998). However, 1,1-DCE should be a key intermediate for the proposed pathway scheme, but it was not observed and may have been below the detection limit. Alternatively, carbene intermediate can form as a result of α-elimination of 1,1-DCE that can hydrogenate to form ethene and ethane. In other words, α-elimination pathway may play a critical role in a direct transformation of 1,1,1-TCA into ethane and ethene (Cwiertny et al., 2006). Song and Carraway (2005) reported that 1,1,1-TCA was rapidly transformed by unstabilized nZVI to form 1,1-DCA as the major product that should

occur via hydrogenolysis pathway. However, the result from this study suggests that nZVI/FeS produce a higher yield of fully dechlorinated byproduct than by unstabilized nZVI.

3.2.2.2 Effect of sulfide loading on 1,1,1-TCA degradation

Similar to previous sections of this study, section 3.2.1.3 and 3.2.1.6 of this study, possible explanation for decreasing degradation kinetic at higher sulfide percentages(>1%) is that more FeS can block the active sites on the nZVI surface. Byproduct yields did not change much due to increase in sulfide loading from 0.5-1.5 wt. %. This study suggests that nZVI/FeS produced lower 1,1-DCA yield (m/m_0) compare to stabilized nZVI, thus indicating less toxic byproducts due to greater dechlorination. The study also shows that 0.1 g/L nZVI/FeS modified with 1 wt. % sulfide has the optimal effect on the reaction kinetics.

3.2.3 Effect of Iron loading on 1,1,1-TCA degradation.

Increasing nZVI/FeS loading causes k_{obs} to increase. This trend was expected because increase in nZVI/FeS loading increases its surface area that participates in reaction with 1,1,1-TCA. This study indicates that linearity between the reaction rate-constant and the nZVI/FeS concentration holds, at least over the range investigated. Song and Carraway (2005) observed a similar relationship between 1,1,1-TCA degradation rate constants at various nZVI concentrations. The 1,1,1-TCA remaining (m/m_0) shows decline from 0.23 at 0.1 g/L nZVI/FeS to 0.12 at 0.5 g/L nZVI/FeS at the end of 2 hr. Further, increase in ethane and ethene yields at 2 hr is also evident at increasing nZVI/FeS concentration. Higher nZVI/FeS loading can create stronger reducing condition, facilitate larger total nZVI surface area and favor greater yields of non-toxic byproducts.

3.2.4 nZVI/FeS longevity.

The longevity of the nZVI/FeS nanoparticles can be defined by the reactivity (k_m) remaining after a certain period (performance), where the decline in k_m may suggest loss of reactive nZVI/FeS mass during the period. Given the price of nZVI, multiple injections are unlikely at most sites. Therefore, longevity is critical to determining the return on investment (ROI) by the end-user. This relationship between longevity and ROI makes longevity a critical parameter in the utilization of nZVI for site remediation (Liles, 2009).

3.2.4.1 Degradation of 1,1,1-TCA by fresh and aged nZVI/FeS

As reported in section 3.1.4.1, Sarathy et al. (2008) studied the effects of aging on CCl_4 degradation using RNIP immersed in an aqueous solution at different intervals. The degradation kinetics was decreasing in the medium- to long- term period due to the formation of more protective, magnetite- rich oxides (Sarathy et al., 2008).

The high reactivity of nZVI is related to its core–shell structure, which consists of a metallic iron (Fe^0) core encapsulated by a thin oxide shell (Martin et al., 2008). The Fe^0 core in the nZVI oxidizes upon reaction with an oxidant (e.g., water and oxygen), and eventually, the metallic iron is exhausted to form iron oxides and hydroxides. In a similar study by Liu et al., 2015, the aging of nZVI was investigated over a period of 90 days in static water. The results indicated that initially Fe^{2+} ion in the Fe^0 core diffused outwardly through the shell, and hollowed-out iron oxide shells emerge. Then, the iron oxide shell collapsed and became a flaky, acicular-shaped structure. The type and the crystal phase of second iron oxide minerals are vastly different at various aging times (Liu et al., 2015).

The heterogeneous reactions on the corroding ZVI surface were complicated and resulted in a variety of reactive surface sites for contaminant removal (Satapanajaru et al., 2003). The loss of nZVI/FeS reactivity could be due to the dislodgment of FeS from the aged nZVI/FeS particles and encapsulation of sulfide islets by iron oxides film that developed/thickened over the aging period. Also, CMC is known to adversely affect reaction kinetics. Phenrat et al. (2009) showed that CMC stabilization can cause up to a 24-fold decrease in reactivity when treating TCE with nZVI. There are a variety of potential causes for loss in nZVI/FeS reactivity and there may be multiple processes occurring simultaneously that can lead to loss in nZVI/FeS reactivity.

3.2.5 Effect of CMC concentration on reactivity

It has been demonstrated in several studies that CMC of varying molecular weights outperformed other polyelectrolytes by producing nanoparticles with smaller size, higher reactivity, and better transport characteristics (Cirtiu et al., 2011). While CMC coatings increase the reactive surface area of nZVI by decreasing particle size and inhibit interparticle aggregation, CMC can also decreases nZVI reactivity by blocking the reactive surface sites (Phenrat et al., 2009). At an nZVI loading of 0.10 g/L, He and Zhao (2007, 2008) determined that 4.0 g/L and 2.0 g/L CMC loading gave the smallest and the most reactive nZVI particles, respectively. Although optimal CMC loading was reported relative to nZVI loading in the past, there is evidence that the absolute CMC concentration, regardless of nZVI loading, is a better predictor of performance (He and Zhao, 2008). It was previously observed that failure of polyelectrolytes to prevent nanoparticle aggregation is not caused by insufficient amounts of stabilizer, but rather the slow rate of particle coating at low stabilizer concentrations (Ditsch et al, 2005). Furthermore, during particle synthesis polyelectrolytes mediate the formation of more numerous,

smaller particles, an effect dependent on absolute polyelectrolyte concentration (He and Zhao, 2007).

Optimization of CMC loading in nZVI/FeS system may be complicated as FeS deposition on the nZVI surface can significantly influence nanoparticle interactions with the polyelectrolyte. The roles of CMC in blocking reactive sites on FeS/nZVI surface and preventing the nanoparticles from agglomeration are the two competing processes that have not been examined in this study.

Earlier in this study it was confirmed that 1wt% sulfide has the optimal effect on degradation CHCs, regardless of a CHC type. In this study, it was assumed that increasing CMC concentration to > 4 g/L in the given set-up can block more reactive surface sites and reduce reactivity. However, the effect of higher CMC concentration on potential decrease in nZVI/FeS particle size thus affecting an increase its reactivity was beyond the scope of this study.

3.2.5.1. Degradation of 1,1,1-TCA by varying CMC concentrations.

It is assumed beyond 4.0 g/L CMC loading, a plateau in reactivity would be observed, based on the two factors: (1) higher CMC concentrations may have no further effect on particle size or stability, and (2) continued improvements in particle size or stability may be negated by the reaction-inhibiting effect of the CMC surface coating (Phenrat et al., 2009). There was this possibility that at CMC concentration <4.0 g/L, nZVI surface would be more available for FeS particles to deposit and this might increase reactivity. However, the result, section 3.1.5.1, shows experiment with 0.4 g/L CMC had 3.3 fold smaller k_{obs} than with 4g/L CMC, which suggests that 0.4 g/L CMC concentration is not sufficient to stablize the nZVI particles and significant agglomeration may have occurred and subsequent FeS deposition on the surface was ineffective

Chapter 4

CONCLUSIONS

4.1.Review of Findings

The five research objectives presented in the introduction were as follows: (1) evaluate the effect of sulfide loading and nZVI loading on degradation of CHCs, (2) measure degradation kinetics of select CHCs using a pseudo first-order modeling to compare the performance of nZVI/FeS to nZVI, (3) determine the degradation byproduct distribution and identify degradation pathways/ mechanisms resulting from reactions involving nZVI/FeS and various CHCs, (4) evaluate the effect of stabilizer loading on nZVI/FeS system, and (5) measure nZVI/FeS system longevity.

1) Evaluate the effect of sulfide loading and nZVI loading on degradation of CHCs.

Sulfide loading experiments showed that increasing the sulfide loading (0 – 10 wt. %) caused a linear increase in k_{obs} followed by a drastic decrease, with the change occurring at 1 wt.% sulfide. The same set of experiments were conducted for CF (0-2 wt.% sulfide) and 1,1,1-TCA (0-1.5 wt.% sulfide) and it was observed regardless of CHC type, 1 wt.% sulfide is the optimal sulfide loading that shows the highest k_{obs} in nZVI/FeS system. The possible explanation for this fact is that more FeS is formed with increasing levels of sulfide, which can block the active sites on the surface thereby inhibiting the dissolution of the core of nZVI particles. nZVI

concentration experiments with 1 wt.% sulfide showed that increasing nZVI concentrations increased k_{obs} but decreased k_M so it will be less efficient when applied at an industrial scale.

2) Measure degradation kinetics of select CHCs using a pseudo first-order model to compare the performance of nZVI/FeS to nZVI.

The application of nZVI/FeS improves CHCs degradation and reaction kinetic could increase compare to unamended nZVI. In the range of (0.5-2 wt. %) sulfide loading, CT, CF, and 1,1,1-TCA all degraded more rapidly in nZVI/FeS system compared to the unamended nZVI. Sulfide clearly has a favorable effect on degradation kinetics with regard to chlorinated methanes and ethanes.

3) Determine the degradation byproduct distribution and identify degradation pathways/ mechanisms resulting from reactions involving nZVI/FeS and various CHCs.

In this study of chlorinated methane, the rate constants increased with increasing chlorination, consistent with previous studies on this group of compounds (Matheson and Tratnyek, 1994; Lien and Zhang, 1999). Direct transformation of CT and CF to methane seems to be occurring with nZVI coated by sulfide, as the rapid appearance of methane observed could not have been produced from DCM hydrogenalysis which has slow degradation kinetics. Byproducts generated by nZVI/FeS reduction of 1,1,1-TCA resulted in the formation of ethane, ethane and 1,1-DCA. 1,1,1-TCA asymmetrical structure makes it a subject of reductive α-elimination pathway which result in less toxic products in nZVI/FeS system.

4) Evaluate the effect of stabilizer loading on nZVI/FeS system.

A set of experiments with 1 wt. % sulfide and lower CMC concentrations toward 1,1,1-TCA were conducted and results relived a drastically decrease in k_{obs}. Although at lower CMC concentration there would potentially be more room on nZVI surface for FeS particles, CMC amount is not sufficient to stablize all the nZVI particles. Therefore, agglomeration occurred before FeS particles can settle on the surface.

5) Measure nZVI/FeS system longevity.

The longevity experiments confirmed that nZVI/FeS particles remain highly reactive with 1,1,1-TCA nine days after particle synthesis. The Fe^0 core in the nZVI oxidizes upon reaction with water and oxygen, and eventually, the metallic iron is exhausted to form iron oxides and hydroxides which decrease reactivity.

4.2. Future research

This thesis identified one the most promising opportunities for improving nZVI reactivity by coating it with FeS. Based on the current state of the technology, nZVI appears to be too expensive for mainstream use as a remediation tool (Crane and Scott, 2012). Increasing the reactivity of nZVI toward chlorinated contaminants makes it a more viable, cost-effective option for remediation of contaminated groundwater. However, many opportunities for future research can be identified. There have been few field-scale studies of nZVI and no studies for nZVI/FeS system. Therefore, many possibilities for future research exist. Field studies are needed to discover how nZVI/FeS can be successfully transported to reach and mix with target contaminants in situ. In laboratory scale there are also additional CHCs that should be evaluated for degradation by nZVI/FeS. The toxicological effects of nZVI/FeS and use of engineered copolymers to stabilize nZVI/FeS should be considered for future studies as well.

REFERENCES

Ajayan, Pulickel M., Linda S. Schadler, and Paul V. Braun. *Nanocomposite Science and Technology*. John Wiley & Sons, 2006.

Arnold, William A., William P. Ball, and A. Lynn Roberts. "Polychlorinated ethane reaction with zero-valent zinc: pathways and rate control." *Journal of Contaminant Hydrology* 40, no. 2 (1999): 183-200.

Barbee, Gary C. "Fate of chlorinated aliphatic hydrocarbons in the vadose zone and ground water." *Groundwater Monitoring & Remediation* 14, no. 1 (1994): 129-140.

Boronina, Tatyana, Kenneth J. Klabunde, and Gleb Sergeev. "Destruction of organohalides in water using metal particles: carbon tetrachloride/water reactions with magnesium, tin, and zinc." *Environmental Science & Technology*29, no. 6 (1995): 1511-1517

Bradley, Paul M., and Francis H. Chapelle. "Kinetics of DCE and VC mineralization under methanogenic and Fe (III)-reducing conditions." *Environmental Science & Technology* 31, no. 9 (1997): 2692-2696.

Butler, E. C., Y. Dong, L. R. Krumholz, X. Liang, H. Shao, and Y. Tan. "Rate controlling processes in the transformation of tetrachloroethylene and carbon tetrachloride under iron reducing and sulfate reducing conditions." *Aquatic Redox Chemistry* ACS Symposium Series 1041; American Chemical Society: Washington, DC, 2011; pp 519−538.

Chen, Chun, Jaakko A. Puhakka, and John F. Ferguson. "Transformations of 1, 1, 2, 2-tetrachloroethane under methanogenic conditions." *Environmental Science & Technology* 30, no. 2 (1996): 542-547.

Cirtiu, Ciprian M., Trishikhi Raychoudhury, Subhasis Ghoshal, and Audrey Moores. "Systematic comparison of the size, surface characteristics and colloidal stability of zero-valent iron nanoparticles pre-and post-grafted with common polymers." *Colloids and Surfaces A: Physicochemical and Engineering Aspects* 390, no. 1 (2011): 95-104.

Crane, R. A., and T. B. Scott. "Nanoscale zero-valent iron: future prospects for an emerging water treatment technology." *Journal of Hazardous Materials*, no. 211 (2012): 112-125

Cundy, Andrew B., Laurence Hopkinson, and Raymond LD Whitby. "Use of iron-based technologies in contaminated land and groundwater remediation: A review." *Science of the Total Environment* 400, no. 1 (2008): 42-51.

Cwiertny, David M., Stephen J. Bransfield, Kenneth JT Livi, D. Howard Fairbrother, and A. Lynn Roberts. "Exploring the influence of granular iron additives on 1, 1, 1-trichloroethane reduction." *Environmental Science & Technology* 40, no. 21 (2006): 6837-6843

Ditsch, Andre, Paul E. Laibinis, Daniel I.C. Wang, and T. Alan Hatton. "Controlled clustering and enhanced stability of polymer-coated magnetic nanoparticles." *Langmuir* 21, no. 13 (2005): 6006-6018.

Doherty, Richard E. "A History of the Production and Use of Carbon Tetrachloride, Tetrachloroethylene, Trichloroethylene and 1, 1, 1-Trichloroethane: Part 1--Historical Background; Carbon Tetrachloride and Trichloroethylene." *Environmental Forensics* 1, no. 2 (2000): 69-81.

Fam, Sami A., David M. Falatko, Glenn McGillicuddy, George Pon, Louis J. Burkhardt, and Jonathan Hone. "Successful full-scale enhanced anaerobic dechlorination at a NAPL strength 1, 1, 1-TCA source area." *Remediation Journal* 22, no. 2 (2012): 33-47.

Feng, Jing, and Teik-Thye Lim. "Pathways and kinetics of carbon tetrachloride and chloroform reductions by nano-scale Fe and Fe/Ni particles: comparison with commercial micro-scale Fe and Zn." *Chemosphere* 59, no. 9 (2005): 1267-1277

Fennelly, Jay P., and A. Lynn Roberts. "Reaction of 1, 1, 1-trichloroethane with zero-valent metals and bimetallic reductants." *Environmental Science & Technology* 32, no. 13 (1998): 1980-1988.

Gavaskar A, Tatar L, Condit W. Cost and Performance Report: Nanoscale Zero-Valent Iron Technologies for Source Remediation. CR-05-007-ENV. Port Hueneme, CA, 2005: Naval Facilities Engineering Command. https://clu-in.org/download/techdrct/td_CR-05-007-ENV.pdf

He, Feng, and Dongye Zhao. "Hydrodechlorination of trichloroethene using stabilized Fe-Pd nanoparticles: Reaction mechanism and effects of stabilizers, catalysts and reaction conditions." *Applied Catalysis B: Environmental* 84, no. 3 (2008): 533-540.

He, Feng, and Dongye Zhao. "Manipulating the size and dispersibility of zerovalent iron nanoparticles by use of carboxymethyl cellulose stabilizers."*Environmental Science & Technology* 41, no. 17 (2007): 6216-6221.

He, Feng, and Dongye Zhao. "Preparation and characterization of a new class of starch-stabilized bimetallic nanoparticles for degradation of chlorinated hydrocarbons in water." *Environmental Science & Technology* 39, no. 9 (2005): 3314-3320.

He, Feng, Dongye Zhao, and Chris Paul. "Field assessment of carboxymethyl cellulose stabilized iron nanoparticles for in situ destruction of chlorinated solvents in source zones." *Water Research* 44, no. 7 (2010): 2360-2370.

He, Y. Thomas, John T. Wilson, and Richard T. Wilkin. "Impact of iron sulfide transformation on trichloroethylene degradation." *Geochimica et Cosmochimica Acta* 74, no. 7 (2010): 2025-2039

Henderson, Andrew D., and Avery H. Demond. "Long-term performance of zero-valent iron permeable reactive barriers: a critical review." *Environmental Engineering Science* 24, no. 4 (2007): 401-423.

Hotze, Ernest M., Tanapon Phenrat, and Gregory V. Lowry. "Nanoparticle aggregation: challenges to understanding transport and reactivity in the environment." *Journal of Environmental Quality* 39, no. 6 (2010): 1909-1924.

Johnson, Timothy L., Michelle M. Scherer, and Paul G. Tratnyek. "Kinetics of halogenated organic compound degradation by iron metal." *Environmental Science & Technology* 30, no. 8 (1996): 2634-2640.

Kim, Eun-Ju, Jae-Hwan Kim, Abdul-Majeed Azad, and Yoon-Seok Chang. "Facile synthesis and characterization of Fe/FeS nanoparticles for environmental applications." *ACS Applied Materials & Interfaces* 3, no. 5 (2011): 1457-1462.

Kim, Eun-Ju, Jae-Hwan Kim, Yoon-Seok Chang, David Turcio-Ortega, and Paul G. Tratnyek. "Effects of metal ions on the reactivity and corrosion electrochemistry of Fe/FeS nanoparticles." *Environmental Science & Technology* 48, no. 7 (2014): 4002-4011.

Kim, Eun-Ju, Kumarasamy Murugesan, Jae-Hwan Kim, Paul G. Tratnyek, and Yoon-Seok Chang. "Remediation of trichloroethylene by FeS-coated iron nanoparticles in simulated and real groundwater: Effects of water chemistry. *"Industrial & Engineering Chemistry Research* 52, no. 27 (2013): 9343-9350.

Kim, Hye-Jin, Tanapon Phenrat, Robert D. Tilton, and Gregory V. Lowry. "Fe0 nanoparticles remain mobile in porous media after aging due to slow desorption of polymeric surface modifiers." *Environmental Science & Technology* 43, no. 10 (2009): 3824-3830

Liles, David S. "Treatment of Chlorinated Hydrocarbon Contaminated Ground water with Injectable Nanoscale Bimetallic Particles." ESTCP-Project-ER-007 (2009). https://clu in.org/download/techfocus/prb/NZVI-ER-0017-LL.pdf

Lien, Hsing-Lung, and Wei-xian Zhang. "Transformation of chlorinated methanes by nanoscale iron particles." *Journal of Environmental Engineering*125, no. 11 (1999): 1042-1047.

Liu, Airong, Jing Liu, and Wei-xian Zhang. "Transformation and composition evolution of nanoscale zero-valent iron (nZVI) synthesized by borohydride reduction in static water." *Chemosphere* 119 (2015): 1068-1074.

Mackay, Douglas M., and John A. Cherry. "Groundwater contamination: Pump-and-treat remediation." *Environmental Science & Technology* 23, no. 6 (1989): 630-636.

Mackay, Donald, Wan Ying Shiu, Aila Maijanen, and Stan Feenstra. "Dissolution of non-aqueous phase liquids in groundwater." *Journal of Contaminant Hydrology* 8, no. 1 (1991): 23-42

Martin, John E., Andrew A. Herzing, Weile Yan, Xiao-qin Li, Bruce E. Koel, Christopher J. Kiely, and Wei-xian Zhang. "Determination of the oxide layer thickness in core-shell zero-valent iron nanoparticles." *Langmuir* 24, no. 8 (2008): 4329-4334.

Matheson, Leah J., and Paul G. Tratnyek. "Reductive dehalogenation of chlorinated methanes by iron metal." *Environmental Science & Technology* 28, no. 12 (1994): 2045-2053.

Mohn, William W., and James M. Tiedje. "Microbial reductive dehalogenation."*Microbiological Reviews* 56, no. 3 (1992): 482-507.

Nobre, Rosane C.M., and Manoel M.M. Nobre. "Natural attenuation of chlorinated organics in a shallow sand aquifer." *Journal of Hazardous Materials* 110, no. 1 (2004): 129-137.

NRC, 1994.Alternatives for Groundwater Cleanup, National Academy Press, Washington D.C, USA. 316 p

Nyer, Evan K., and David B. Vance. "Nano-Scale Iron for Dehalogenation. *"Groundwater Monitoring & Remediation* 21, no. 2 (2001): 41-46.

Park, Sang-Won, Sung-Kuk Kim, Jeong-Bae Kim, Sung-Woo Choi, Hilary I. Inyang, and Shuzo Tokunaga. "Particle surface hydrophobicity and the dechlorination of chloro-compounds by iron sulfides." *Water, Air, & Soil Pollution: Focus* 6, no. 1-2 (2006): 97-110.

Parshetti, Ganesh K., and Ruey-an Doong. "Dechlorination of trichloroethylene by Ni/Fe nanoparticles immobilized in PEG/PVDF and PEG/nylon 66 membranes." *Water Research* 43, no. 12 (2009): 3086-3094.

Petosa, Adamo R., Deb P. Jaisi, Ivan R. Quevedo, Menachem Elimelech, and Nathalie Tufenkji. "Aggregation and deposition of engineered nanomaterials in aquatic environments: role of physicochemical interactions." *Environmental Science & Technology* 44, no. 17 (2010): 6532-6549.

Phenrat, Tanapon, Yueqiang Liu, Robert D. Tilton, and Gregory V. Lowry. "Adsorbed polyelectrolyte coatings decrease Fe0 nanoparticle reactivity with TCE in water: conceptual model and mechanisms." *Environmental Science & Technology* 43, no. 5 (2009): 1507-1514.

Phenrat, Tanapon, Navid Saleh, Kevin Sirk, Hye-Jin Kim, Robert D. Tilton, and Gregory V. Lowry. "Stabilization of aqueous nanoscale zero-valent iron dispersions by anionic polyelectrolytes: adsorbed anionic polyelectrolyte layer properties and their effect on aggregation and sedimentation." *Journal of Nanoparticle Research* 10, no. 5 (2008): 795-814.

Plumb, R. H. "The occurrence of Appendix IX organic constituents in disposal site ground water." *Groundwater Monitoring & Remediation* 11, no. 2 (1991): 157-164

Poulton, Simon W. "Sulfide oxidation and iron dissolution kinetics during the reaction of dissolved sulfide with ferrihydrite." *Chemical Geology* 202, no. 1 (2003): 79-94.

Richardson, John P., and John W. Nicklow. "In situ permeable reactive barriers for groundwater contamination." *Soil and Sediment Contamination* 11, no. 2 (2002): 241-268.

Rickard, David, and George W. Luther. "Chemistry of iron sulfides." *Chemical Reviews* 107, no. 2 (2007): 514-562.

Roehl, K. E., Meggyes, T., Simon, F. G. and Stewart, D. I. eds., "Long-term Performance of Permeable Reactive Barriers. Trace Metals and Other Contaminants in the Environment. Vol. 7. (Series editor: J. O. Nriagu). Amsterdam, Elsevier. 326 pp.

Sakulchaicharoen, Nataphan, Denis M. O'Carroll, and Jose E. Herrera. "Enhanced stability and dechlorination activity of pre-synthesis stabilized nanoscale FePd particles." *Journal of Contaminant Hydrology* 118, no. 3 (2010): 117-127.

Satapanajaru, Tunlawit, Patrick J. Shea, Steve D. Comfort, and Yul Roh. "Green rust and iron oxide formation influences metolachlor dechlorination during zero-valent iron treatment." *Environmental Science & Technology* 37, no. 22 (2003): 5219-5227.

Sale, Tom, Charles Newell, Hans Stroo, Robert Hinchee, and Paul Johnson. " Frequently Asked Questions Regarding Management of Chlorinated Solvents in Soils and Groundwater.", Developed for the Environmental Security Technology Certification Program (ESTCP), (2008).http://www.savethepoudre.org/docs/faq-regarding-management-of-chlorinated-solvents-in-soils-and-groundwater.pdf

Salter-Blanc, Alexandra J., Eric J. Suchomel, John H. Fortuna, James T. Nurmi, Chris Walker, Tom Krug, Suzanne O'Hara, Nancy Ruiz, Theresa Morley, and Paul G. Tratnyek. "Evaluation of Zero-valent Zinc for Treatment of 1, 2, 3-Trichloropropane-Contaminated Groundwater: Laboratory and Field Assessment." *Groundwater Monitoring & Remediation* 32, no. 4 (2012): 42-52.

Sarathy, Vaishnavi, Paul G. Tratnyek, James T. Nurmi, Donald R. Baer, James E. Amonette, Chan Lan Chun, R. Lee Penn, and Eric J. Reardon. "Aging of iron nanoparticles in aqueous solution: effects on structure and reactivity." *The Journal of Physical Chemistry C* 112, no. 7 (2008): 2286-2293.

Shimmin, Robert G., Andrew B. Schoch, and Paul V. Braun. "Polymer size and concentration effects on the size of gold nanoparticles capped by polymeric thiols." *Langmuir* 20, no. 13 (2004): 5613-5620.

Song, Hocheol, and Elizabeth R. Carraway. "Reduction of chlorinated ethanes by nanosized zero-valent iron: kinetics, pathways, and effects of reaction conditions." *Environmental Science & Technology* 39, no. 16 (2005): 6237-6245.

Song, Hocheol, and Elizabeth R. Carraway. "Reduction of chlorinated methanes by nano-sized zero-valent iron. Kinetics, pathways, and effect of reaction conditions." *Environmental Engineering Science* 23, no. 2 (2006): 272-284.

Stroo, Hans F., and C. Herb Ward. In situ remediation of chlorinated solvent plumes. Springer Science & Business Media, 2010.

Tobiszewski, Marek, and Jacek Namieśnik. "Abiotic degradation of chlorinated ethanes and ethenes in water." *Environmental Science and Pollution Research* 19, no. 6 (2012): 1994-2006.

Vogel, T. M., R. D. Norris, R. E. Hinchee, R. Brown, P. L. McCarty, L. Semprini, J. T. Wilson "Natural bioremediation of chlorinated solvents." Handbook of Bioremediation. Lewis Publishers, Boca Raton, FL (1994): 201-225.

Wang, Chuan-Bao, and Wei-Xian Zhang. "Synthesizing nanoscale iron particles for rapid and complete dechlorination of TCE and PCBs." *Environmental Science & Technology* 31, no. 7 (1997): 2154-2156.

Xu, Jian, and Dibakar Bhattacharyya. "Membrane-based bimetallic nanoparticles for environmental remediation: Synthesis and reactive properties." *Environmental Progress* 24, no. 4 (2005): 358-366.

1. CHLORINATED METHANES

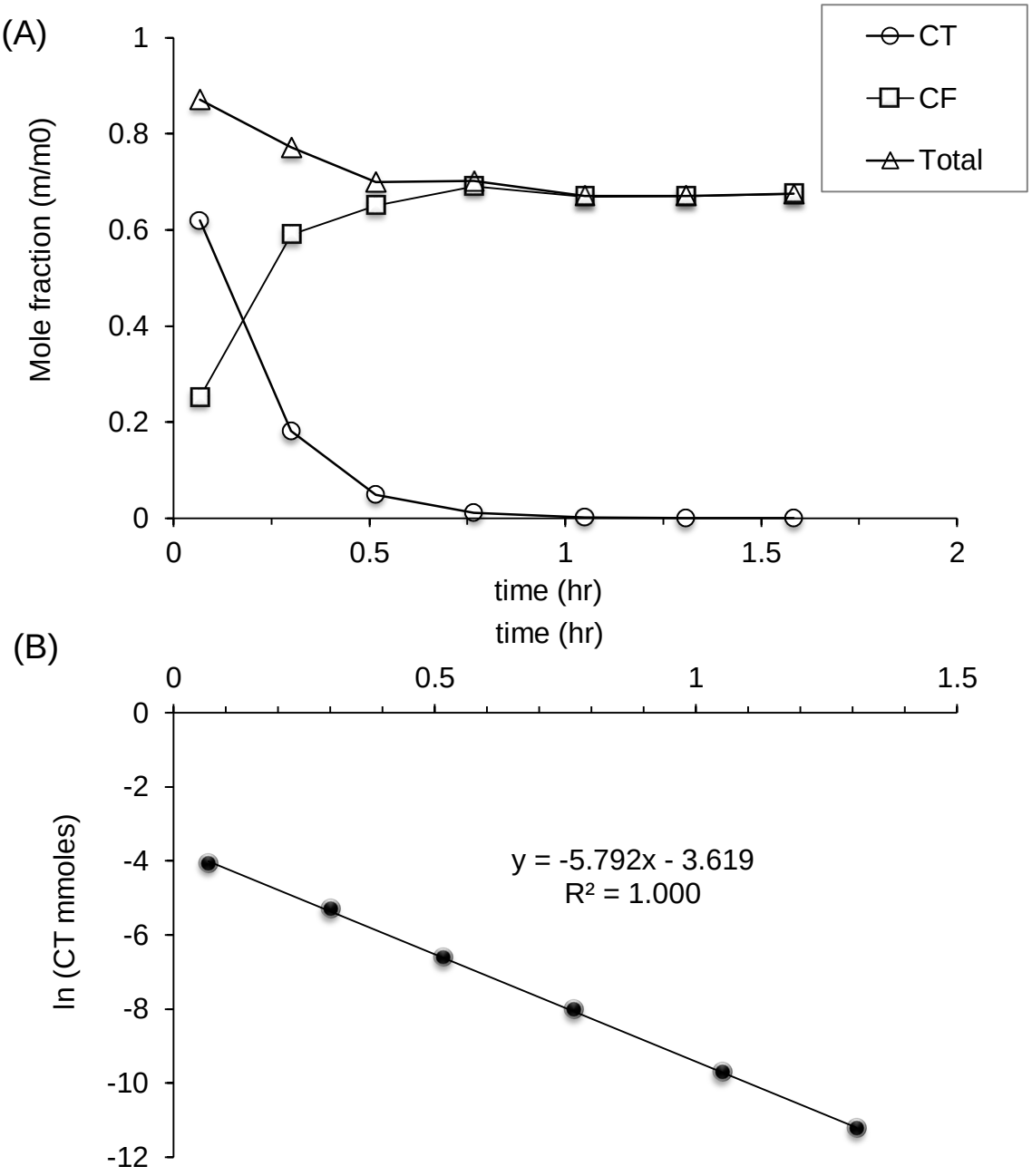

Figure 3.1: CT degradation with fresh 0.05 g/L nZVI prepared in 4 g/L CMC. Initial CT = 0.035 μmoles, or 54.45 μg/L (50 μL of 108.9 mg/L CT stock solution). CT degraded completely in about 1 hour, with chloroform as the only reaction byproduct. (A) CT degradation and byproduct (mole fraction); (B) ln [CT] vs. time plot showing CT degradation rate constant.

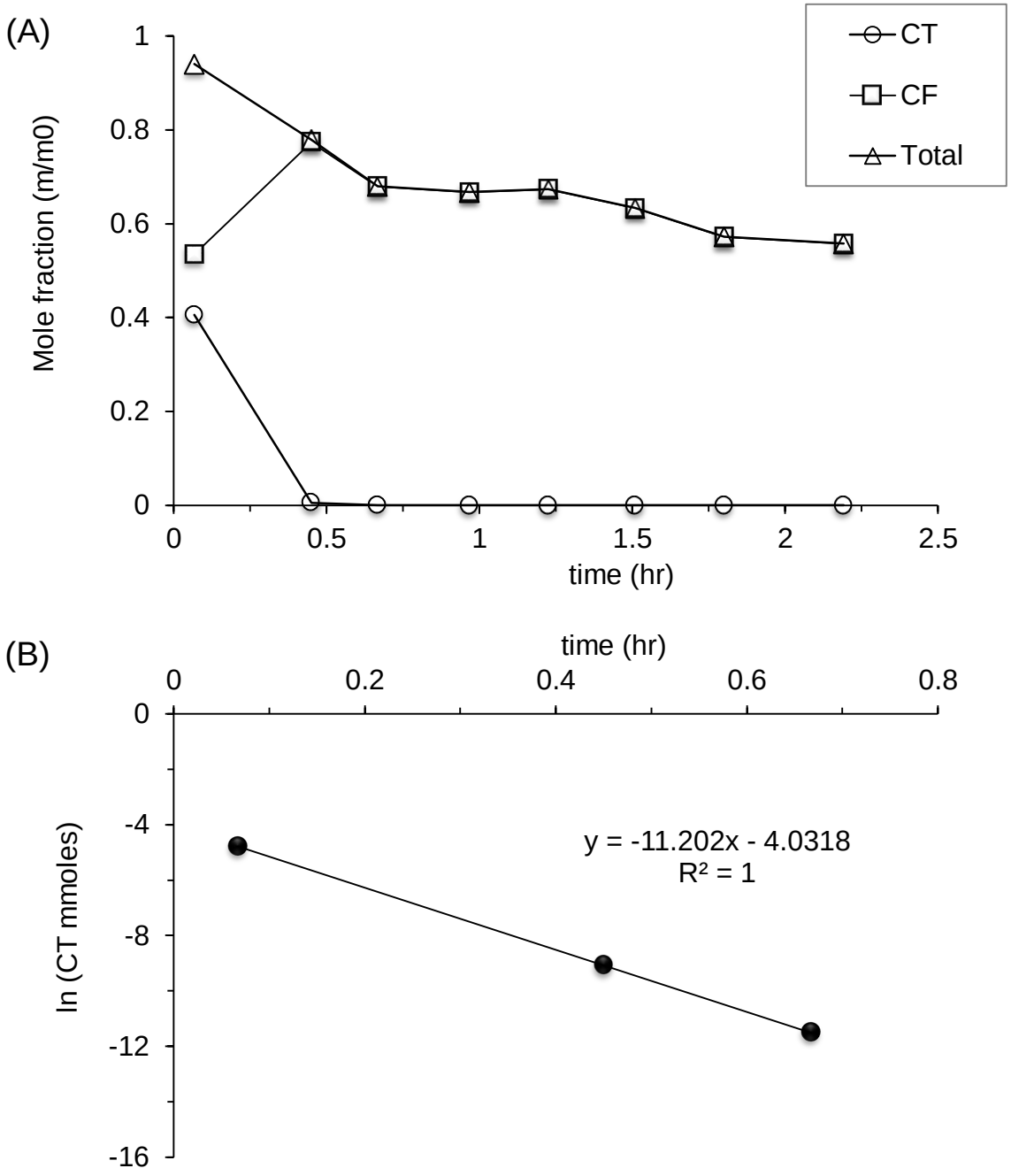

Figure 3.2: CT degradation with fresh 0.05 g/L nZVI modified with 1 wt. % sulfide, prepared in 4 g/L CMC. Initial CT = 0.035 μmoles, or 54.45 μg/L (50 μL of 108.9 mg/L CT stock solution). CT degraded completely in 1 hour, with chloroform as the only reaction byproduct. . (A) CT degradation and byproduct (mole fraction); (B) ln [CT] vs. time plot showing CT degradation rate constant.

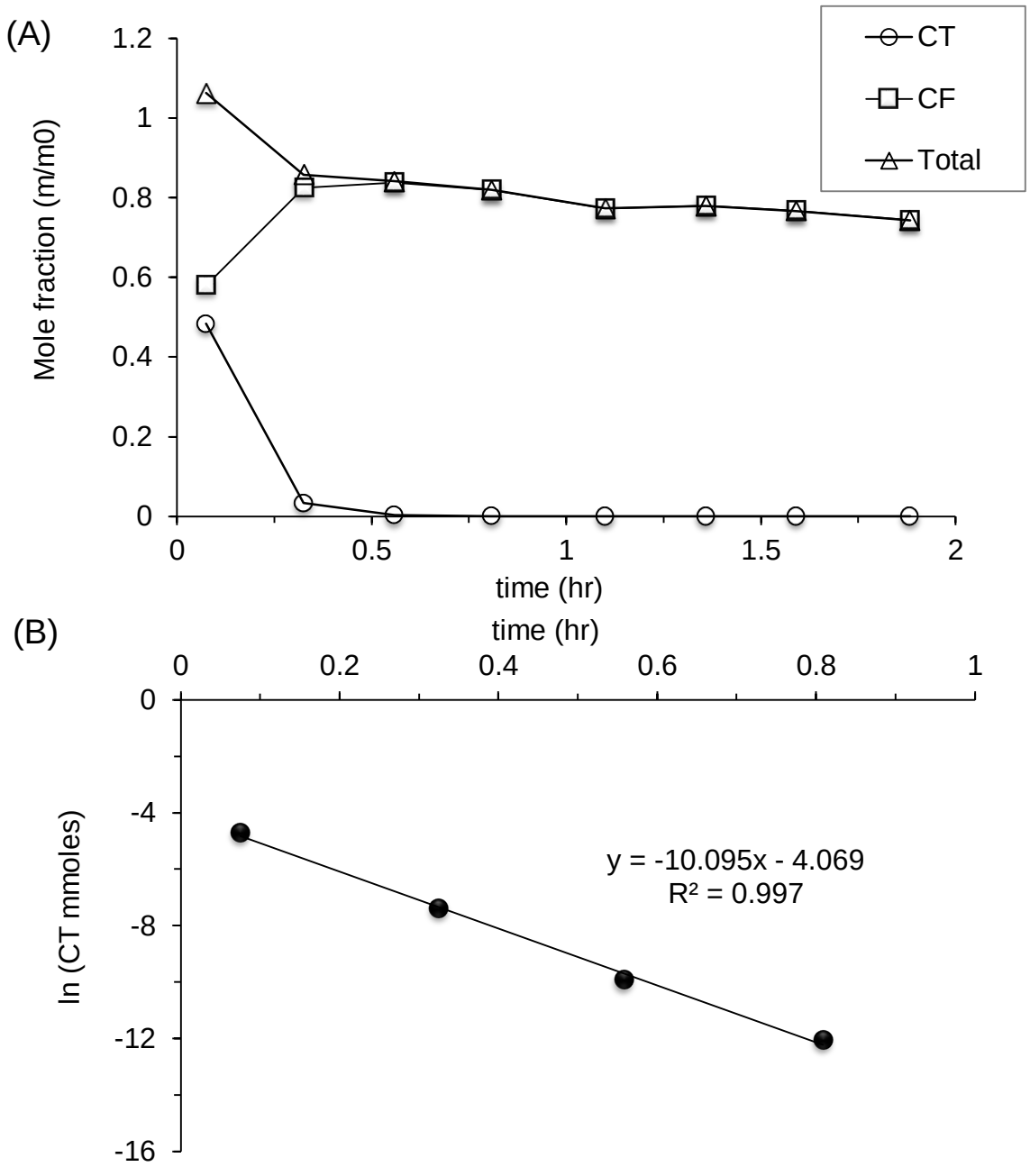

Figure 3.3: CT degradation with fresh 0.05 g/L nZVI modified with 0.5 wt. % sulfide prepared in 4 g/L CMC. Initial CT = 0.035 μmoles, or 54.45 μg/L (50 μL of 108.9 mg/L CT stock solution).CT degraded completely in 1 hour, with chloroform as the only reaction byproduct. (A) CT degradation and byproduct (mole fraction); ln [CT] vs. time plot showing CT degradation rate constant.

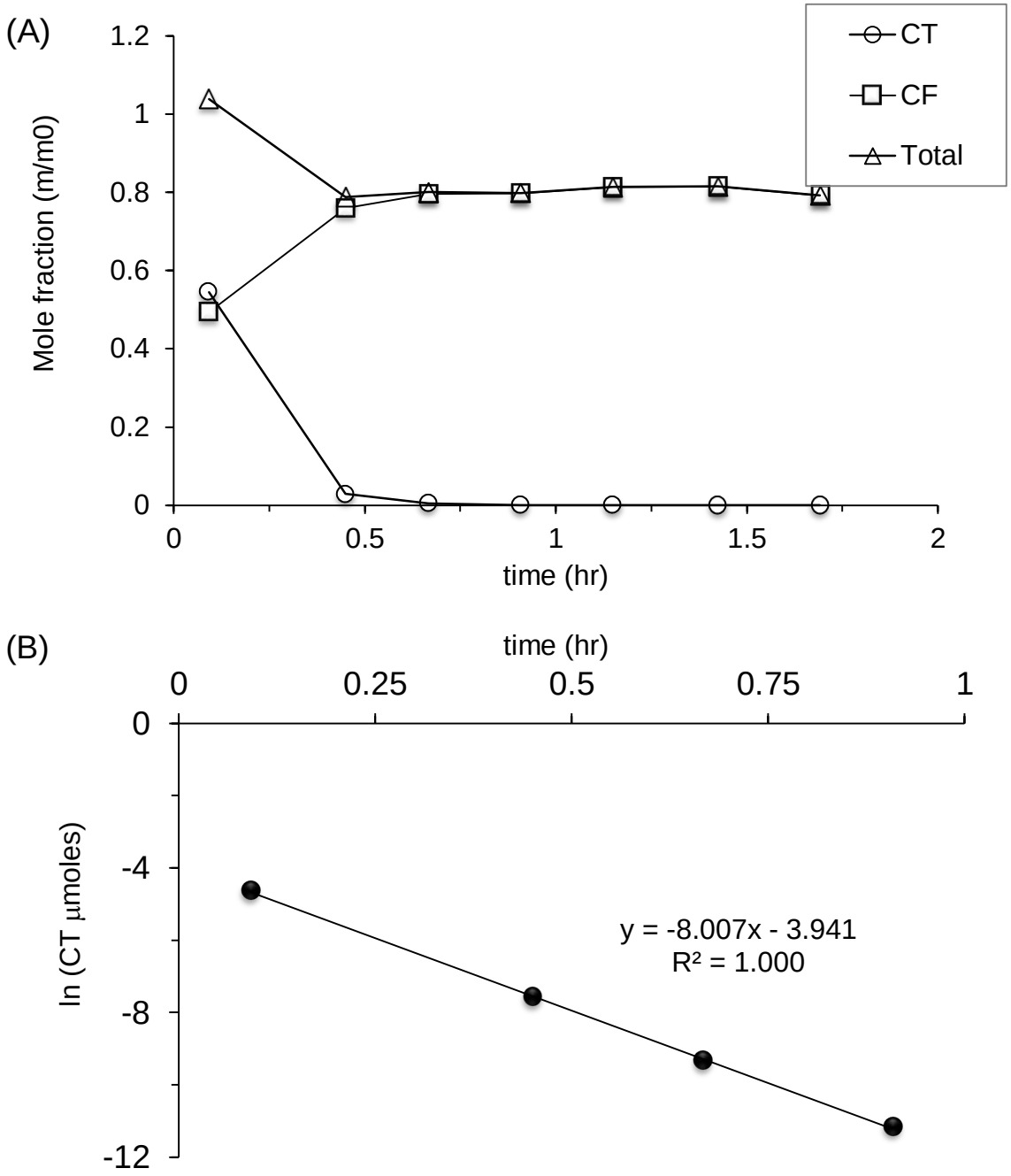

Figure 3.4: CT degradation with fresh 0.05 g/L nZVI modified with 1.5 wt. % sulfide, prepared in 4 g/L CMC. Initial CT = 0.035 µmoles, or 54.45 µg/L (50 µL of 108.9 mg/L CT stock solution). CT degraded completely in 1 hour, with chloroform as the only reaction byproduct. (A) CT degradation and byproduct (mole fraction); (B) ln [CT] vs. time plot showing CT degradation rate constant.

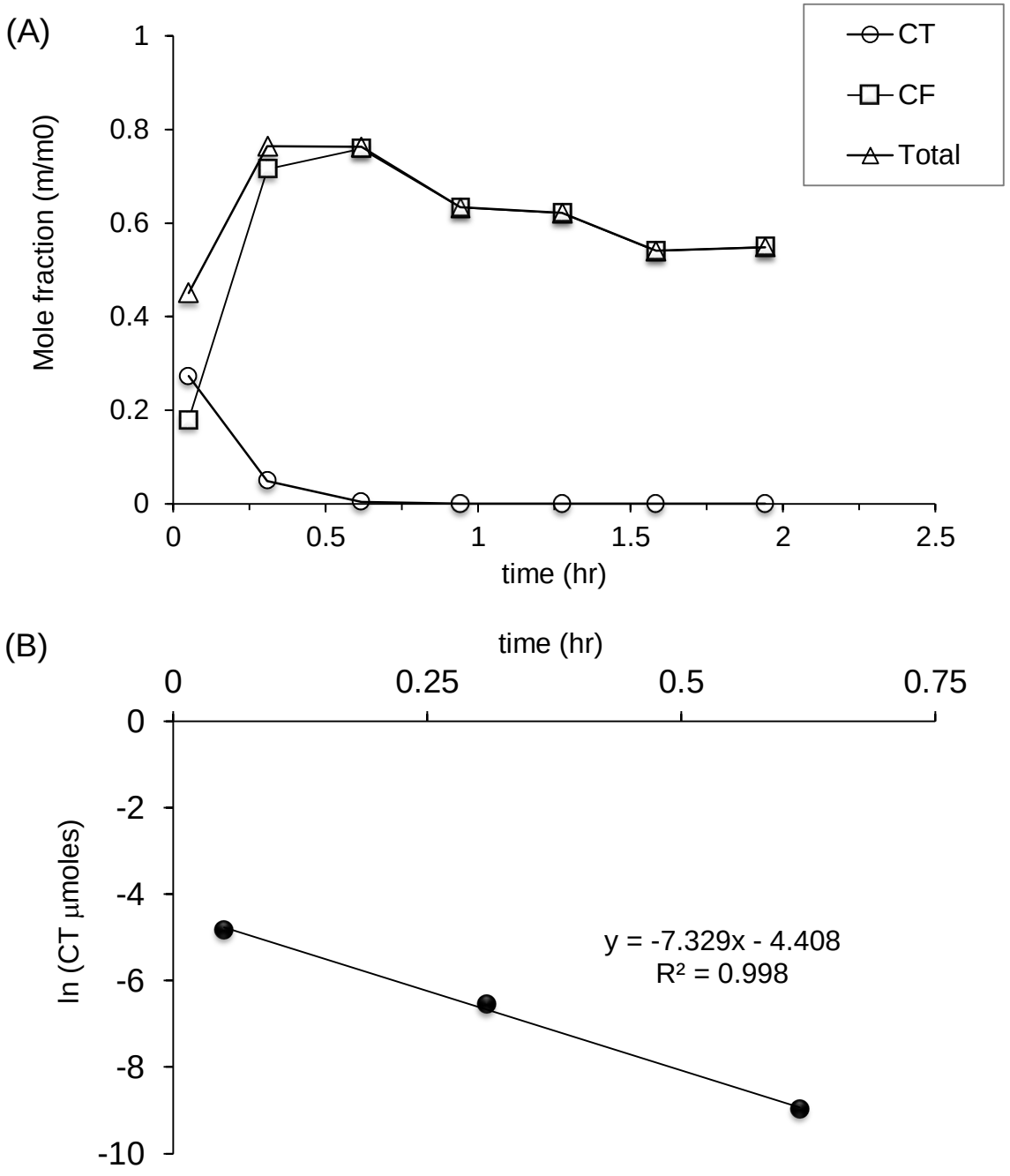

Figure 3.5: CT degradation with fresh 0.05 g/L nZVI modified with 2 wt. % sulfide prepared in 4 g/L CMC. Initial CT = 0.035 µmoles, or 54.45 µg/L (50 µL of 108.9 mg/L CT stock solution).CT degraded completely in 1 hour, with chloroform as the only reaction byproduct. (A) CT degradation and byproduct (mole fraction); (B) ln [CT] vs. time plot showing CT degradation rate constant.

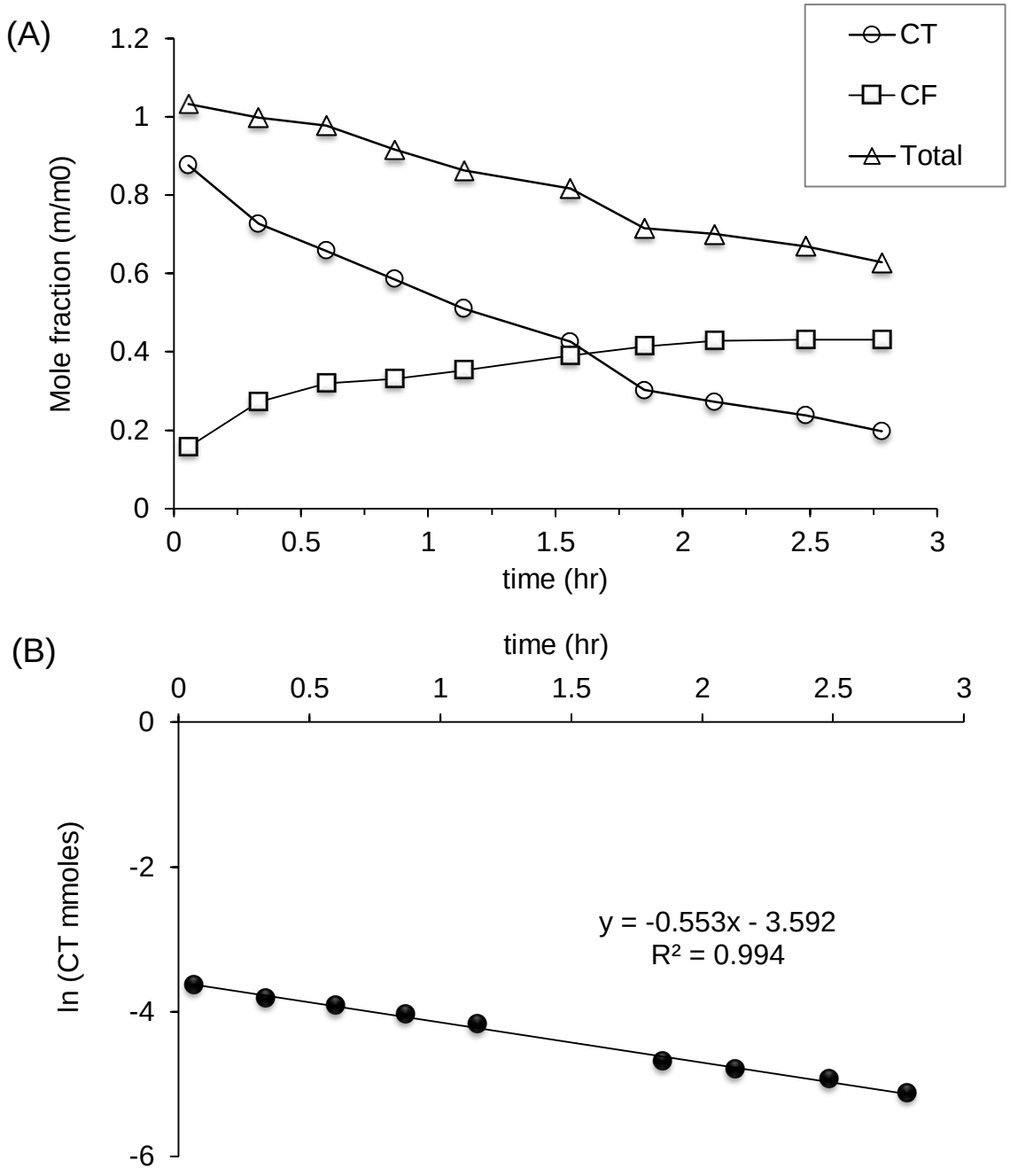

Figure 3.6: CT degradation with fresh 0.05 g/L nZVI modified with 3 wt. % sulfide prepared in 4 g/L CMC. Initial CT = 0.035 moles, or 54.45 g/L (50 μL of 108.9 mg/L CT stock solution). About 80% of CT degraded in 3 hours, with chloroform as the only reaction byproduct. (A) CT degradation and byproduct (mole fraction); (B) ln [CT] vs. time plot showing CT degradation rate constant

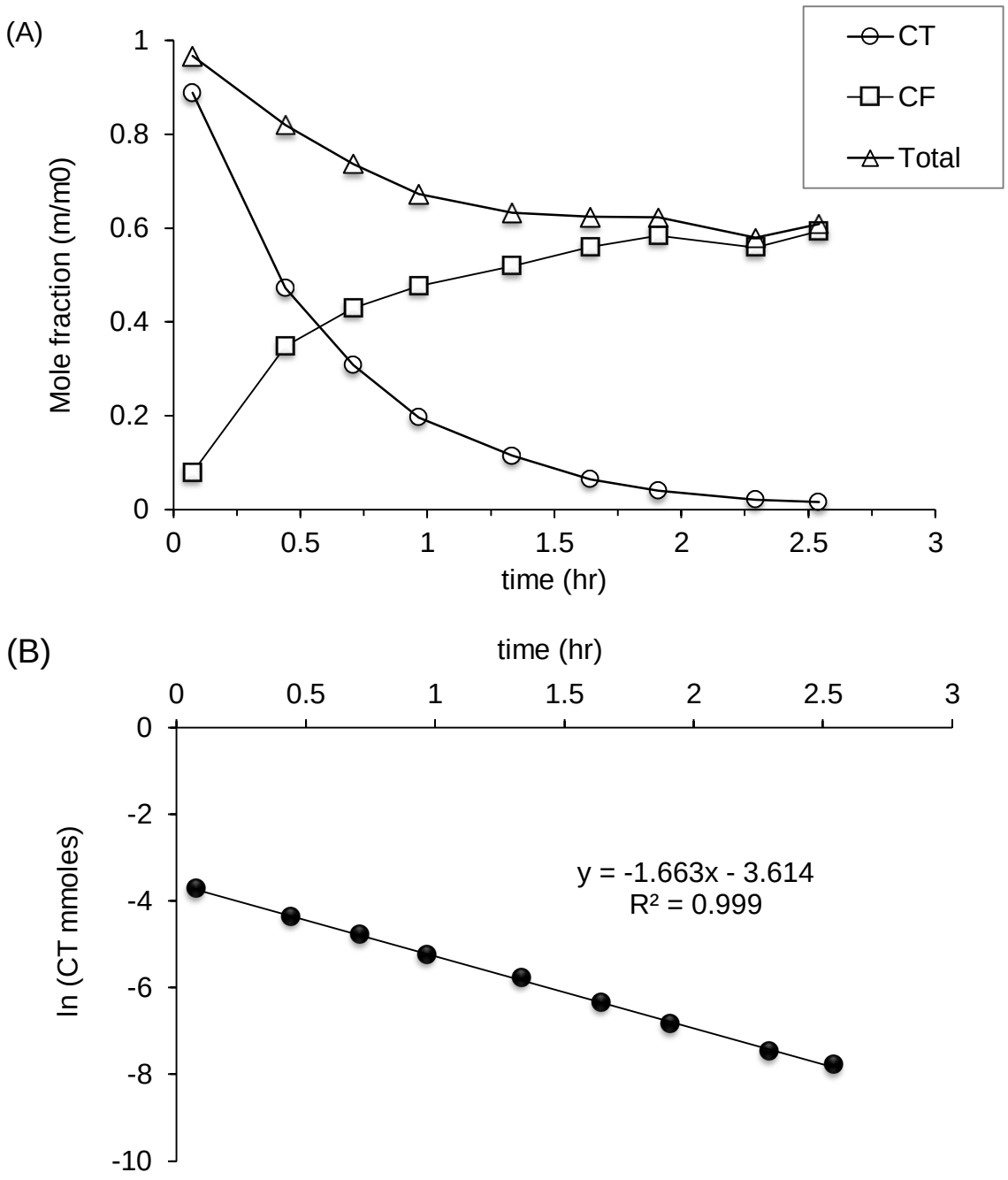

Figure 3.7: CT degradation with fresh 0.05 g/L nZVI modified with 4 wt. % sulfide prepared in 4 g/L CMC. Initial CT = 0.035 μmoles, or 54.45 μg/L (50 μL of 108.9 mg/L CT stock solution). CT degraded completely in 2.6 hours, with chloroform as the only reaction byproduct. (A) CT degradation and byproduct (mole fraction); (B) ln [CT] vs. time plot showing CT degradation rate constant.

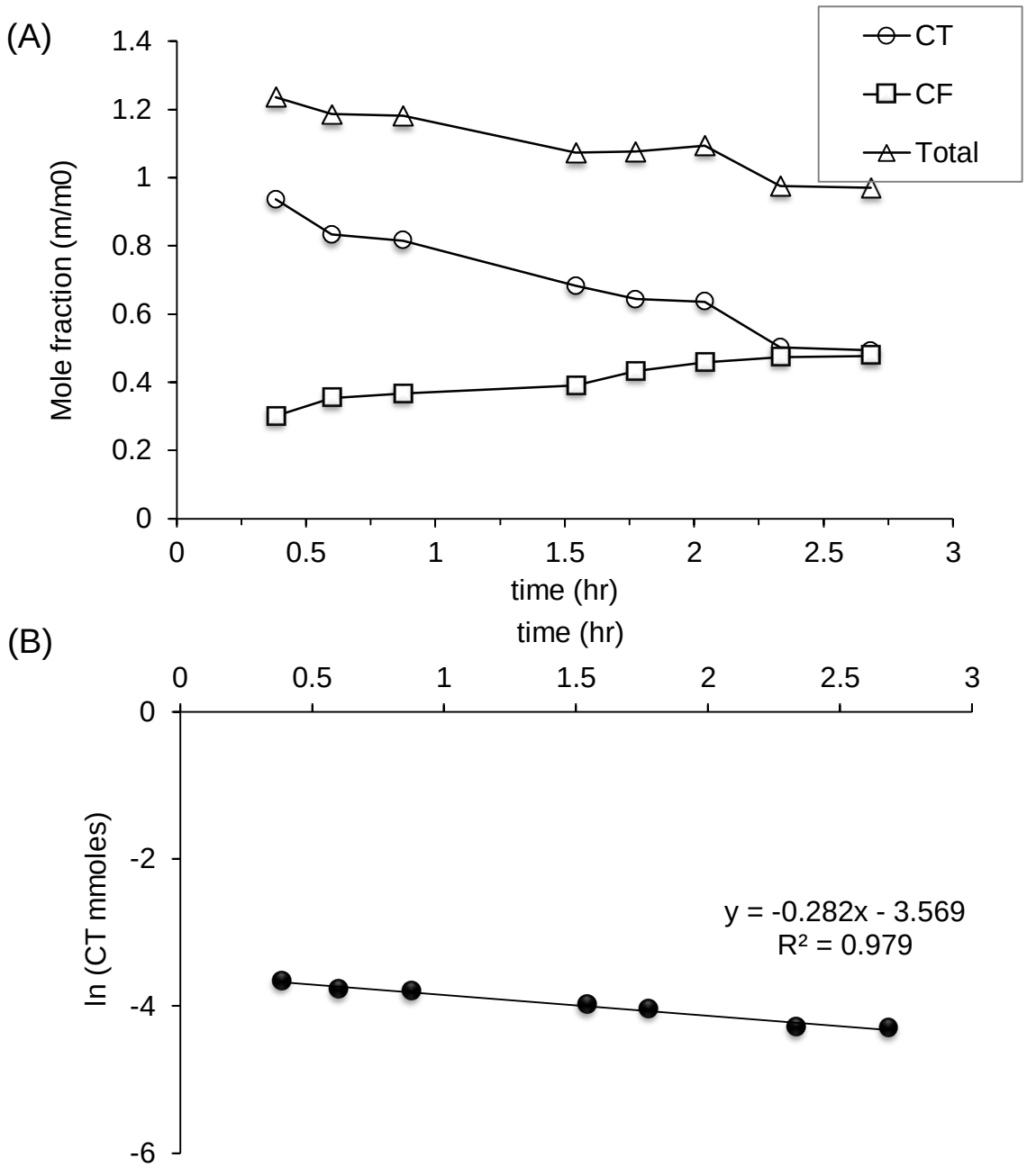

Figure 3.8: CT degradation with fresh 0.05 g/L nZVI modified with 5 wt. % sulfide prepared in 4 g/L CMC. Initial CT = 0.035 μmoles, or 54.45 μg/L (50 μL of 108.9 mg/L CT stock solution). About 50% CT degraded in 3 hours, with chloroform as the only reaction byproduct. (A) CT degradation and byproduct (mole fraction); (B) ln [CT] vs. time plot showing CT degradation rate constant.

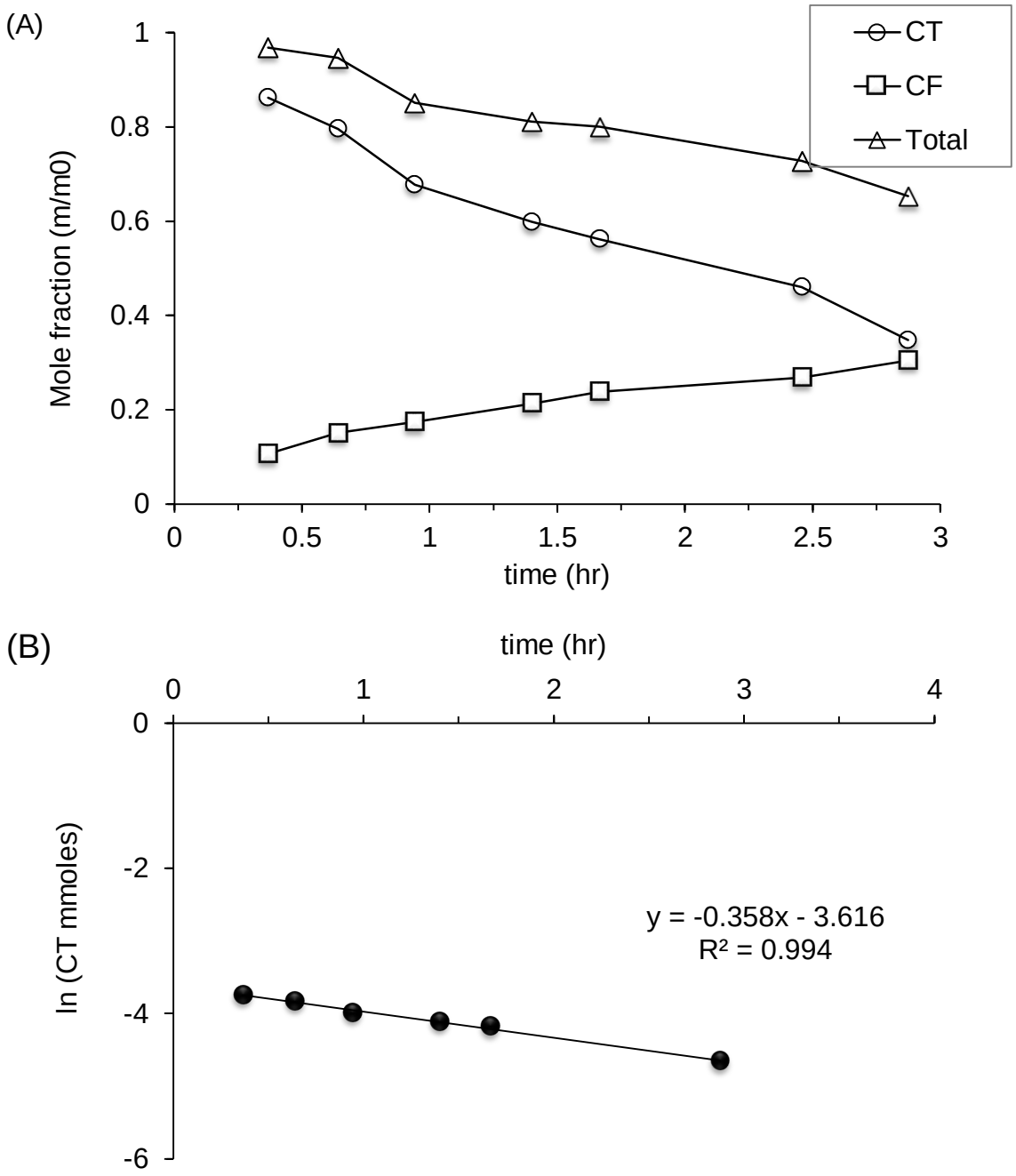

Figure 3.9: CT degradation with fresh 0.05 g/L nZVI modified with 6 wt. % sulfide prepared in 4 g/L CMC. Initial CT = 0.035 μmoles, or 54.45 μg/L (50 μL of 108.9 mg/L CT stock solution).About 70% CT degraded in 3 hours, with chloroform as the only reaction byproduct. (A) CT degradation and byproduct (mole fraction); (B) ln [CT] vs. time plot showing CT degradation rate constant.

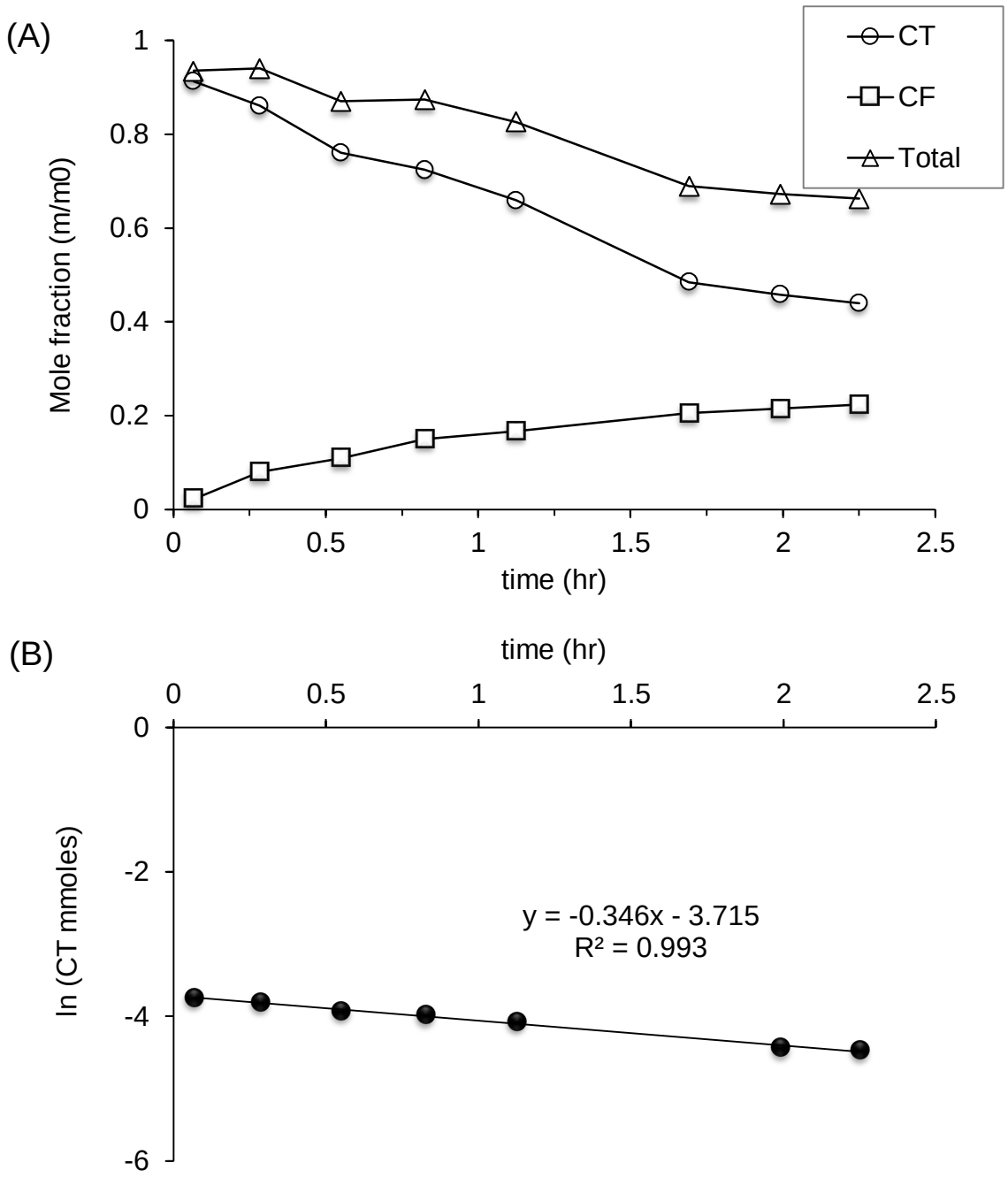

Figure 3.10: CT degradation with fresh 0.05 g/L nZVI modified with 8 wt. % sulfide prepared in 4 g/L CMC. Initial CT = 0.035 μmoles, or 54.45 μg/L (50 μL of 108.9 mg/L CT stock solution).About 60% CT degraded in 2.2 hours, with chloroform as the only reaction byproduct. . (A) CT degradation and byproduct (mole fraction); (B) ln [CT] vs. time plot showing CT degradation rate constant.

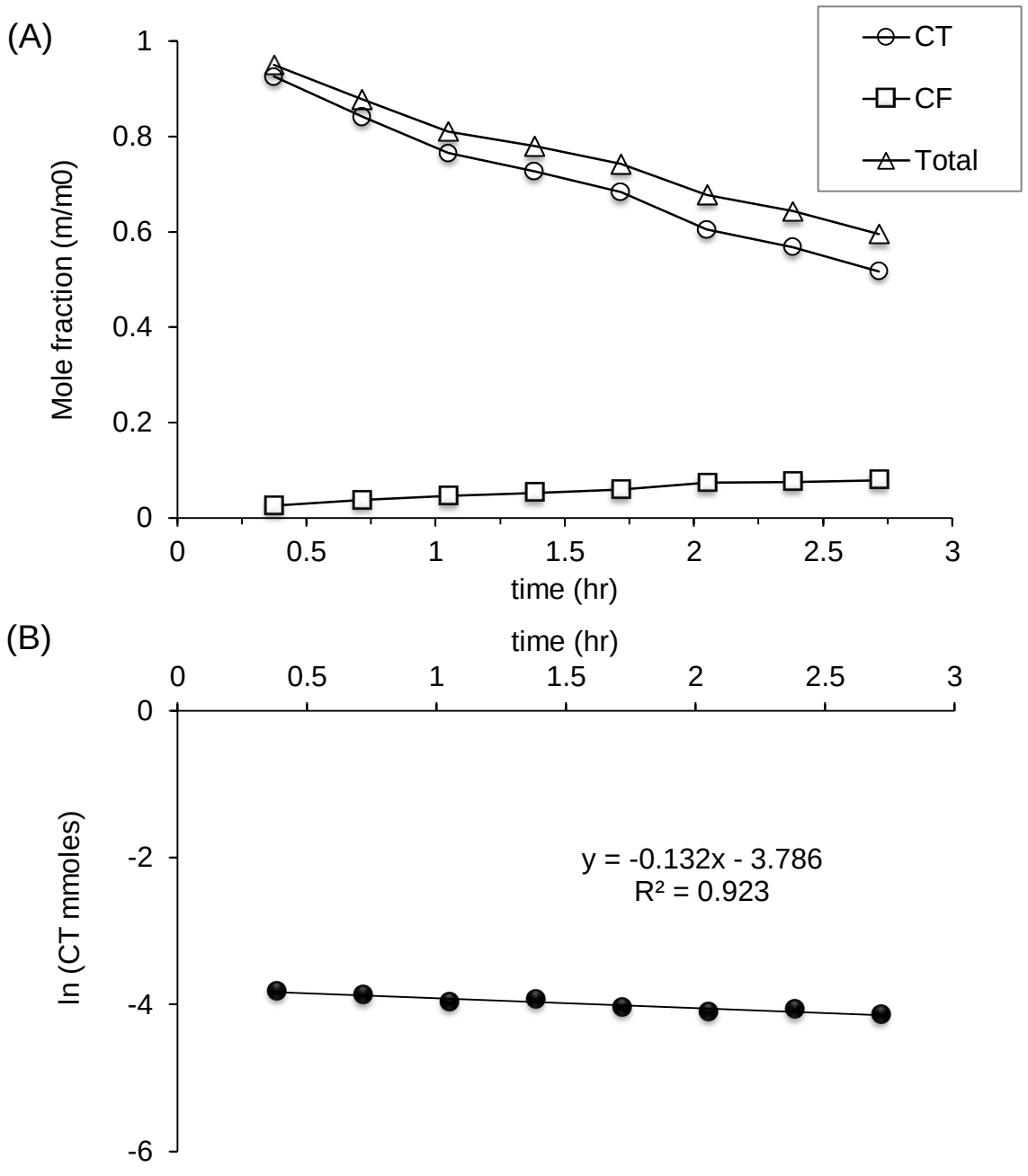

Figure 3.11: CT degradation with fresh 0.05 g/L nZVI modified with 10 wt. % sulfide prepared in 4 g/L CMC. Initial CT = 0.035 μmoles, or 54.45 μg/L (50 μL of 108.9 mg/L CT stock solution).About 50% CT degraded in 3 hours, with chloroform as the only reaction byproduct. (A) CT degradation and byproduct (mole fraction); (B) ln [CT] vs. time plot showing CT degradation rate constant.

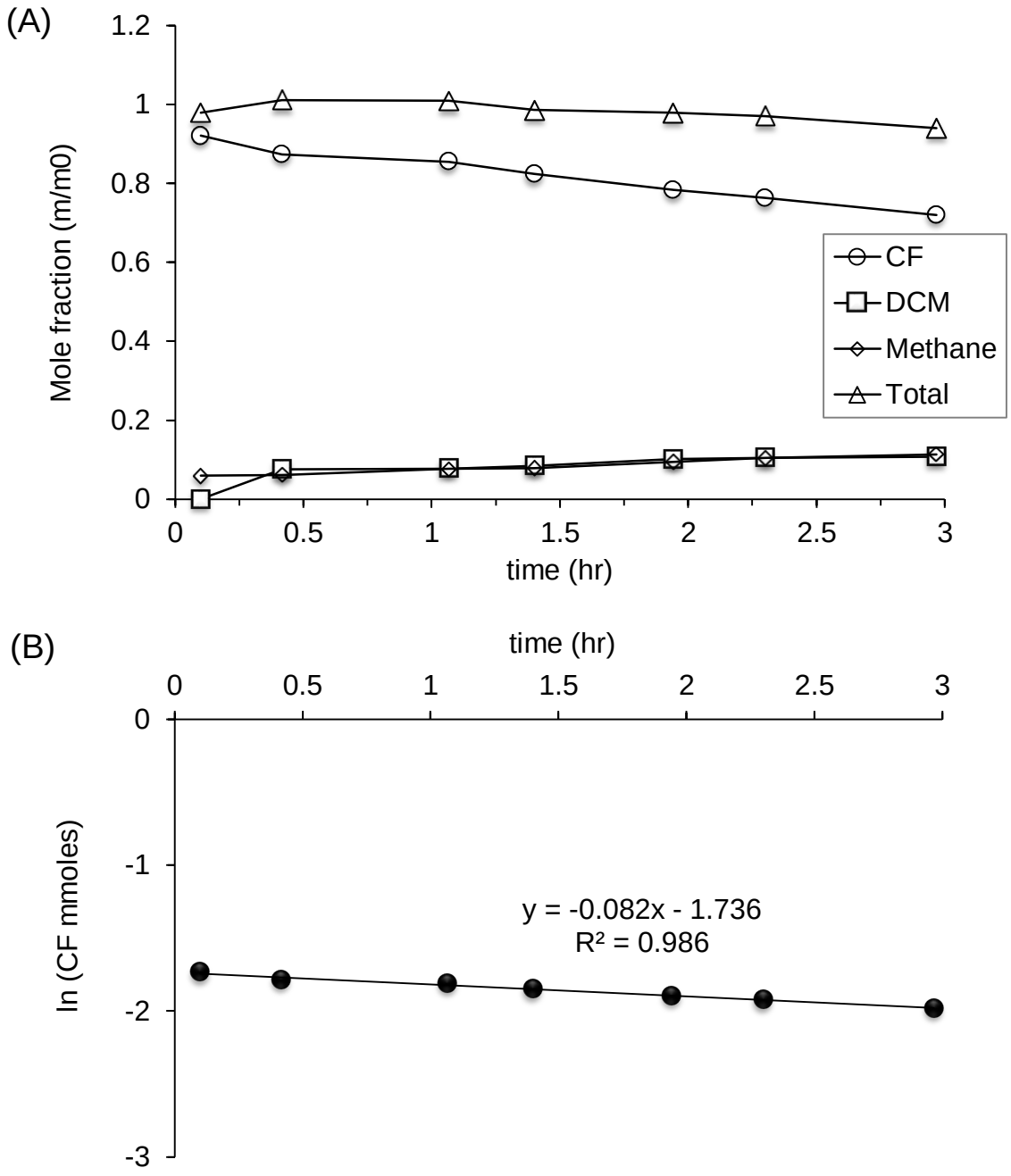

Figure 3.12: CF degradation with fresh 0.1 g/L nZVI prepared in 4 g/L CMC. Initial CF = 0.097 μmoles, or 110.58 μg/L (50 μL of 233.12 mg/L CF stock solution). About 28 % of CF degraded in 3 hours, with DCM and Methane as byproducts. (A) CF degradation and byproduct (mole fraction); (B) ln [CF] vs. time plot showing CT degradation rate constant.

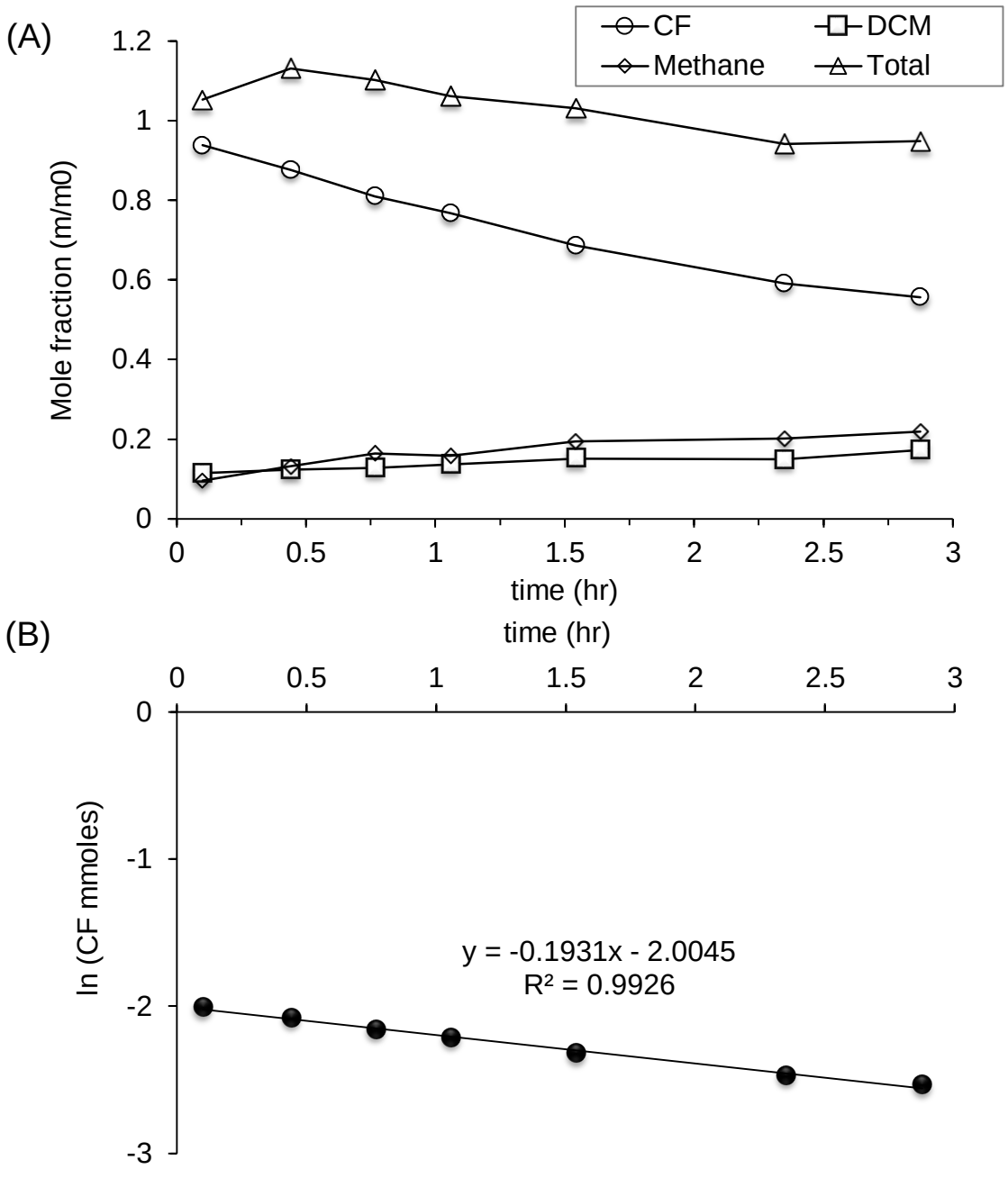

Figure 3.13: CF degradation with fresh 0.1 g/L nZVI modified with 1 wt. % sulfide prepared in 4g/L CMC. Initial CF = 0.097 μmoles, or 110.58 μg/L (50 μL of 233.12 mg/L CF stock solution). About 36 % of CF degraded in 3 hours, with DCM and Methane as byproducts. (A) CF degradation and byproduct (mole fraction); (B) ln [CF] vs. time plot showing CT degradation rate constant.

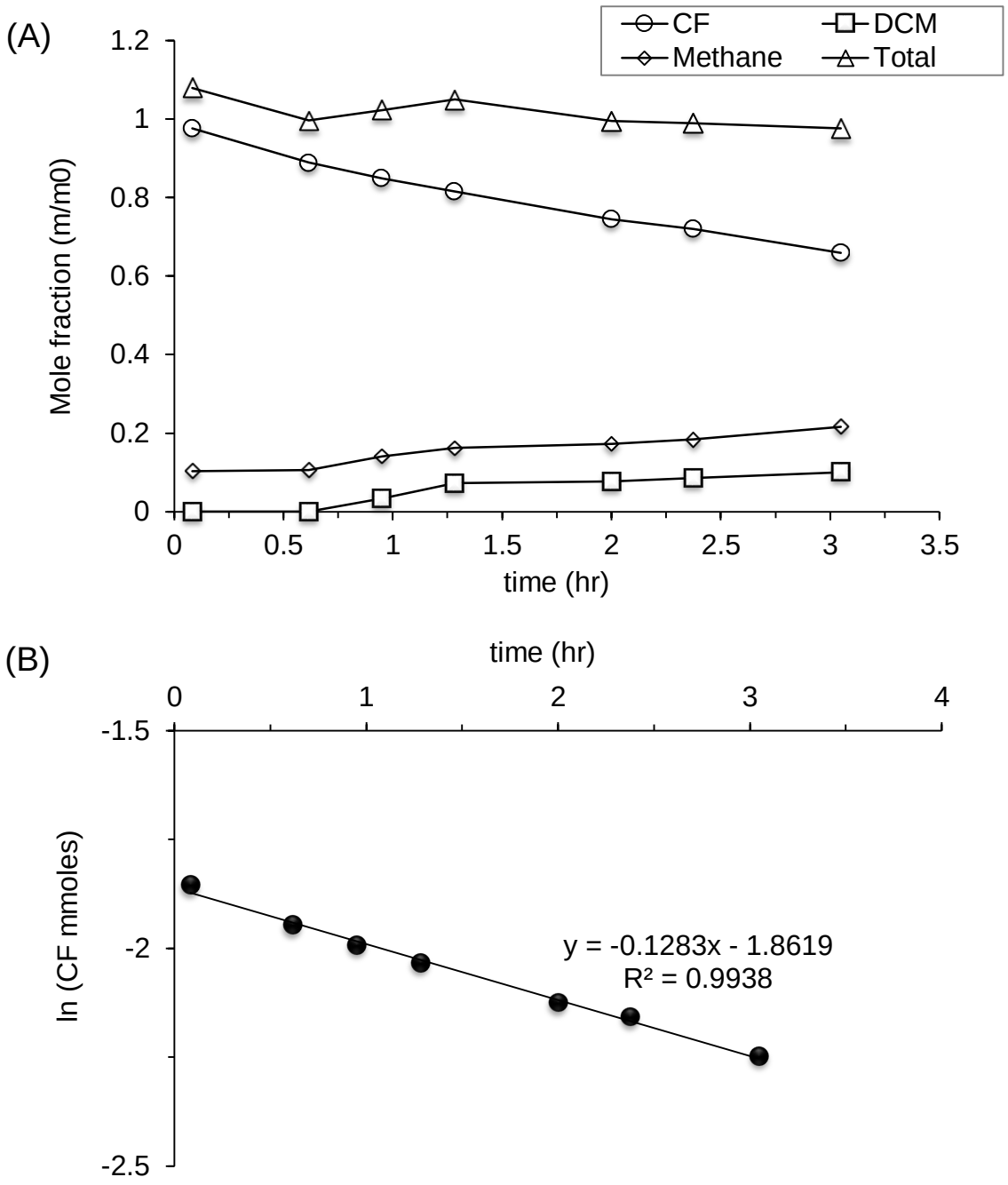

Figure 3.14: CF degradation with fresh 0.1 g/L nZVI modified with 0.5 wt. % sulfide prepared in 4g/L CMC. Initial CF = 0.097 μmoles, or 110.58 μg/L (50 μL of 233.12 mg/L CF stock solution). About 35 % of CF degraded in 3 hours, with DCM and Methane as byproducts. (A) CF degradation and byproduct (mole fraction); (B) ln [CF] vs. time plot showing CT degradation rate constant.

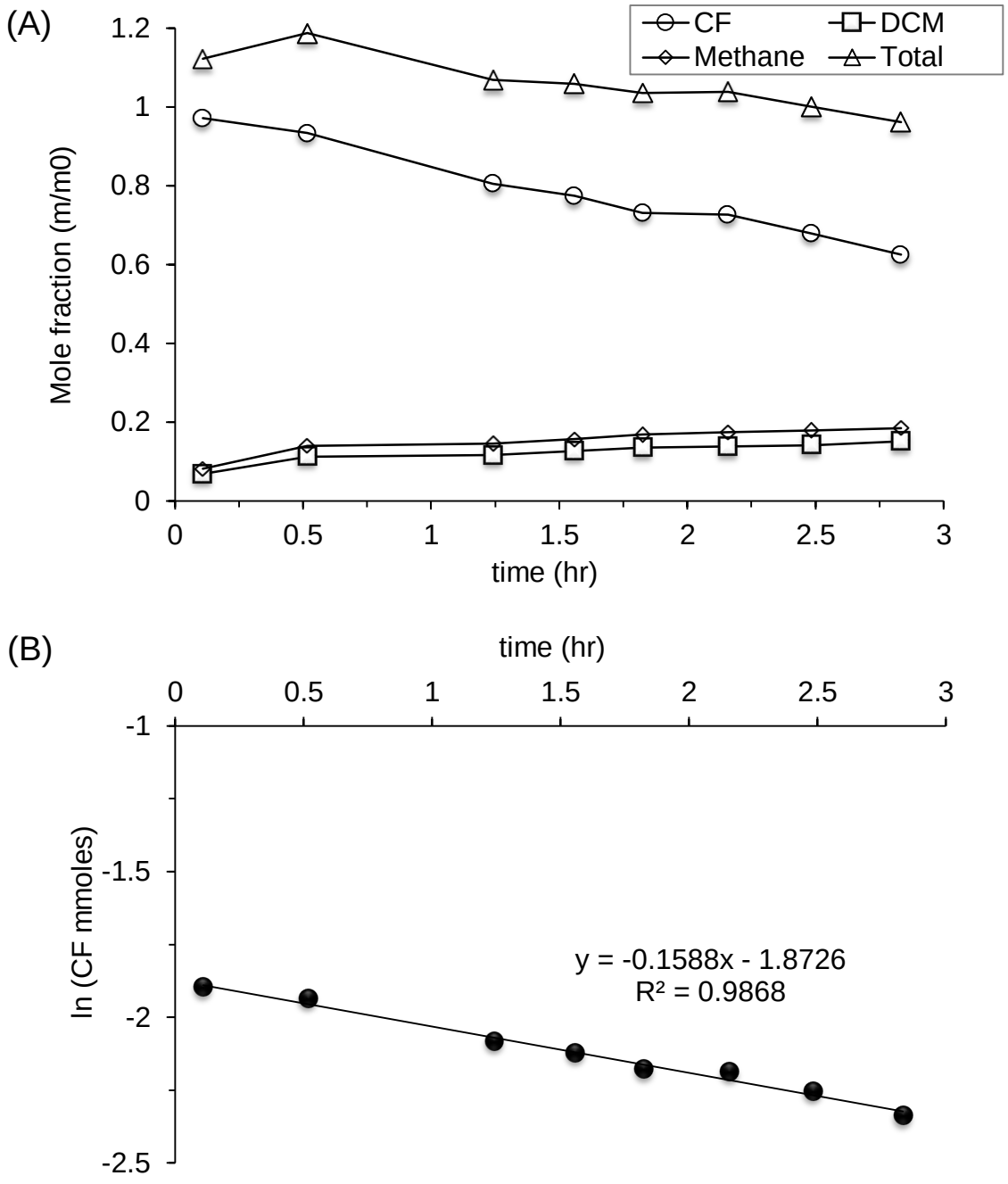

Figure 3.15: CF degradation with fresh0.1 g/L nZVI modified with 1.5 wt. % sulfide prepared in 4g/L CMC. Initial CF = 0.097 μmoles, or 110.58 μg/L (50 μL of 233.12 mg/L CF stock solution). About 37 % of CF degraded in 3 hours, with DCM and Methane as byproducts. (A) CF degradation and byproduct (mole fraction); (B) ln [CF] vs. time plot showing CT degradation rate constant.

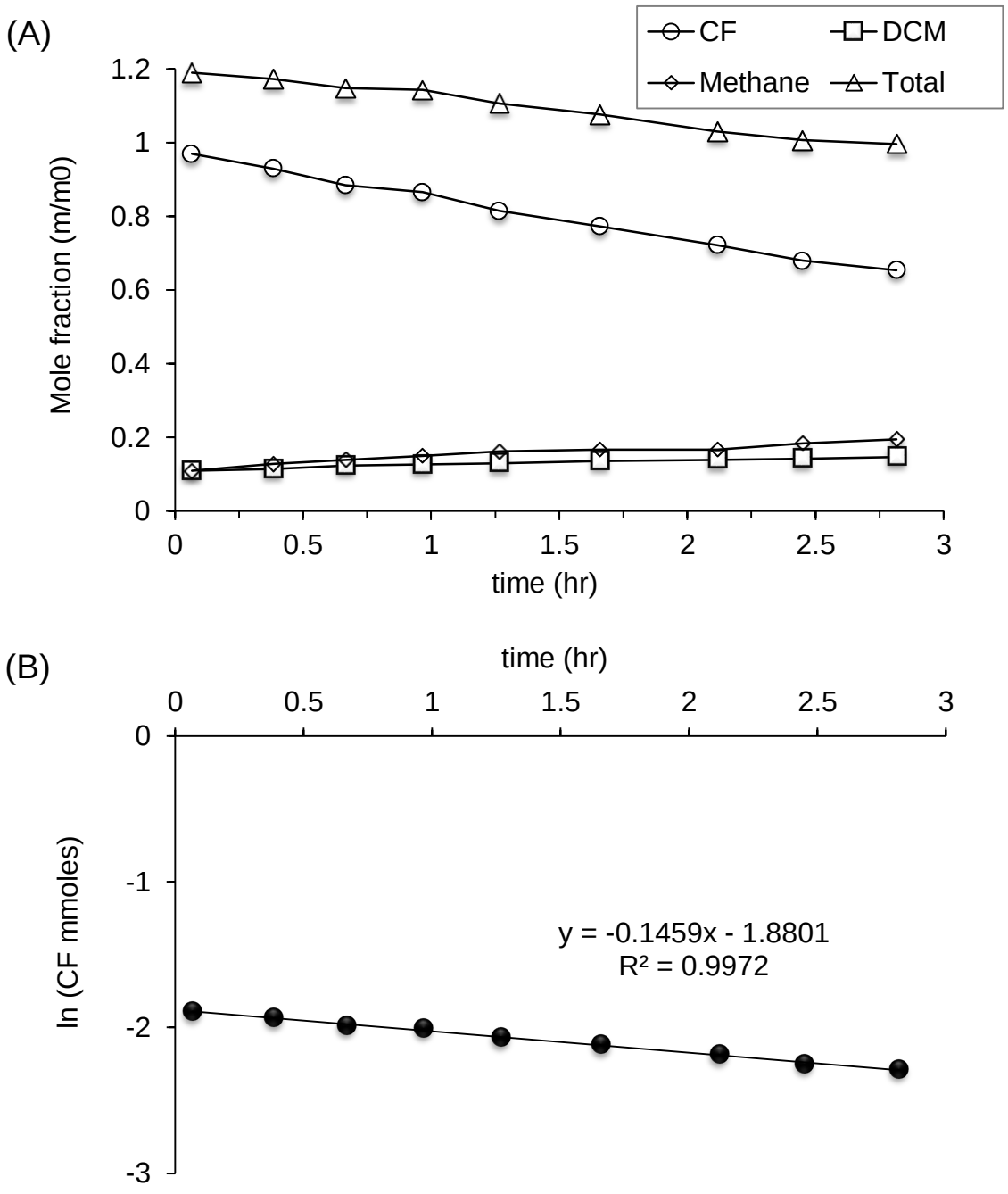

Figure 3.16: CF degradation with fresh0.1 g/L nZVI modified with 2 wt. % sulfide prepared in 4g/L CMC. Initial CF = 0.097 μmoles, or 110.58 μg/L (50 μL of 233.12 mg/L CF stock solution). About 35 % of CF degraded in 3 hours, with DCM and Methane as byproducts. (A) CF degradation and byproduct (mole fraction); (B) ln [CF] vs. time plot showing CT degradation rate constant.

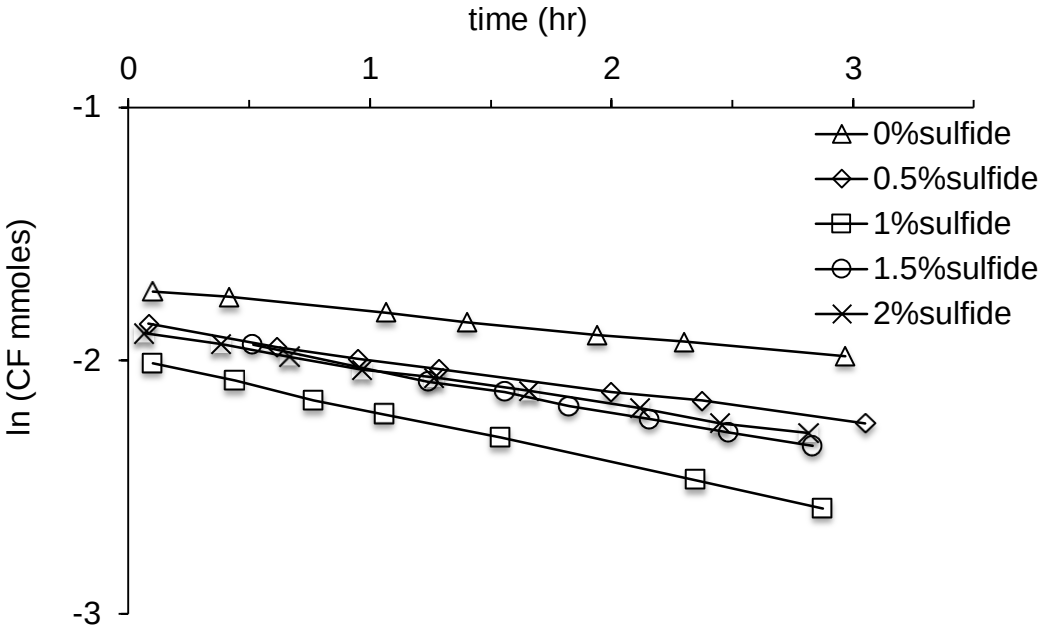

Figure 3.17: CF degradation with fresh0.1 g/L nZVI prepared in 4g/L CMC and modified at varied sulfide loading. Initial CF = 0.097 μmoles, or 110.58 μg/L (50 μL of 233.12 mg/L CF stock solution).

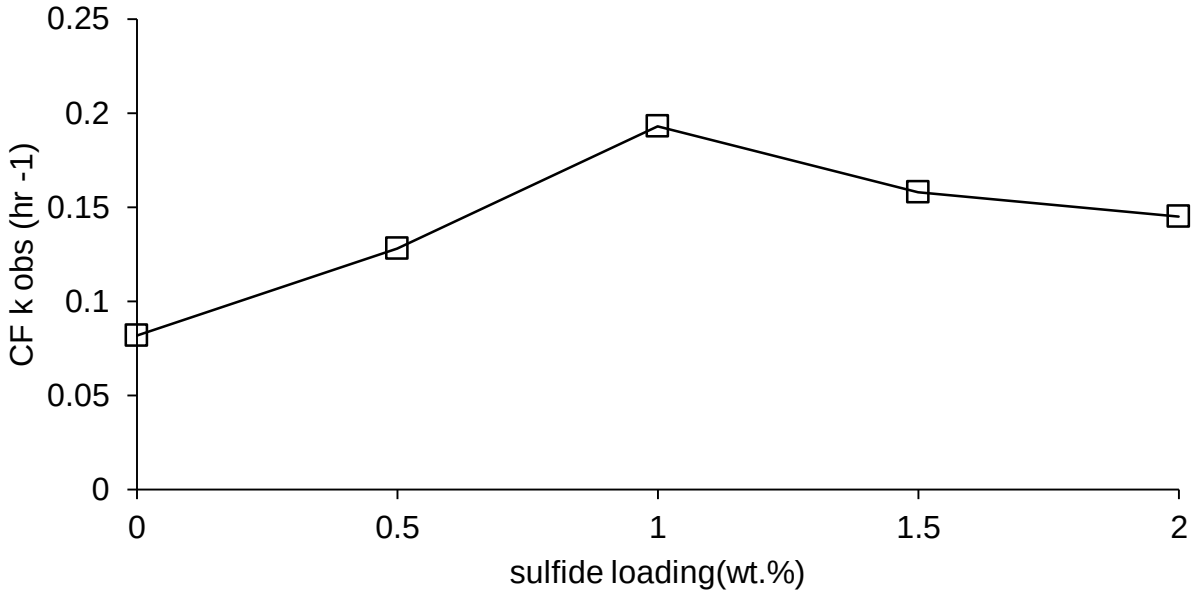

Figure 3.18: Comparison of CF degradation kinetics (k_{obs} values) with fresh 0.1 g/L nZVI and different sulfide loading prepared in 4g/L CMC. Initial CF = 0.097 μmoles, or 110.58 μg/L (50 μL of 233.12 mg/L CF stock solution).

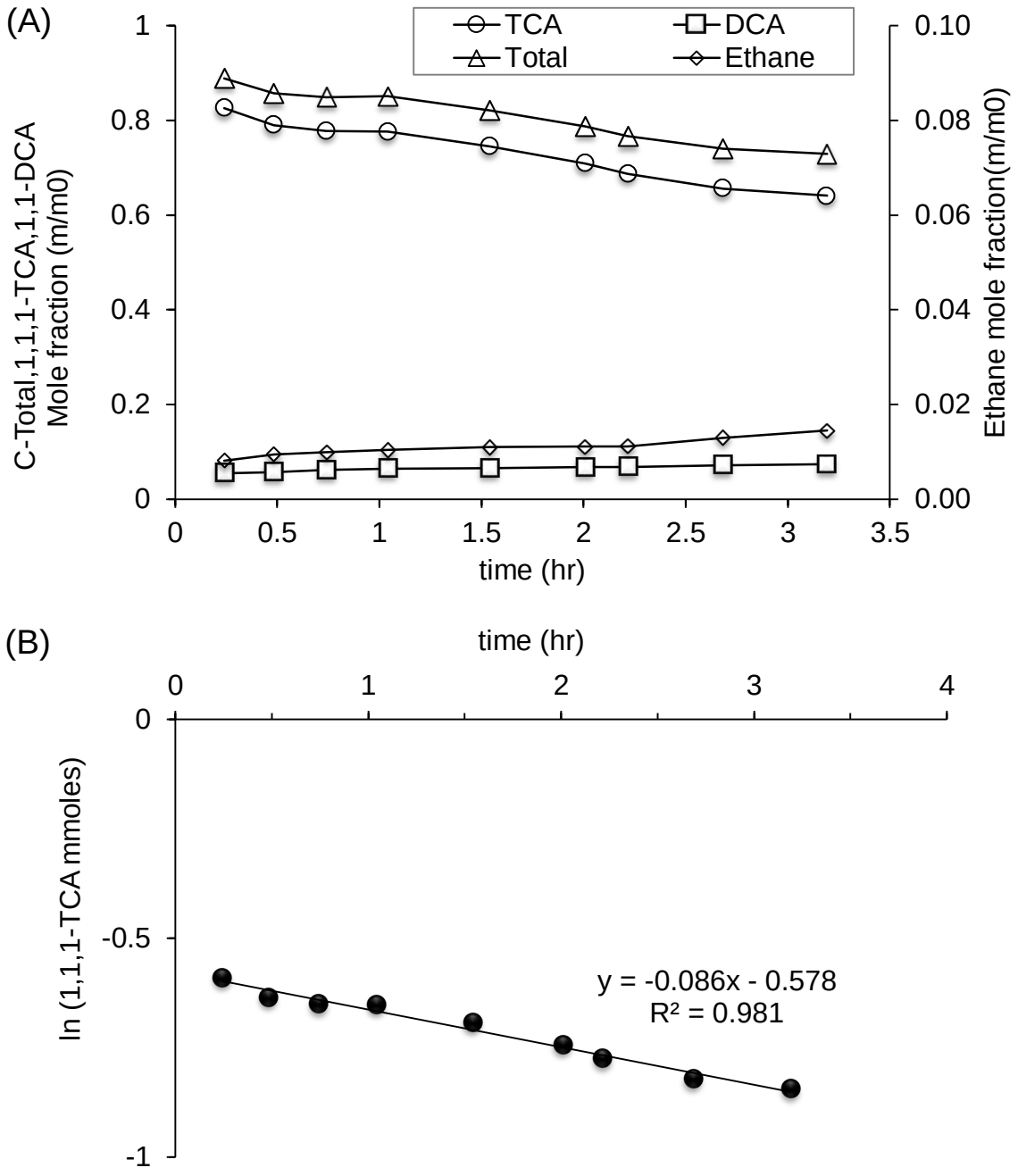

Figure 3.19: 1,1,1-TCA degradation with fresh 0.1 g/L nZVI prepared in 4 g/L CMC. Initial 1,1,1-TCA = 0.077 μmoles, or 103 μg/L (50 μL of 206.25 mg/L 1,1,1-TCA stock solution). About 36% of 1, 1, 1-TCA degraded in 3 hours, with Ethane, Ethene and 1,1-DCA as reaction byproducts. (A) 1,1,1-TCA degradation and byproduct (mole fraction); (B) ln[1,1,1-TCA] vs. time plot showing 1,1,1-TCA degradation rate constant.

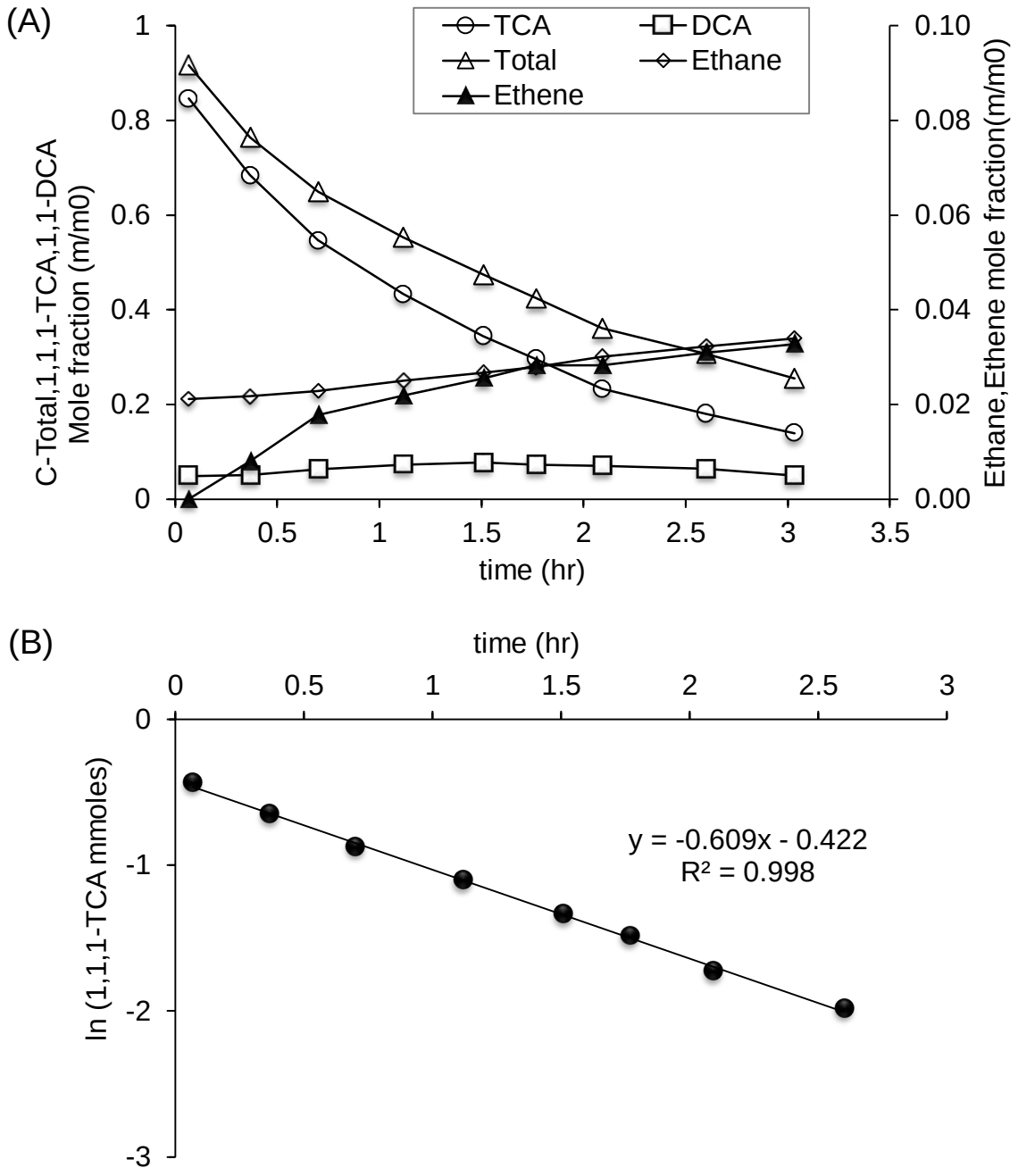

Figure 3.20: 1,1,1-TCA degradation with fresh 0.1 g/L nZVI modified with 1 wt.% sulfide prepared in 4 g/L CMC. Initial 1,1,1-TCA = 0.077 μmoles, or 103 μg/L (50 μL of 206.25 mg/L 1,1,1-TCA stock solution). About 87% of 1,1,1-TCA degraded in 3 hours, with Ethane, Ethene and 1,1-DCA as reaction byproducts. (A) 1,1,1-TCA degradation and byproduct (mole fraction); (B) ln[1,1,1-TCA] vs. time plot showing 1,1,1-TCA degradation rate constant.

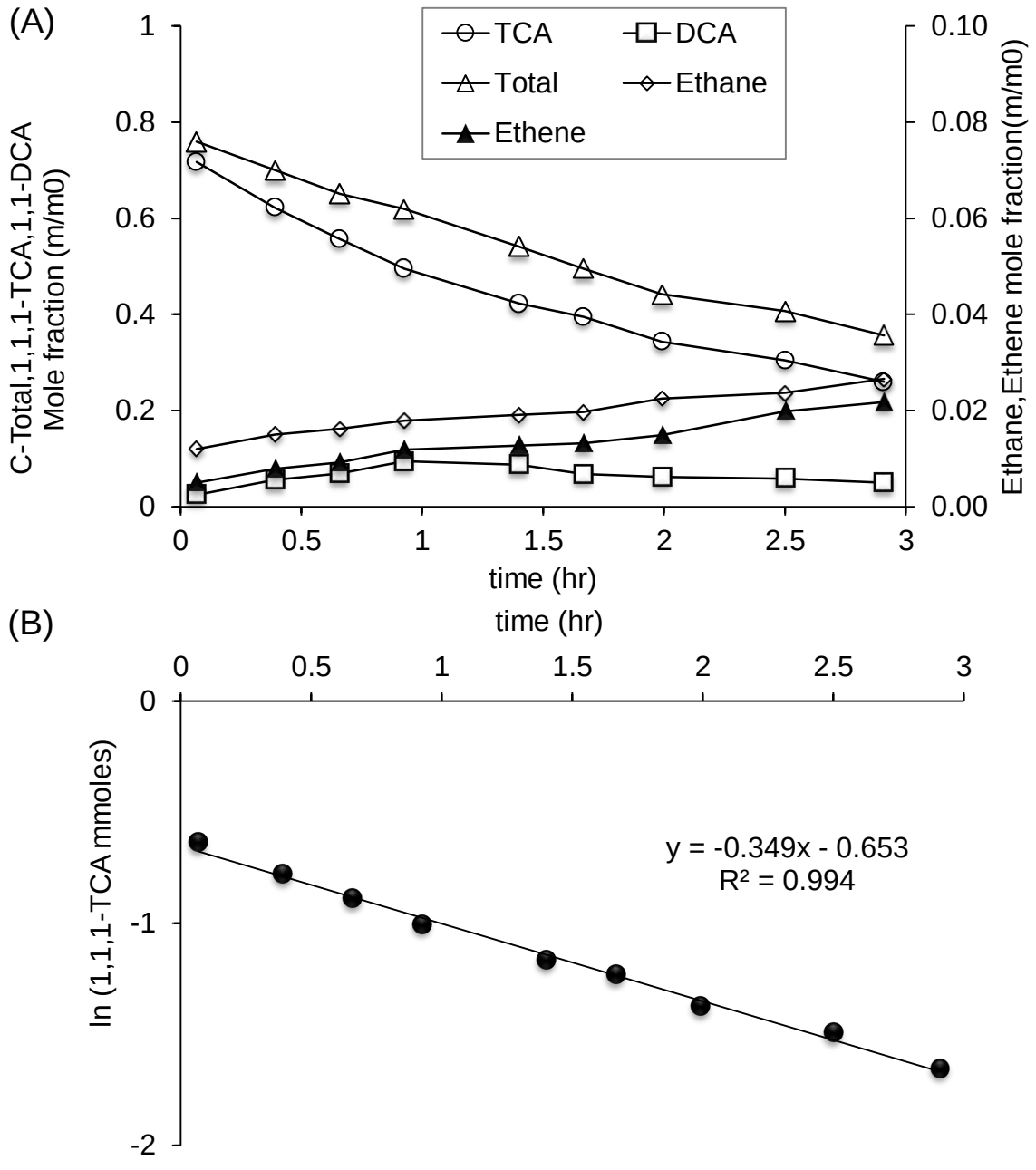

Figure 3.21: 1,1,1-TCA degradation with fresh 0.1 g/L nZVI modified with 0.5 wt.% sulfide prepared in 4 g/L CMC. Initial 1,1,1-TCA = 0.077 μmoles, or 103 μg/L (50 μL of 206.25 mg/L 1,1,1-TCA stock solution). About 74% of 1,1,1-TCA degraded in 3 hours, with Ethane , Ethene and 1,1-DCA as reaction byproducts. (A) 1,1,1-TCA degradation and byproduct (mole fraction); (B) ln[1,1,1-TCA] vs. time plot showing 1,1,1-TCA degradation rate constant.

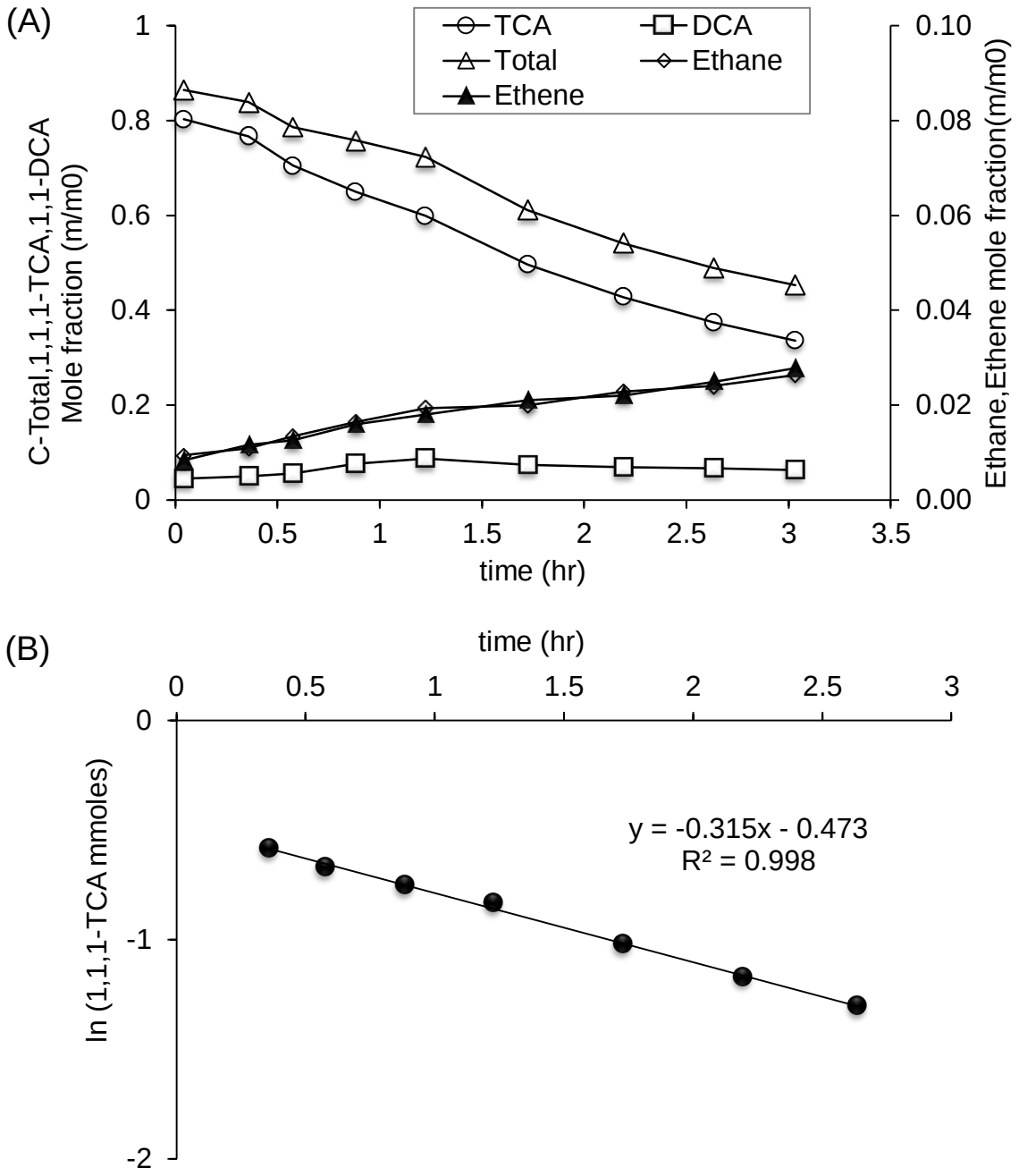

Figure 3.22: 1,1,1-TCA degradation with fresh 0.1 g/L nZVI modified with 1.5 wt.% sulfide prepared in 4 g/L CMC. Initial 1,1,1-TCA = 0.077 μmoles, or 103 μg/L (50 μL of 206.25 mg/L 1,1,1-TCA stock solution). About 67% of 1,1,1-TCA degraded in 3 hours, with ethane, ethene and 1,1-DCA as reaction byproducts. (A) 1,1,1-TCA degradation and byproduct (mole fraction); (B) ln[1,1,1-TCA] vs. time plot showing 1,1,1-TCA degradation rate constant.

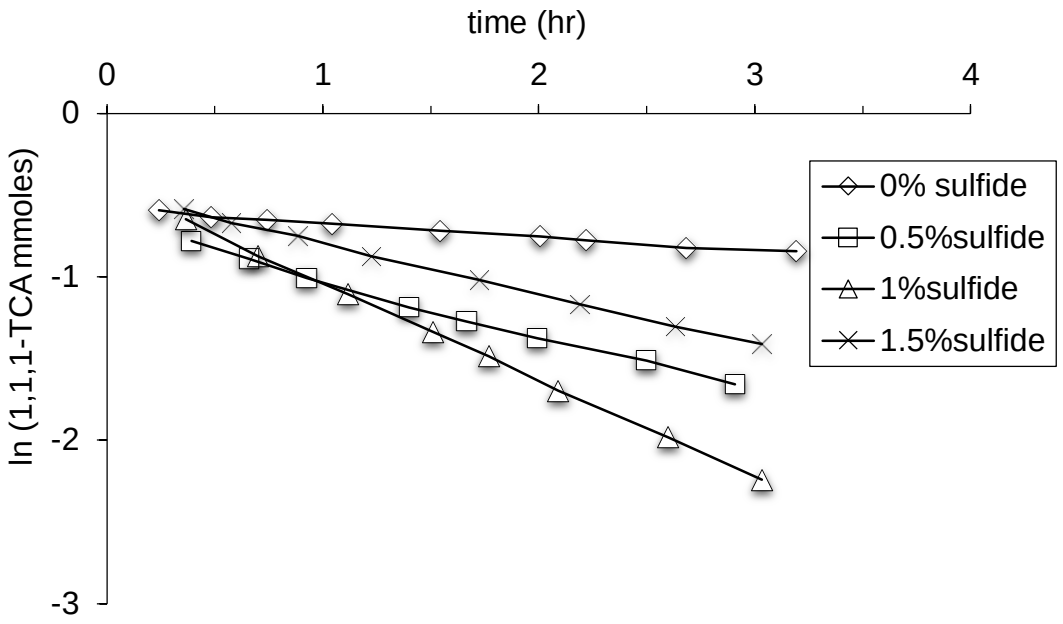

Figure 3.23: 1,1,1-TCA degradation with fresh 0.1 g/L nZVI prepared in 4 g/L CMC and modified with varied sulfide loading. Initial 1,1,1-TCA = 0.077 μmoles, or 103 μg/L (50 μL of 206.25 mg/L 1,1,1-TCA stock solution).

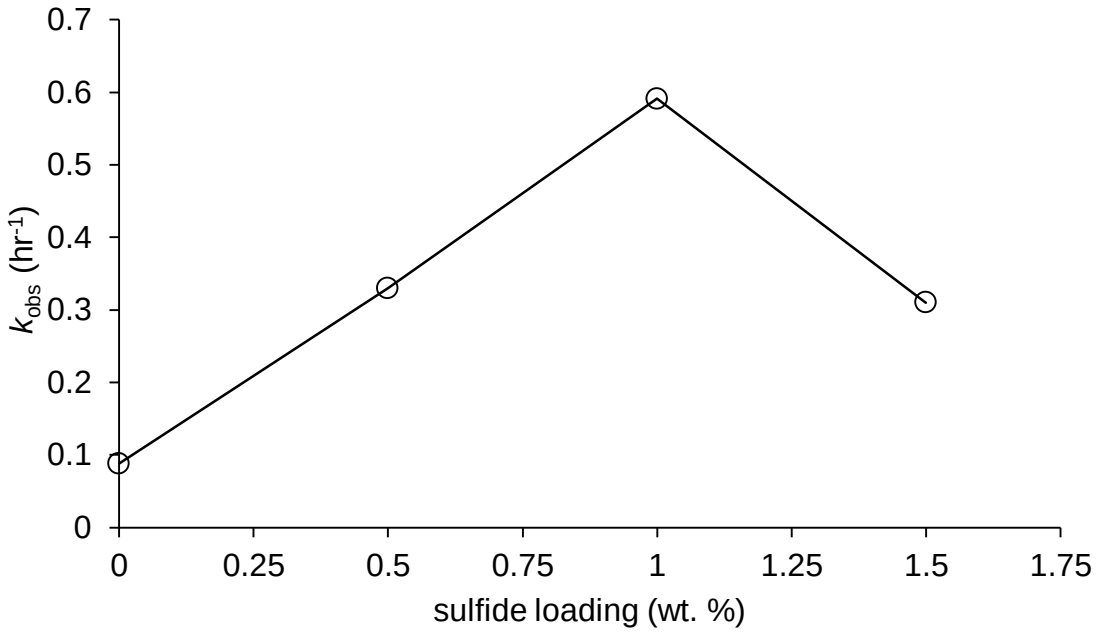

Figure 3.24: Comparison of 1,1,1-TCA degradation kinetics (k_{obs} values) with fresh 0.1 g/L nZVI prepared in 4g/L CMC and modified with different sulfide loading. Initial 1,1,1-TCA = 0.077 μmoles, or 103 μg/L (50 μL of 206.25 mg/L 1,1,1-TCA stock solution.

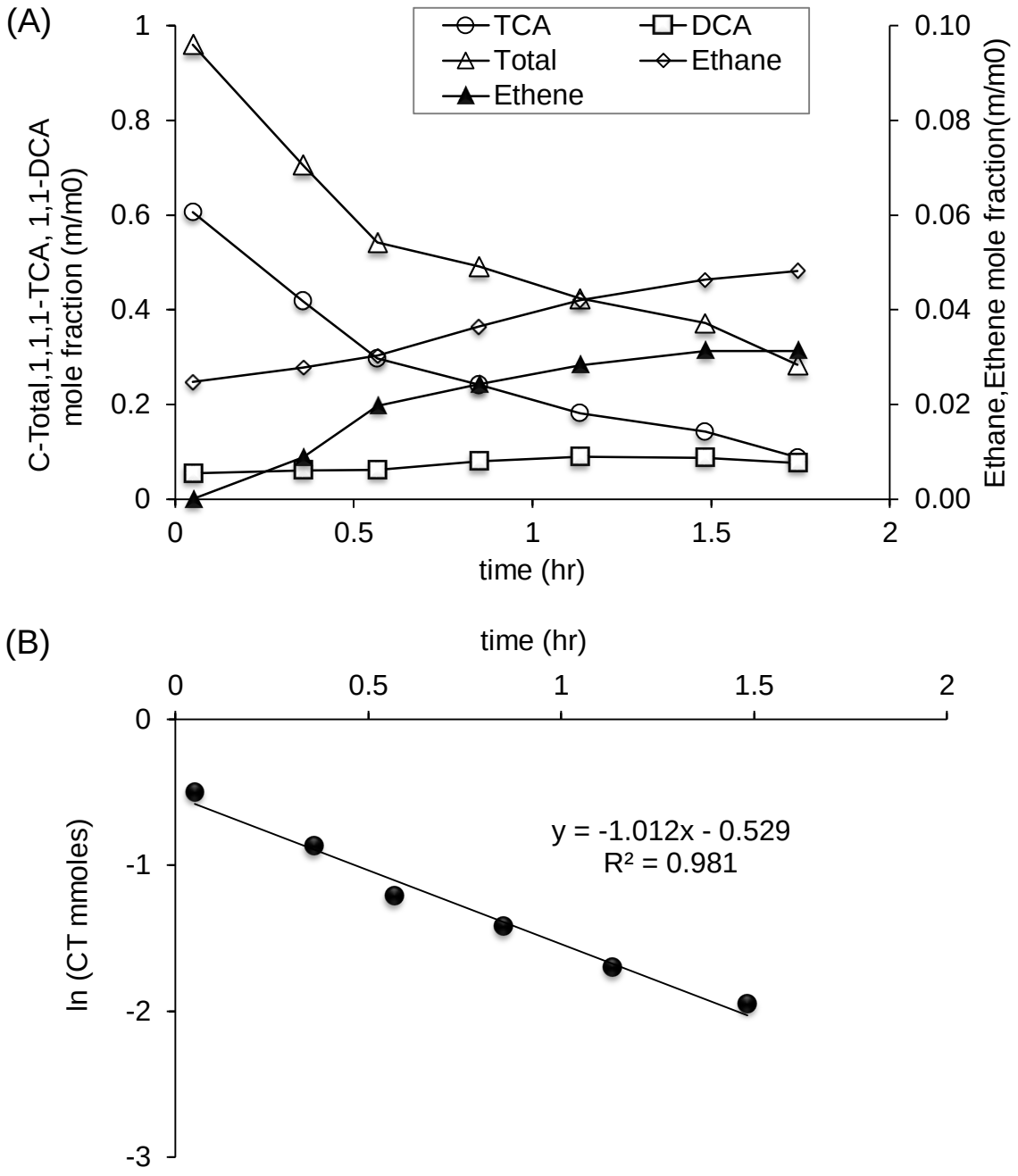

Figure 3.25: : 1,1,1-TCA degradation with fresh 0.5 g/L nZVI prepared in 4 g/L CMC and modified with 1 wt.% sulfide. Initial 1,1,1-TCA = 0.077 μmoles, or 103 μg/L (50 μL of 206.25 mg/L 1,1,1-TCA stock solution). About 89% of 1,1,1-TCA degraded in 3 hours, with ethane, ethene and 1,1-DCA as reaction byproducts. (A) 1,1,1-TCA degradation and byproduct (mole fraction); (B) ln[1,1,1-TCA] vs. time plot showing 1,1,1-TCA degradation rate constant.

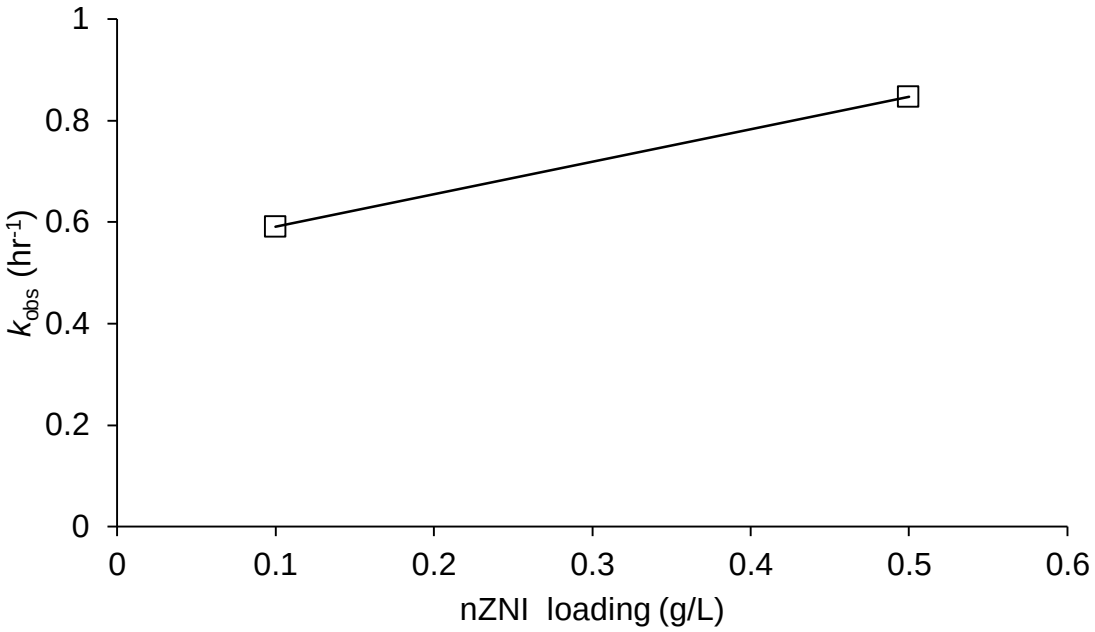

Figure 3.26: Comparison of 1,1,1-TCA degradation kinetics (k_{obs} values) for 2 different fresh nZVI concentrations prepared in 4 g/L CMC and modified with 1 wt% sulfide. Initial 1,1,1-TCA = 0.077 μmoles, or 103 μg/L (50 μL of 206.25 mg/L 1,1,1-TCA stock solution.

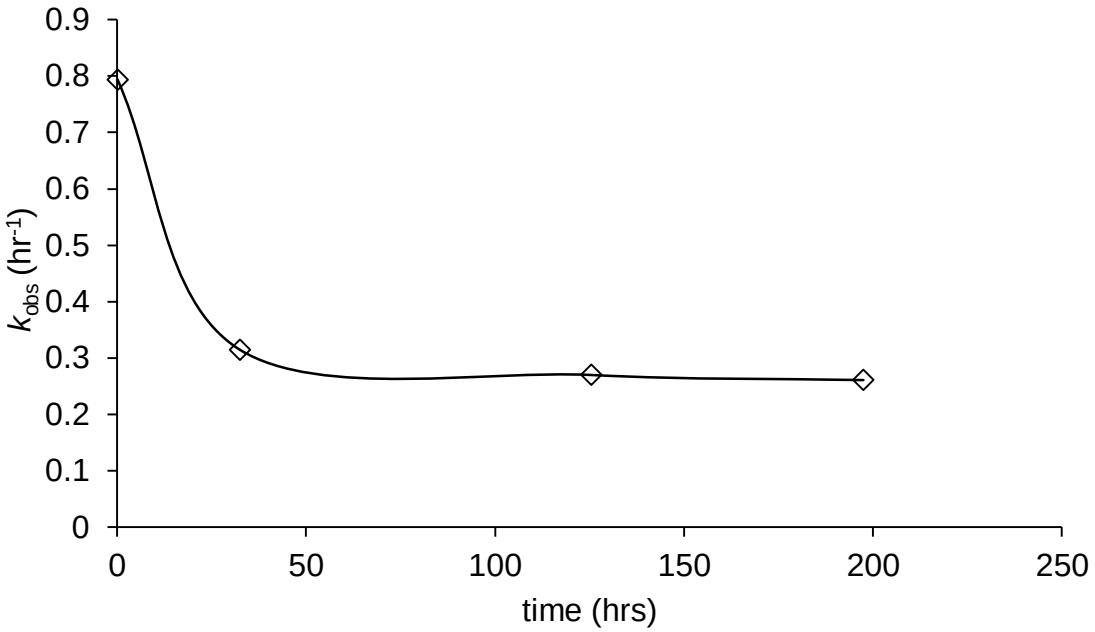

Figure 3.27: 1,1,1-TCA degradation by aged 0.5 g/L nZVI prepared in 4 g/L CMC modified with 1 wt.% sulfide. Initial 1,1,1-TCA = 0.077 μmoles, or 103 μg/L (50 μL of 206.25 mg/L 1,1,1-TCA stock solution). The variation in 1,1,1-TCA k_{obs} appears to show a power function decline in nZVI/FeS reactivity with time.

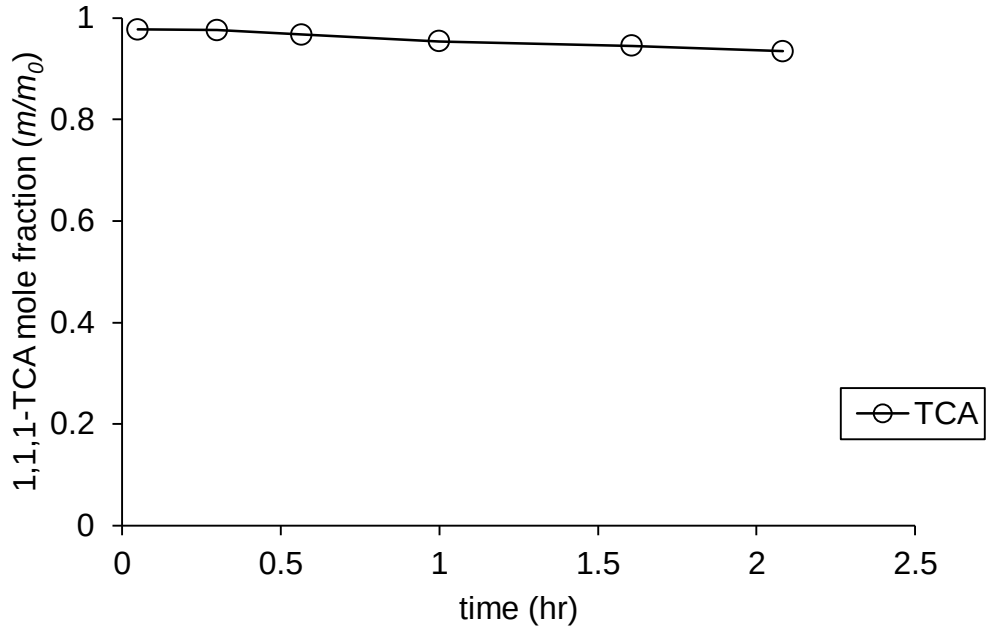

Figure 3.28: 1,1,1-TCA degradation with fresh unstable 0.5 g/L nZVI modified with 1 wt.% sulfide. Initial 1,1,1-TCA = 0.077 μmoles, or 103 μg/L (50 μL of 206.25 mg/L 1,1,1-TCA stock solution). About 7% of 1,1,1-TCA degraded in 2 hours, with no byproduct.

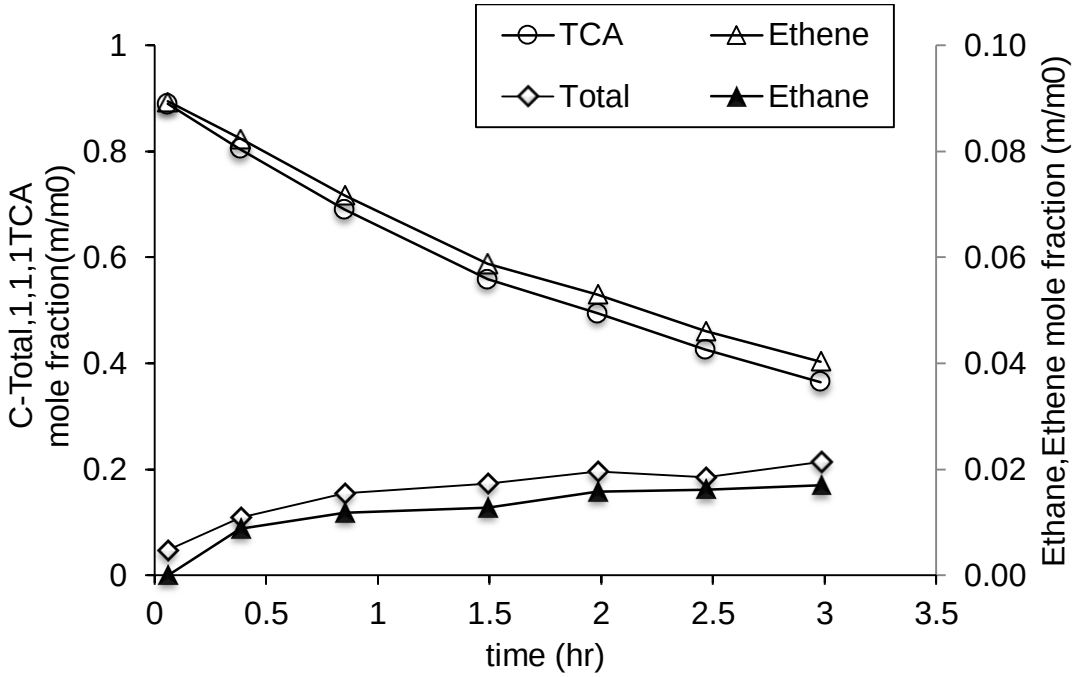

Figure 3.29: 1,1,1-TCA degradation with fresh 0.5 g/L nZVI prepared in 0.4 g/L CMC and modified with 1 wt.% sulfide. Initial 1,1,1-TCA = 0.077 μmoles, or 103 μg/L (50 μL of 206.25 mg/L 1,1,1-TCA stock solution). About 74% of 1,1,1-TCA degraded in 3 hours, with ethane and ethene as reaction byproducts.

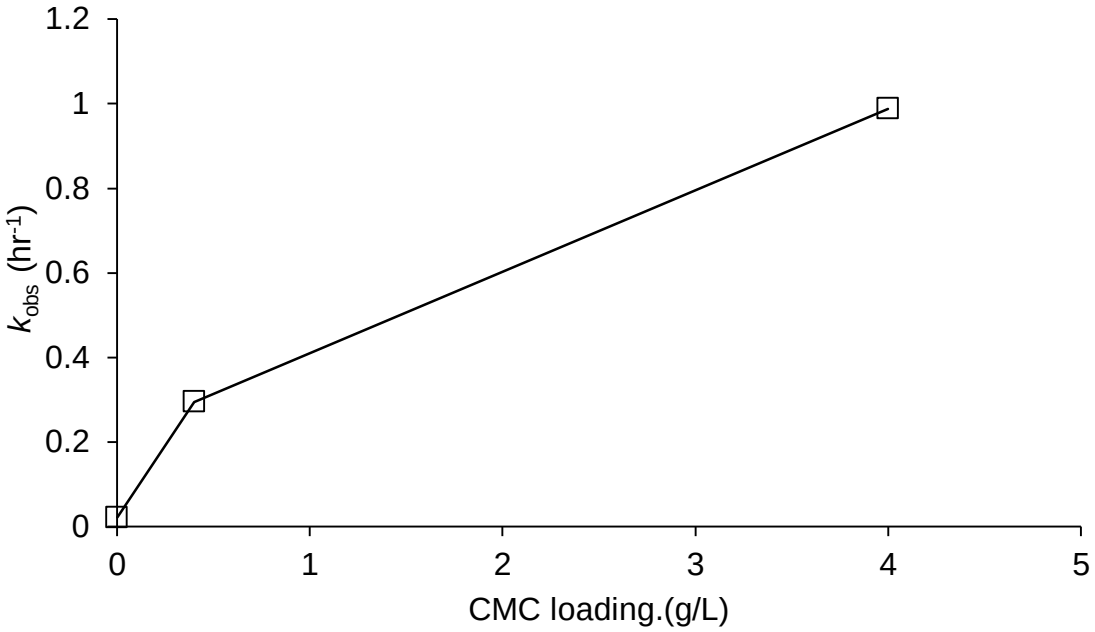

Figure 3.30: Comparison of 1,1,1-TCA degradation kinetics (k_{obs} values) with fresh 0.5 g/L nZVI prepared at 0, 0.4, and 4 g/L CMC loading and modified with 1 wt% sulfide. Initial 1,1,1-TCA = 0.077 μmoles, or 103 μg/L (50 μL of 206.25 mg/L 1,1,1-TCA stock solution).

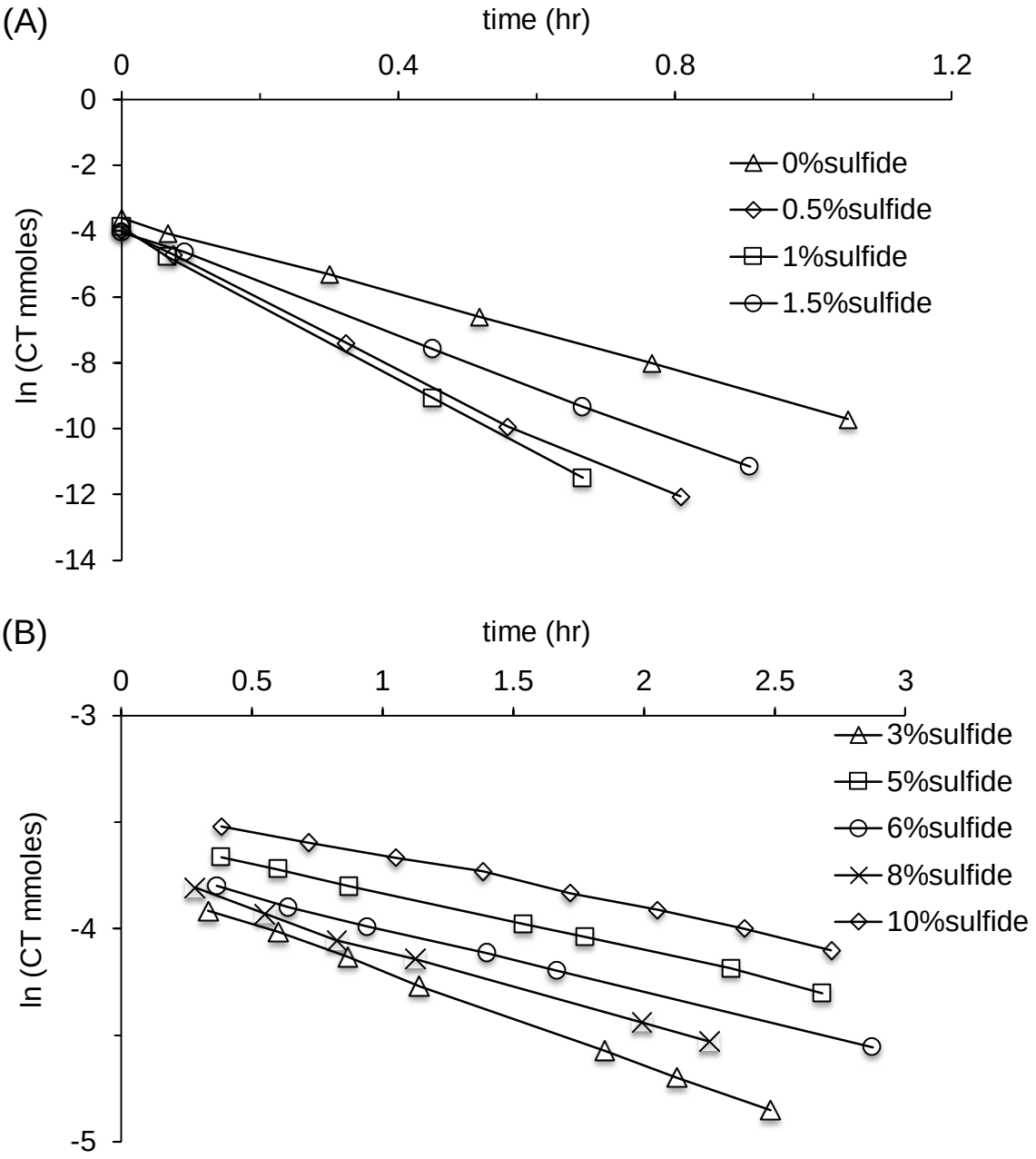

Figure 3.31: CT degradation (ln [CT] vs. time) with fresh 0.05 g/L nZVI prepared in 4 g/L CMC and modified at varied sulfide loading. Initial CT = 0.035 μmoles, or 54.45 μg/L (50 μL of 108.9 mg/L CT stock solution). (A) CT degradation at 0-1.5 wt. % sulfide loading; (B) CT degradation at 3-10 wt. % sulfide loading.

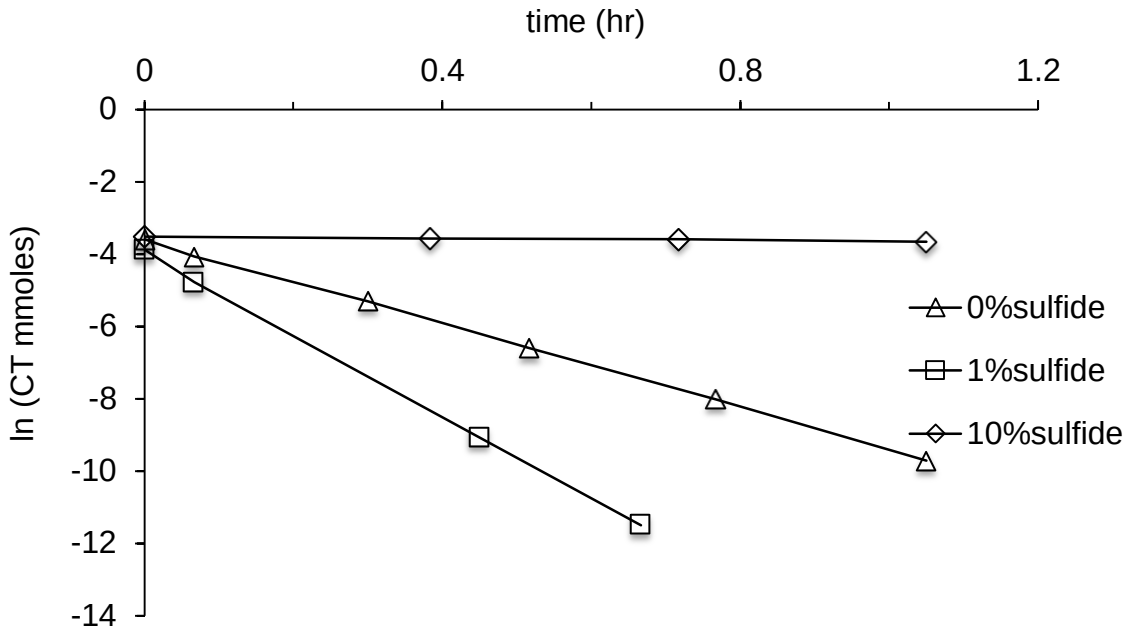

Figure 3.32: Comparison of CT degradation with fresh 0.05 g/L nZVI and different sulfide loading prepared in 4 g/L CMC. Initial CT = 0.035 μmoles, or 54.45 μg/L (50 μL of 108.9 mg/L CT stock solution.

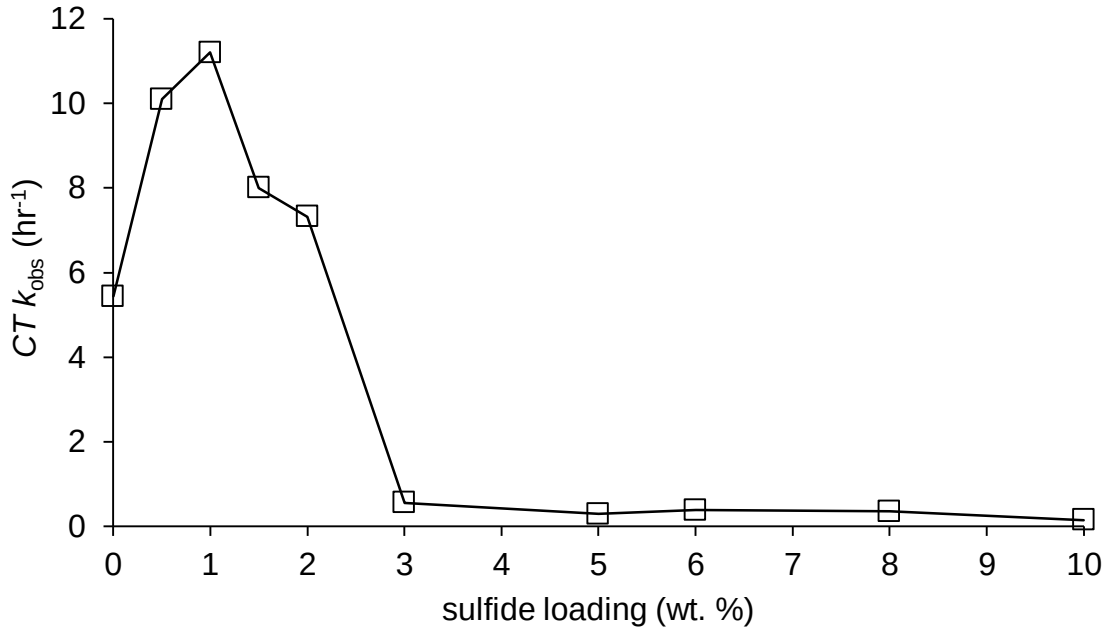

Figure 3.33: Comparison of CT degradation kinetics (k_{obs} values) with fresh 0.05 g/L nZVI and different sulfide loading prepared in 4 g/L CMC. Initial CT = 0.035 μmoles, or 54.45 μg/L (50 μL of 108.9 mg/L CT stock solution.

Table 3.1: Final Carbon Tetrachloride by products mole fraction in degradation with 0.05 g/L fresh nZVI modified with Na_2S (0.1 molar, 0.5-1 wt. % sulfide) in 4 g/L CMC and 30 mM TAPSO at pH 7 after 1.5 hours. $[CT]_0$ = 0.035 μmoles (50μL of 108.9 mg/L CT stock solution).

Sulfide loading (wt. %)	CT remaining *(m/m_0)*	Final CT degradation (%)	Final CF remaining *(m/m_0)*	Carbon mass balance (m/m_0)
0	0	100	0.69	0.69
0.5	0	100	0.74	0.74
1	0	100	0.62	0.62
1.5	0	100	0.78	0.78
2	0	100	0.54	0.54
3	0.42	58	0.39	0.81
4	0.064	94	0.55	0.62
5	0.68	32	0.39	1.07
6	0.56	44	0.23	0.80
8	0.48	52	0.2	0.68
10	0.78	22	0.12	0.90

Table 3.2: Carbon Tetrachloride degradation with 0.05 g/L fresh nZVI modified with Na_2S (0.1 molar, 0.5-10 wt. % sulfide) in 4 g/L CMC and 30 mM TAPSO at pH 7. $[CT]_0$ = 0.035 μmoles (50μL of 108.9 mg/L CT stock solution)

Sulfide Loading (wt. %)	Overall CT k_{obs} (hr^{-1})	CT k_M ($L\ g^{-1}\ hr^{-1}$)	R^2
0	5.79	1.15E+02	1
0.5	10.09	2.02E+02	0.996
1	11.2	2.24 E+02	1
1.5	8	1.6 E+02	1
2	7.32	1.46 E+02	0.997
3	0.55	1.12 E+01	0.994
4	1.66	2.1 E+01	0.999
5	0.28	5.84	0.997
6	0.35	7	0.989
8	0.34	6.8	0.998
10	0.132	2.92	0.923

Table 3.3: Chloroform degradation with 0.1 g/L fresh nZVI modified with Na_2S (0.1 molar, 0.5-2 wt. % sulfide) in 4 g/L CMC and 30 mM TAPSO at pH 7. $[CF]_0$ = 0.097 μmoles (50 μL of 233.12 mg/L CF stock solution).

Sulfide Loading (wt. %)	Overall CF_ k_{obs} (hr^{-1})	CF_ k_M (L g^{-1} hr^{-1})	R^2
0	0.082	8.2E -1	0.954
0.5	0.128	1.28	0.998
1	0.193	1.93	0.992
1.5	0.158	1.58	0.986
2	0146	1.46	0.997

Table 3.4: Final Chloroform mole fraction in degradation with 0.1 g/L fresh nZVI modified with Na_2S (0.1 molar, 0.5-2 wt. % sulfide) in 4 g/L CMC and 30 mM TAPSO at pH 7 after 2 hours. $[CF]_0$ = 0.097 μmoles (50 μL of 233.12 mg/L CF stock solution).

Sulfide loading (wt. %)	Final CF (m/m_0)	Final CF degradation (%)	Final DCM (m/m_0)	Final Methane (m/m_0)	Carbon mass balance (m/m_0)
0	0.73	27	0.101	0.094	0.97
0.5	0.74	26	0.076	0.173	1
1	0.58	42	0.14	0.2	0.94
1.5	0.73	27	0.138	0.174	1.04
2	0.72	28	0.139	0.160	1.03

Table 3.5: Final 1,1,1-TCA mole fraction in degradation with 0.1 g/L fresh nZVI modified with Na_2S (0.1 molar, 0.5-1.5 wt. % sulfide) in 4 g/L CMC and 30 mM TAPSO at pH 7 after 2 hours. $[TCA]_0$ = 0.077 μmoles (50 μL of 206.25 mg/L 1,1,1-TCA stock solution).

Sulfide loading (wt.%)	Final 1,1,1-TCA *(m/m_0)*	Final 1,1,1-TCA degradation (%)	Final 1,1-DCA *(m/m_0)*	Final Ethane *(m/m_0)*	Final Ethene *(m/m_0)*	Carbon Mass balance (m/m_0)
0	0.64	36	0.073	0.014	NA	0.76
0.5	0.25	75	0.049	0.026	0.021	0.44
1	0.13	87	0.049	0.025	0.025	0.36
1.5	0.33	77	0.063	0.026	0.020	0.54

Table 3.6: 1,1,1-TCA degradation with 0.1 g/L fresh nZVI modified with Na_2S (0.1 molar, 0.5-1.5 wt. % sulfide) in 4 g/L CMC and 30 mM TAPSO at pH 7. $[TCA]_0$ = 0.077 μmoles (50 μL of 206.25 mg/L 1,1,1-TCA stock solution).

Sulfide Loading (wt. %)	Overall 1,1,1-TCA k_{obs} (hr^{-1})	1,1,1-TCA k_M (L g^{-1} hr^{-1})	R^2
0	0.086	8.6E-1	0.981
0.5	0.349	3.49	0.994
1	0.609	6.09	0.998
1.5	0.315	3.15	0.998

Table 3.7: 1,1,1-TCA degradation with fresh nZVI modified with Na_2S (1 wt.% sulfide) in 4 g/L CMC and 30 mM TAPSO at pH 7. $[TCA]_0$ = 0.077 μmoles (50 μL of 206.25 mg/L 1,1,1-TCA stock solution).

nZVI conc.(g/L)	Sulfide Loading (wt. %)	Overall 1,1,1-TCA k_{obs} (hr^{-1})	1,1,1TCA k_M (L g^{-1} hr^{-1})	R^2
0.1	1	0.609	6.09	0.998
0.5	1	1.01	2.02	0.981

Table 3.8: Final 1,1,1-TCA mole fraction in degradation with 0.5 g/L fresh nZVI modified with Na_2S (0.1 molar, 1 wt. % sulfide) in 4 g/L CMC and 30 mM TAPSO at pH 7 after 2 hours. $[TCA]_0$ = 0.077 μmoles (50 μL of 206.25 mg/L 1,1,1-TCA stock solution).

nZVI conc.(g/L)	Sulfide Loading (wt. %)	Final 1,1,1-TCA *(m/m_0)*	Final 1,1,1-TCA degradation (%)	Final 1,1-DCA *(m/m_0)*	Final Ethane Mole Fraction *(m/m_0)*	Final Ethene *(m/m_0)*
0.1	1	0.23	77	0.069	0.030	0.028
0.5	1	0.12	86	0.076	0.048	0.031

Table 3.9: 1, 1,1TCA degradation with 0.5 g/L aged nZVI modified with Na_2S (0.1 molar, 1 wt. % sulfide) in 4 g/L CMC and 30 mM TAPSO at pH 7.For each injection, $[TCA]_0$ = 0.077 μmoles (50 μL of 206.25 mg/L 1,1,1-TCA stock solution).

injection	Time(hours)	Overall TCA_ k_{obs} (hr^{-1})	TCA_ k_M (L g^{-1} hr^{-1})	R^2
1	0.083	0.794	7.94	0.994
2	32.42	0.315	3.15	0.988
3	125.46	0.294	2.94	0.982
4	197.47	0.261	2.61	0.976

Table 3.10: Final 1, 1,1TCA and by products mole fraction in degradation with 0.5 g/L aged nZVI modified with Na_2S (0.1 molar, 0.5-1.5 wt. % sulfide) in 4 g/L CMC and 30 mM TAPSO at pH 7 after 2 hours. of each injection sampling . For each injection, $[TCA]_0$ = 0.077 μmoles (50 μL of 206.25 mg/L 1,1,1-TCA stock solution).

Injection	Final TCA (m/m_0)	Final TCA degradation (%)
1	0.13	87
2	0.40	60
3	0.36	64
4	0.35	65

Table 3.11: 1, 1,1-TCA degradation with 0.5 g/L aged nZVI modified with Na_2S (0.1 molar, 1 wt. % sulfide) in 30 mM TAPSO at pH 7at different CMC concentration. $[TCA]_0$ = 0.077μmoles (50 μL of 206.25 mg/L 1,1,1-TCA stock solution).

CMC Conc. (g/L)	Overall 1,1,1-TCA k_{obs} (hr^{-1})	1,1,1TCA_ k_M (L g^{-1} hr^{-1})	R^2
0	0.022	0.044	0.978
0.4	0.295	0.59	0.998
4	0.988	1.97	0.968

Table 3.12: CHC degradation byproduct and pathways with nZVI and Na_2S

Parent	**Products**	**Reaction Pathway**	**Experimental Conditions**
CT	CF Methane	Hydrogenolysis Sequential hydrogenolysis or direct reduction	30 mM TAPSO (pH 7) 4 g/L CMC
CF	DCM Methane	Hydrogenolysis Sequential hydrogenolysis or direct reduction	30 mM TAPSO (pH 7) 4 g/L CMC
1,1,1-TCA	Ethane Ethene 1,1-DCA	Direct transformation (α-elimination/ reactive intermediate) Direct transformation (reactive intermediate) or dehydrohalogenation and hydrogenolysis Hydrogenolysis	30 mM TAPSO (pH 7) 4 g/L CMC

APPENDIX A: CALCULATIONS FOR DETERMINING AMOUNT (μmoles) IN REACTORS

A.1: Chlorinated hydrocarbons quantification

1. Stock solution prepared in 160 mL serum bottle with 160 mL Milli-Q water and 20 μL pure CHC. Concentration of stock was determined as follows:

   $C_s = (\rho_{CHC} * V_{pure}) / V_w$

   Where: C_s = Concentration of stock (mg L^{-1})

   ρ_{CHC} = Density of CHC (mg L^{-1})

   V_{pure} = Volume of pure CHC (L)

   V_w = Volume of water in stock reactor

   Example: Chloroform stock

   C_s = (1,480,000 mg L^{-1} * 0.00002 L) / 0.16 L = 185 mg L^{-1} = 0.185 g L^{-1}

2. Various amounts of stock were then added to reactor bottles or standards containing 96 mL aqueous medium (TAPSO or Milli-Q water, respectively). Calibration curves were constructed with amount (M_t) on the ordinate (y-axis) and corresponding peak areas on the abscissa (x-axis). The amount added to bottle was determined as follows:

   $M_t = [(C_s * V_s) / FW] * 1{,}000{,}000$ μmoles

   Where: M_t = Amount of CHC added to bottle (μmoles)

   C_s = Concentration of stock (g L^{-1})

   V_s = Volume of stock added (L)

   FW = Formula weight of CHC (g mol^{-1})

   1 mol = 1,000,000 μmoles

   Example: Chloroform experiment (50 μL stock added to reactor)

   M_t = [(0.185 g L^{-1} * 0.00005 L) / 119.38 g mol^{-1}] * 1,000,000 μmoles

   = 0.311 μmoles

3. The partitioning coefficient was determined by using a dimensionless Henry's Constant for each CHC according to the following:

$$f_w = \frac{1}{(1+k'_H(\frac{V_a}{V_w}))}$$

Where: f_w = Partitioning coefficient

k'_H = Dimensionless Henry's Constant for CHC at 25°C.

V_a = Volume of head space in reactor (mL)

V_w = Volume of aqueous medium in reactor (mL)

Example: Dimensionless Henry's Constant for CF = 0.148

$$f_w = \frac{1}{(1+0.148(\frac{64\ mL}{96\ mL}))} = 0.910$$

4. The partitioning coefficient was then used to calculate aqueous µmoles after partitioning according to the following:

$$M_w = M_t * f_w$$

Where: M_w = Amount in aqueous phase (µmoles)

M_t = Amount of CHC added to bottle (µmoles)

f_w = Partitioning coefficient

Example: M_w with CF partitioning coefficient

M_w = 0.311 µmoles * 0.910 = 0.282 µmoles

This can also be represented in µg by the following:

0.282 µmoles * 119.38 g mol^{-1} * 1 mol / 10^6 µmoles * 106 µg / 1 g = 33.7 µg

APPENDIX B: CHC DEGRADATION AND BYPRODUCTS (µmoles)

1. CHLORINATED METHANES

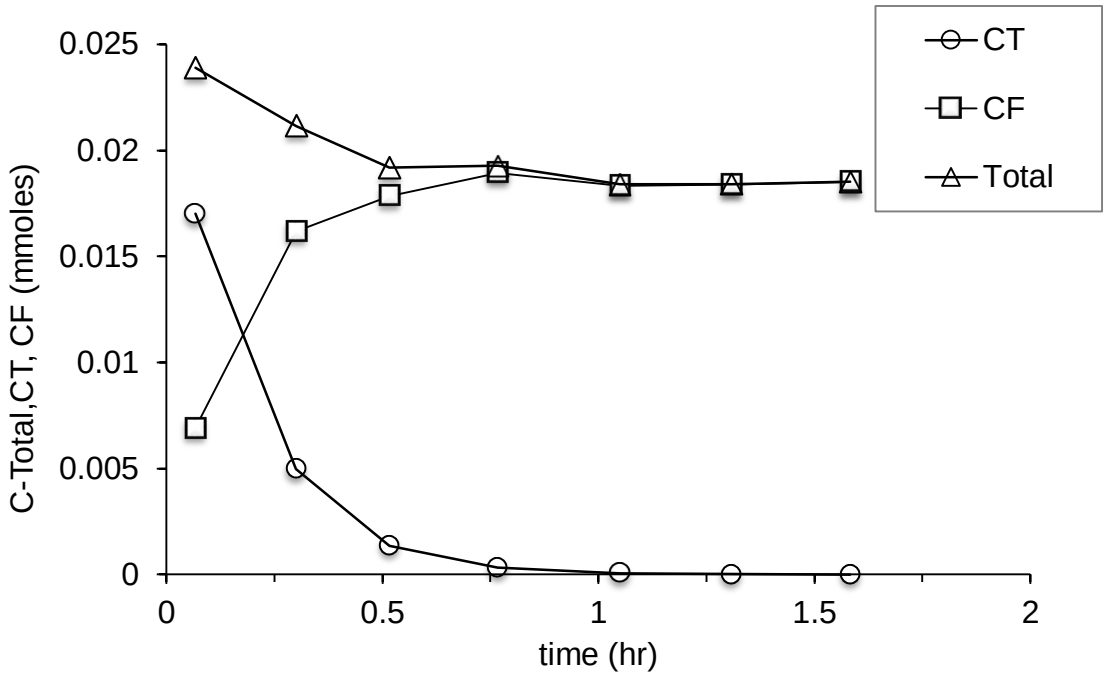

Figure b.1: CT degradation and byproducts (µmoles) with fresh 0.05 g/L nZVI prepared in 4 g/L CMC. Initial CT = 0.035 µmoles, or 54.45 µg/L (50 µL of 108.9 mg/L CT stock solution).

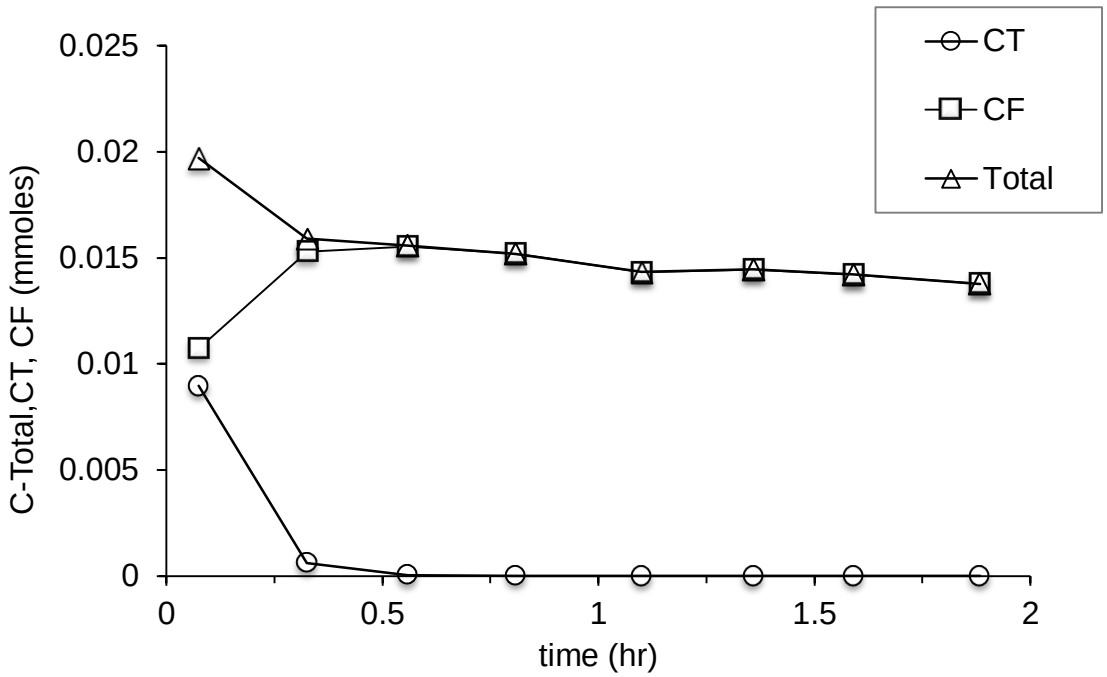

Figure b.2: CT degradation and byproducts (μmoles) with fresh 0.05 g/L nZVI modified with 0.5 wt. % sulfide prepared in 4 g/L CMC. Initial CT = 0.035 μmoles, or 54.45 μg/L (50 μL of 108.9 mg/L CT stock solution).

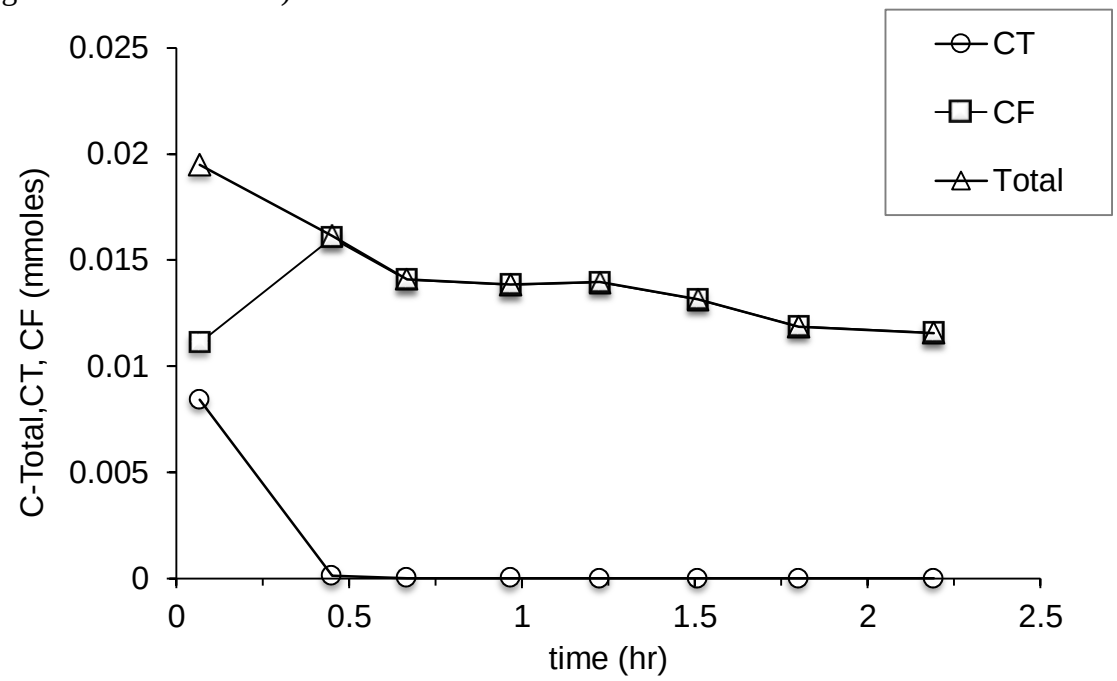

Figure b.3: CT degradation and byproducts (μmoles) with fresh 0.05 g/L nZVI modified with 1 wt. % sulfide prepared in 4 g/L CMC. Initial CT = 0.035 μmoles, or 54.45 μg/L (50 μL of 108.9 mg/L CT stock solution).

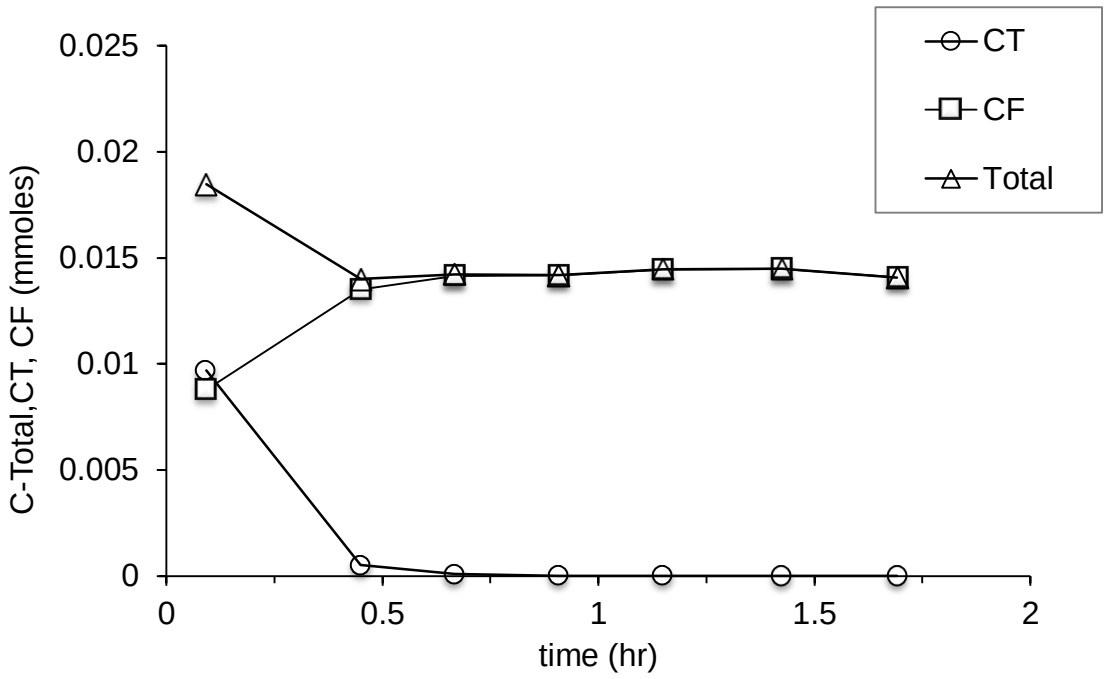

Figure b.4: CT degradation and byproducts (μmoles) with fresh 0.05 g/L nZVI modified with 1.5 wt. % sulfide prepared in 4 g/L CMC. Initial CT = 0.035 μmoles, or 54.45 μg/L (50 μL of 108.9 mg/L CT stock solution).

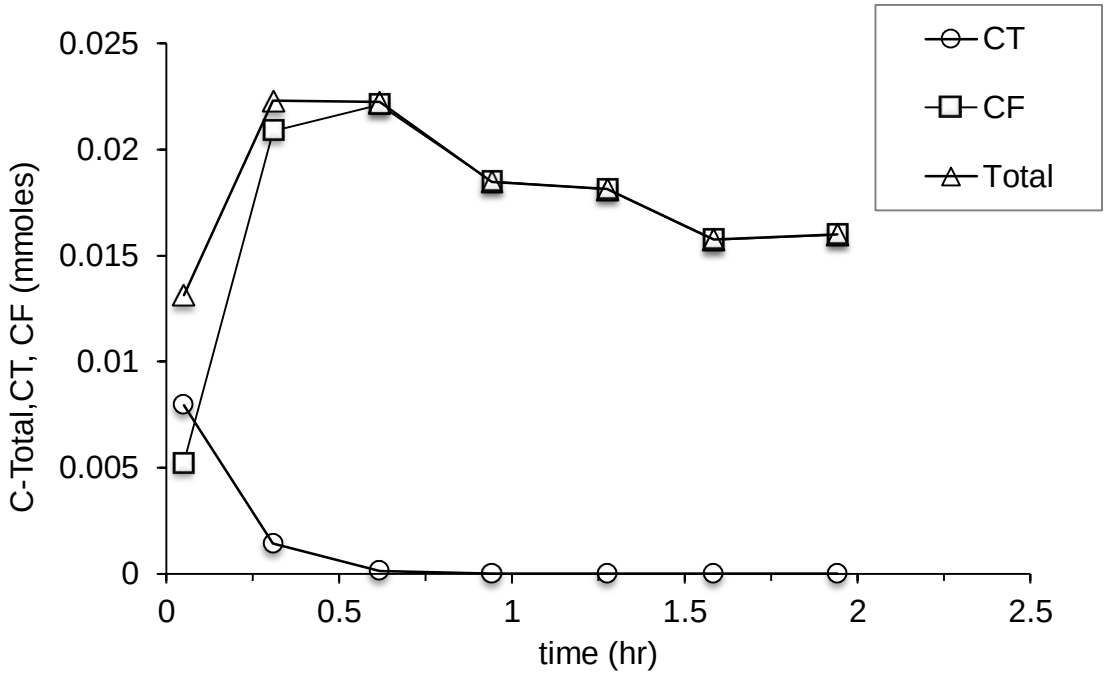

Figure b.5: CT degradation and byproducts (μmoles) with fresh 0.05 g/L nZVI modified with 2.0 wt. % sulfide prepared in 4 g/L CMC. Initial CT = 0.035 μmoles, or 54.45 μg/L (50 μL of 108.9 mg/L CT stock solution).

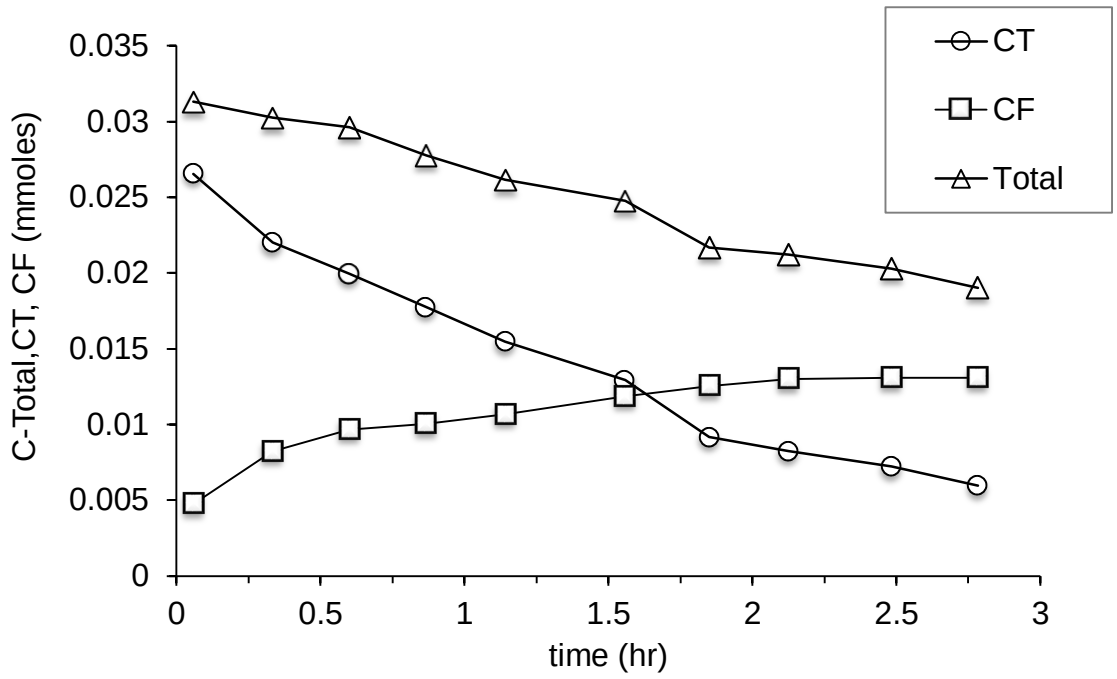

Figure b.6: CT degradation and byproducts (μmoles) with fresh 0.05 g/L nZVI modified with 3.0 wt. % sulfide prepared in 4 g/L CMC. Initial CT = 0.035 μmoles, or 54.45 μg/L (50 μL of 108.9 mg/L CT stock solution).

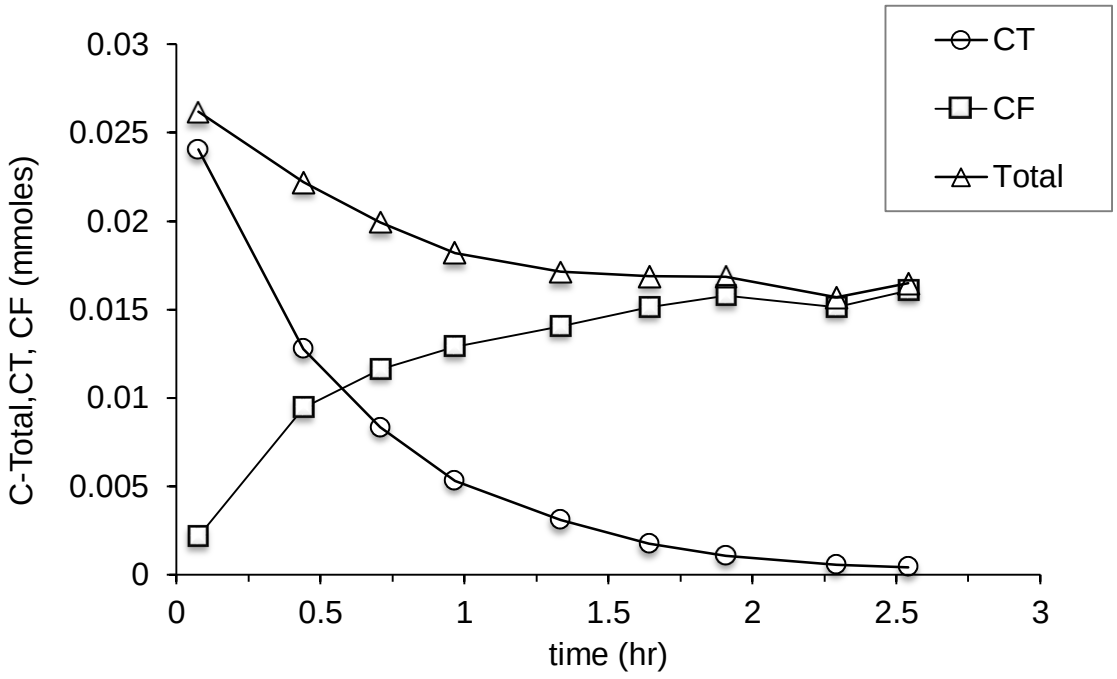

Figure b.7: CT degradation and byproducts (μmoles) with fresh 0.05 g/L nZVI modified with 4.0 wt% sulfide with 4.0 wt% sulfide prepared in 4 g/L CMC. Initial CT = 0.035 μmoles, or 54.45 μg/L (50 μL of 108.9 mg/L CT stock solution).

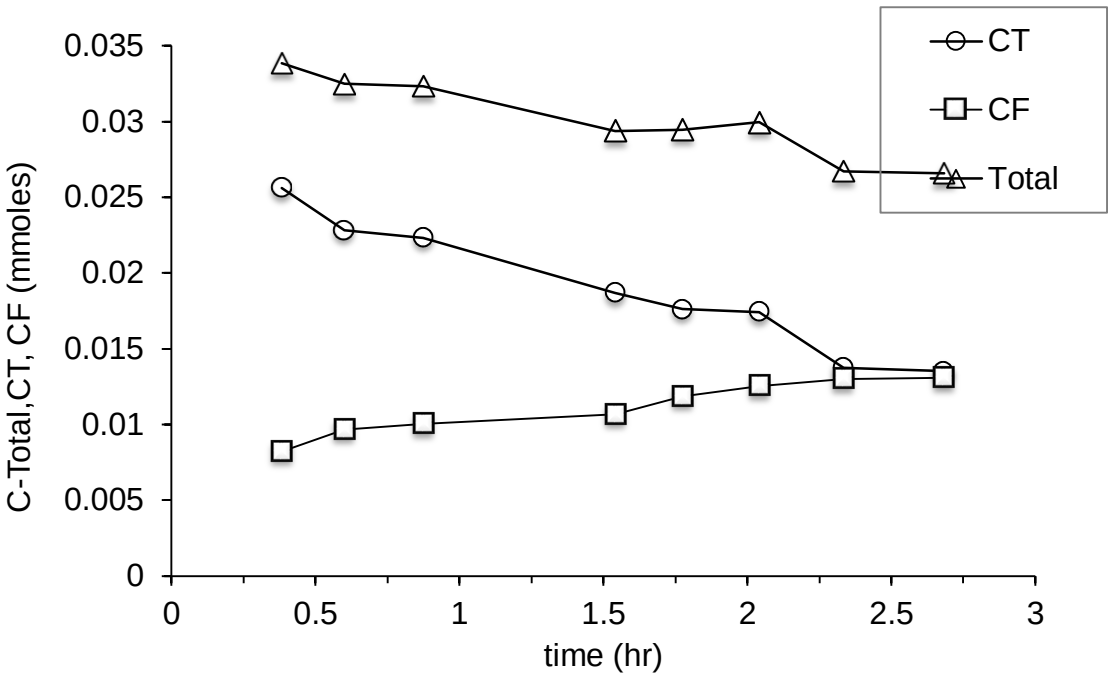

Figure b.8: CT degradation and byproducts (μmoles) with fresh 0.05 g/L nZVI modified with 5.0 wt. % sulfide prepared in 4 g/L CMC. Initial CT = 0.035 μmoles, or 54.45 μg/L (50 μL of 108.9 mg/L CT stock solution).

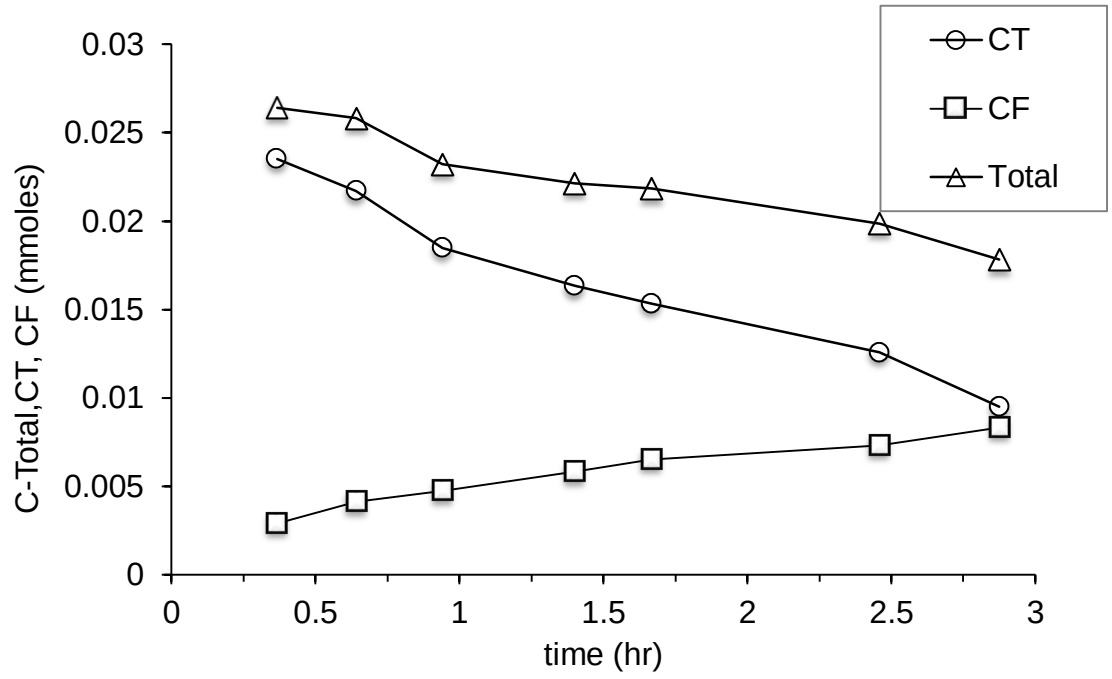

Figure b.9: CT degradation and byproducts (μmoles) with fresh 0.05 g/L nZVI modified with 6.0 wt. % sulfide prepared in 4 g/L CMC. Initial CT = 0.035 μmoles, or 54.45 μg/L (50 μL of 108.9 mg/L CT stock solution).

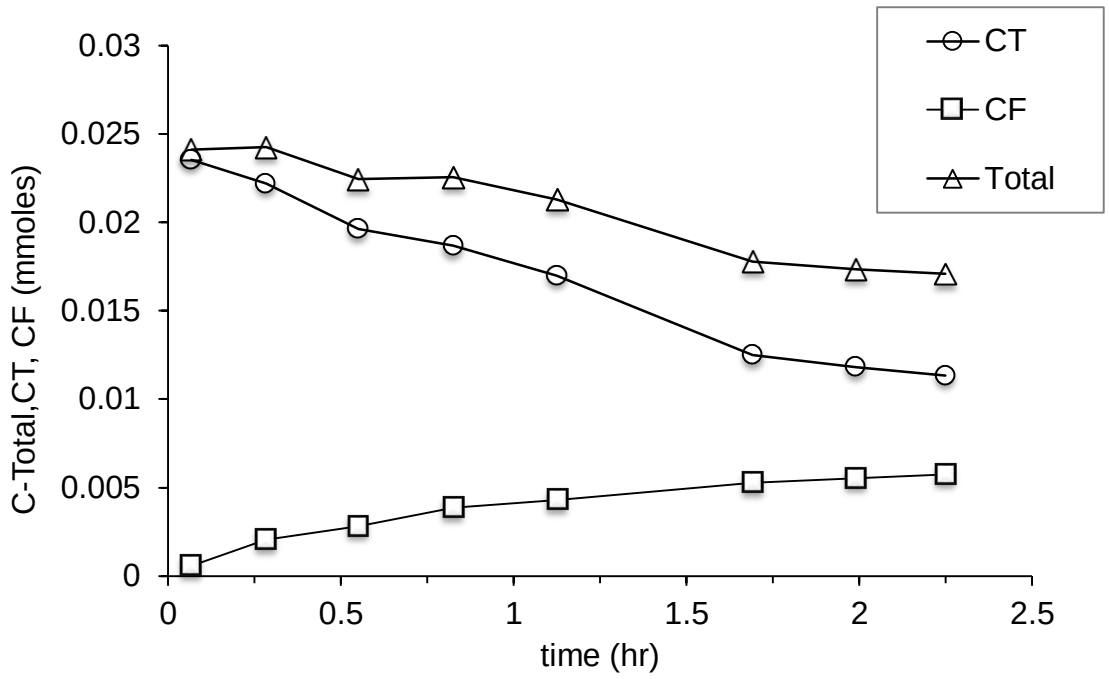

Figure b.10: CT degradation and byproducts (μmoles) with fresh 0.05 g/L nZVI modified with 8.0 wt. % sulfide prepared in 4 g/L CMC. Initial CT = 0.035 μmoles, or 54.45 μg/L (50 μL of 108.9 mg/L CT stock solution).

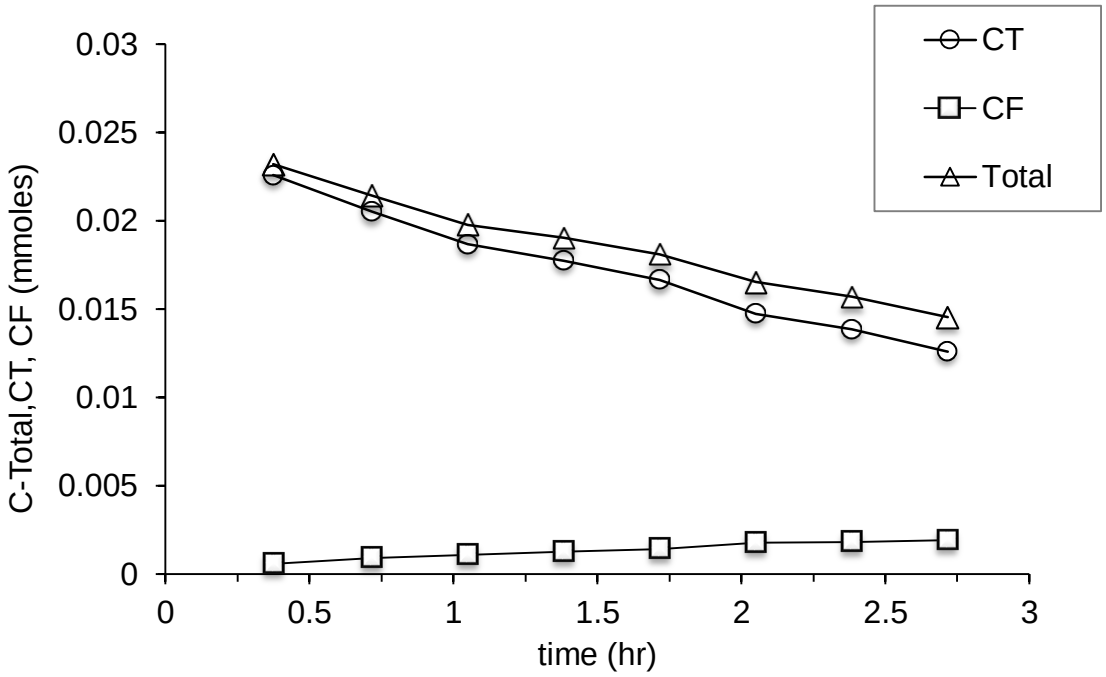

Figure b.11: CT degradation and byproducts (μmoles) with fresh 0.05 g/L nZVI modified with 10.0 wt. % sulfide prepared in 4 g/L CMC. Initial CT = 0.035 μmoles, or 54.45 μg/L (50 μL of 108.9 mg/L CT stock solution).

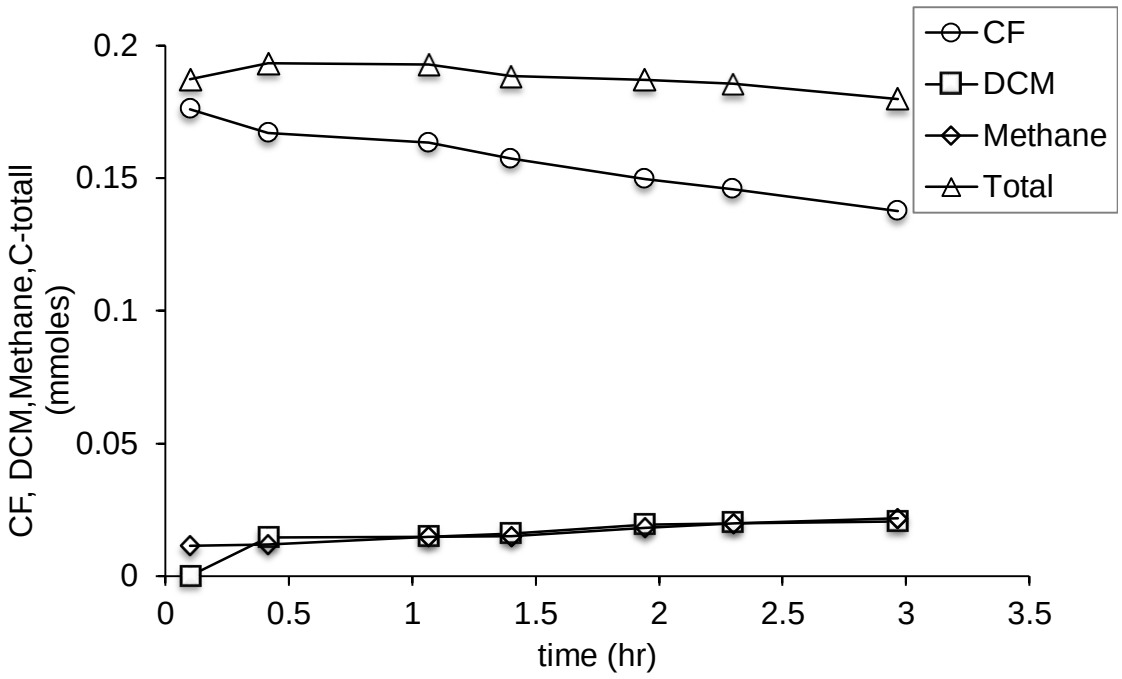

Figure b.12: CF degradation and byproducts (µmoles) with fresh0.1 g/L nZVI prepared in 4g/L CMC. Initial CF = 0.097 µmoles, or 110.58 µg/L (50 µL of 233.12 mg/L CF stock solution).

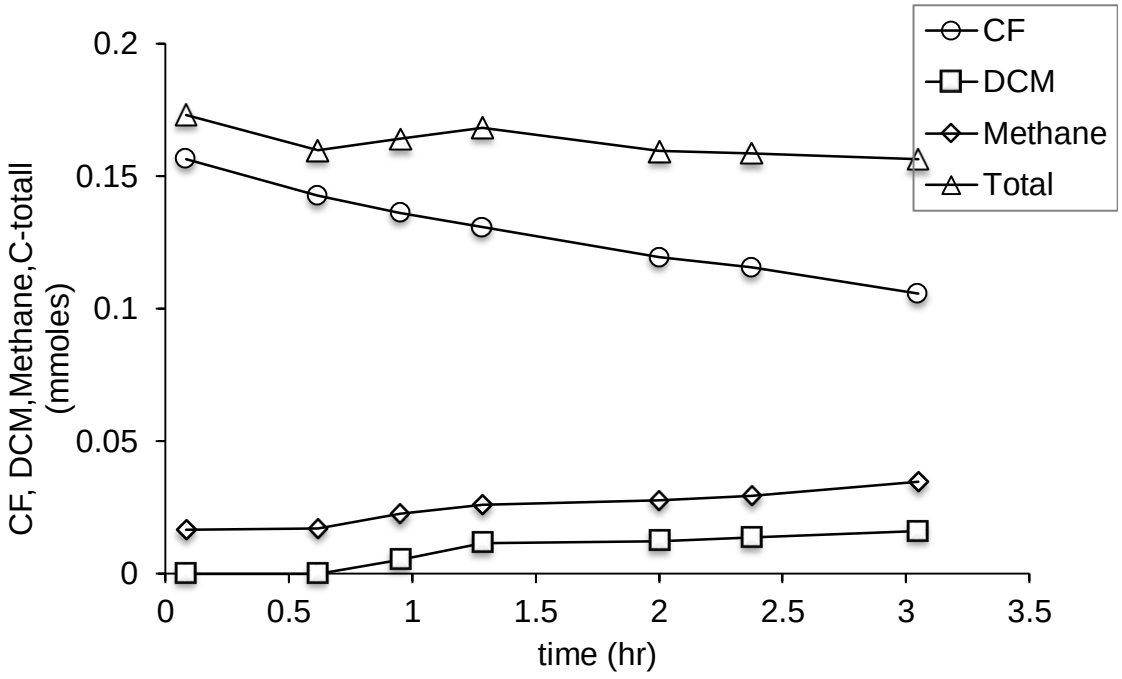

Figure b.13: CF degradation and byproducts (µmoles) with fresh0.1 g/L nZVI modified with 0.5 wt. % sulfide prepared in 4g/L CMC. Initial CF= 0.097 µmoles, or 110.58 µg/L (50 µL of 233.12 mg/L CF stock solution).

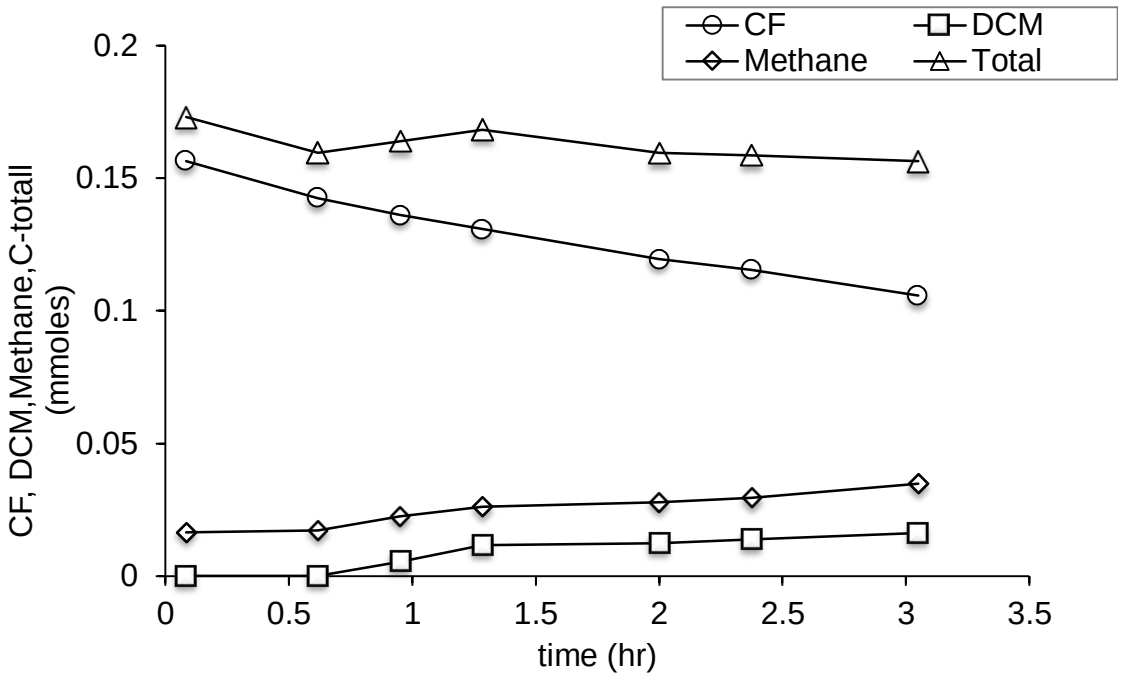

Figure b.14: CF degradation and byproducts (µmoles) with fresh0.1 g/L nZVI modified with 1.0 wt. % sulfide prepared in 4g/L CMC. Initial CF= 0.097 µmoles, or 110.58 µg/L (50 µL of 233.12 mg/L CF stock solution).

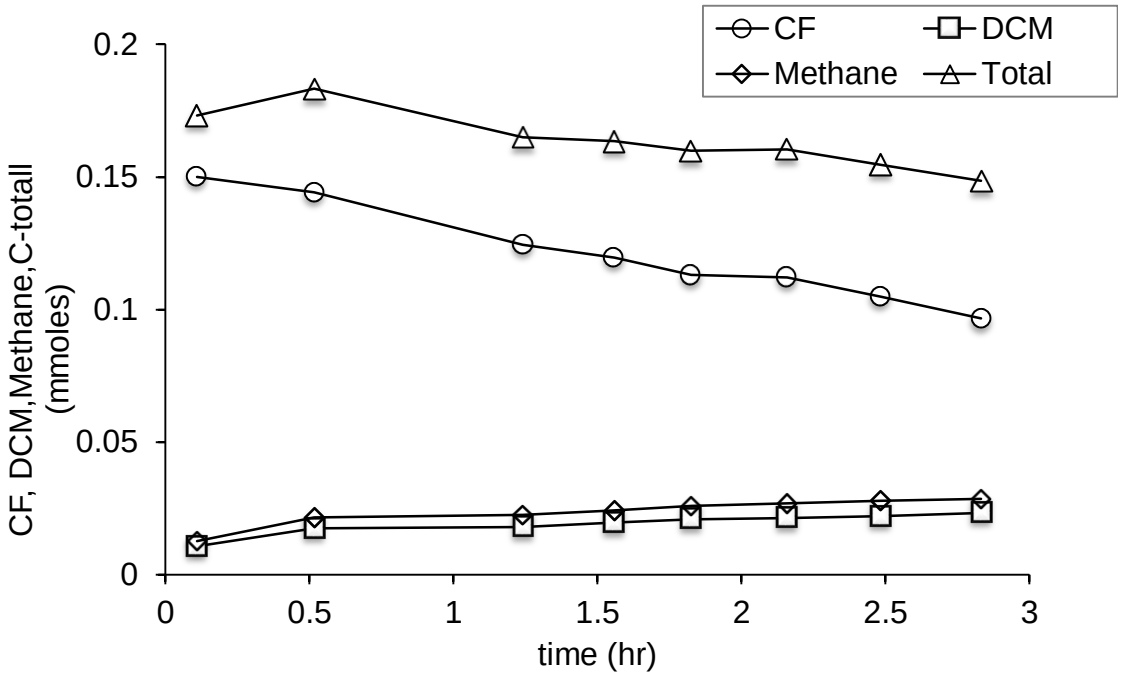

Figure b.15: CF degradation and byproducts (µmoles) with fresh0.1 g/L nZVI modified with 1.5 wt. % sulfide prepared in 4g/L CMC. Initial CF= 0.097 µmoles, or 110.58 µg/L (50 µL of 233.12 mg/L CF stock solution).

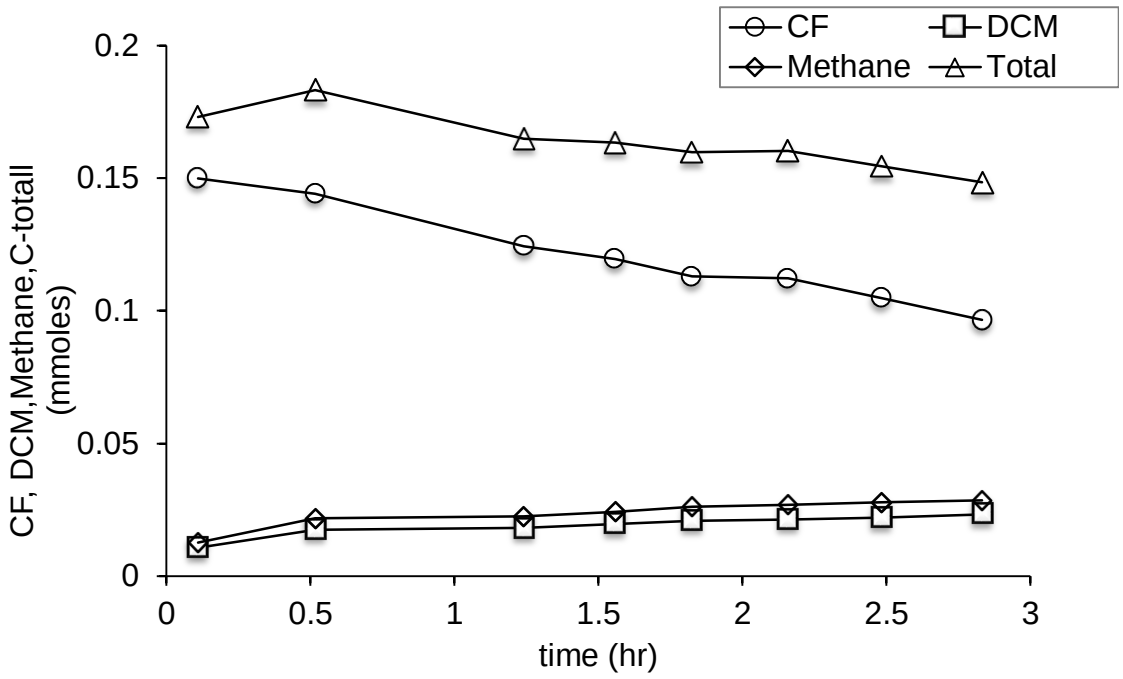

Figure b.16: CF degradation with fresh0.1 g/L nZVI modified with 2 wt% sulfide prepared in 4g/L CMC. Initial CF= 0.097 μmoles, or 110.58 μg/L (50 μL of 233.12 mg/L CF stock solution).

2. CHLORINATED ETHANES

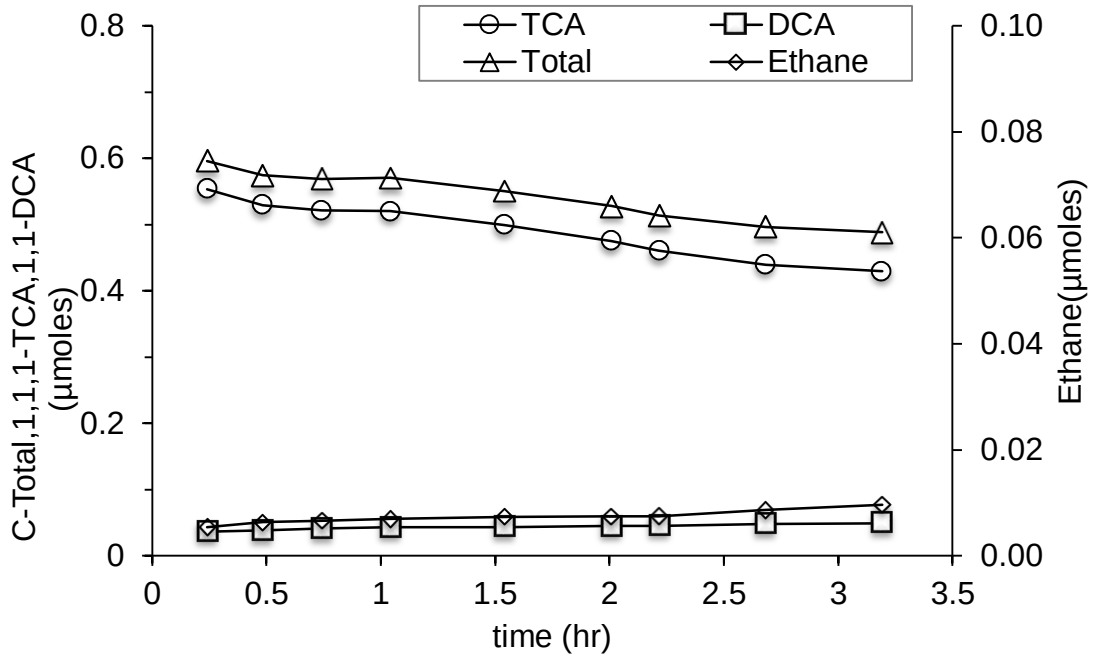

Figure b.17: 1,1,1-TCA degradation and byproducts (µmoles) with fresh 0.1 g/L nZVI prepared in 4 g/L CMC. Initial 1,1,1-TCA = 0.077 µmoles, or 103 µg/L (50 µL of 206.25 mg/L 1,1,1-TCA stock solution).

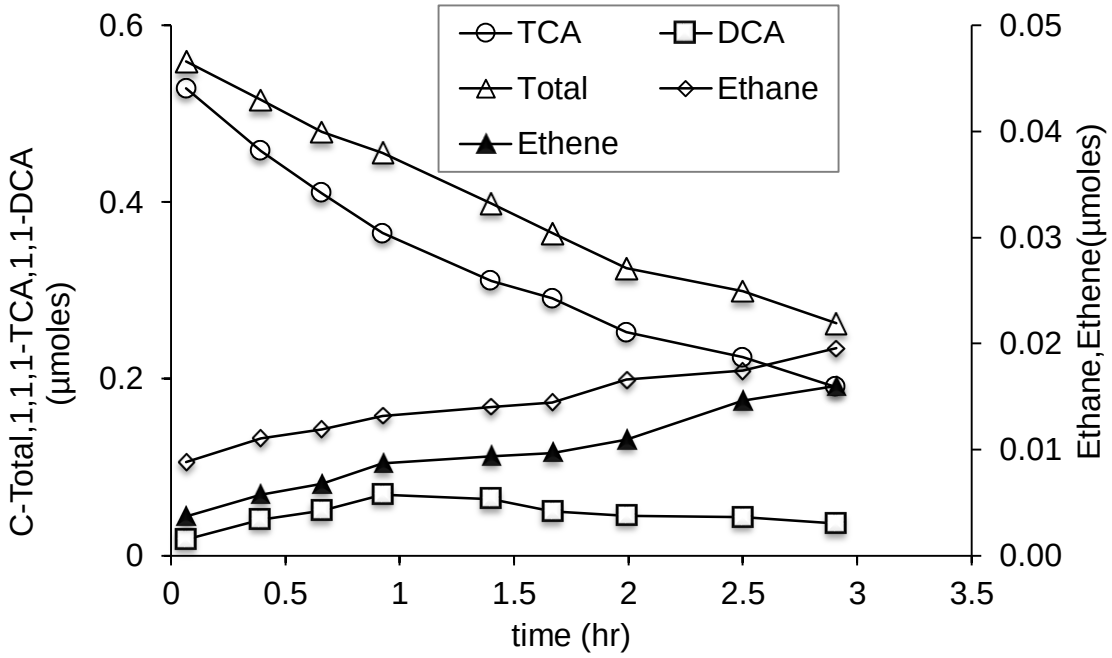

Figure b.18: 1,1,1-TCA degradation and byproducts (µmoles)with fresh 0.1 g/L nZVI modified with 0.5 wt.% sulfide prepared in 4 g/L CMC. Initial 1,1,1-TCA = 0.077 µmoles, or 103 µg/L (50 µL of 206.25 mg/L 1,1,1-TCA stock solution).

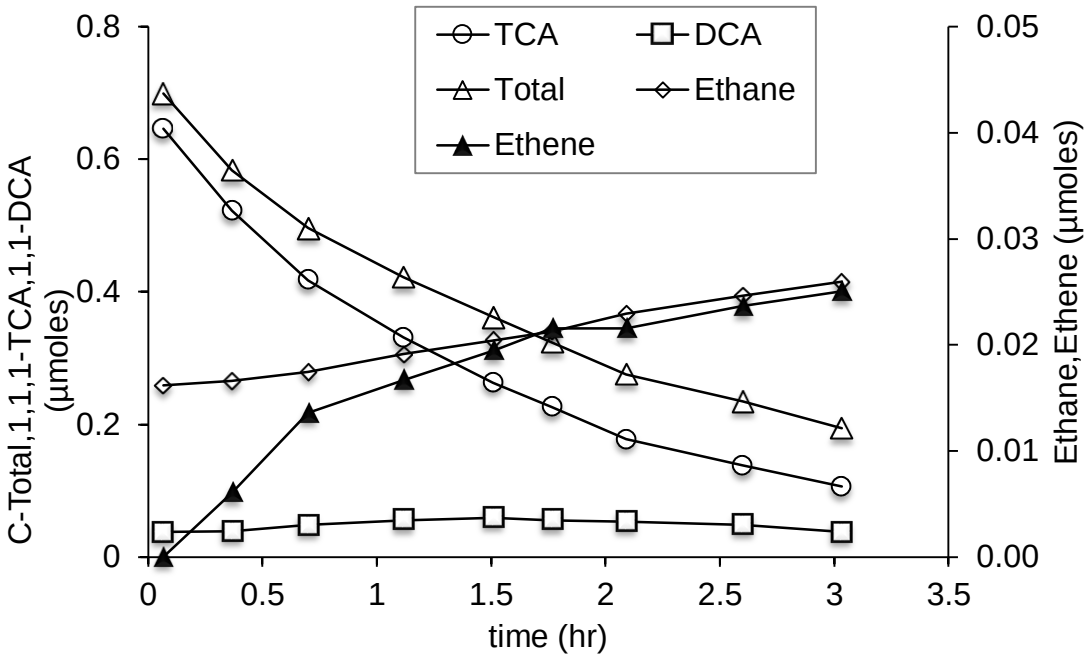

Figure b.19: 1,1,1-TCA degradation and byproducts (µmoles) with fresh 0.1 g/L nZVI modified with 1.0 wt.% sulfide prepared in 4 g/L CMC. Initial 1,1,1-TCA = 0.077 µmoles, or 103 µg/L (50 µL of 206.25 mg/L 1,1,1-TCA stock solution).

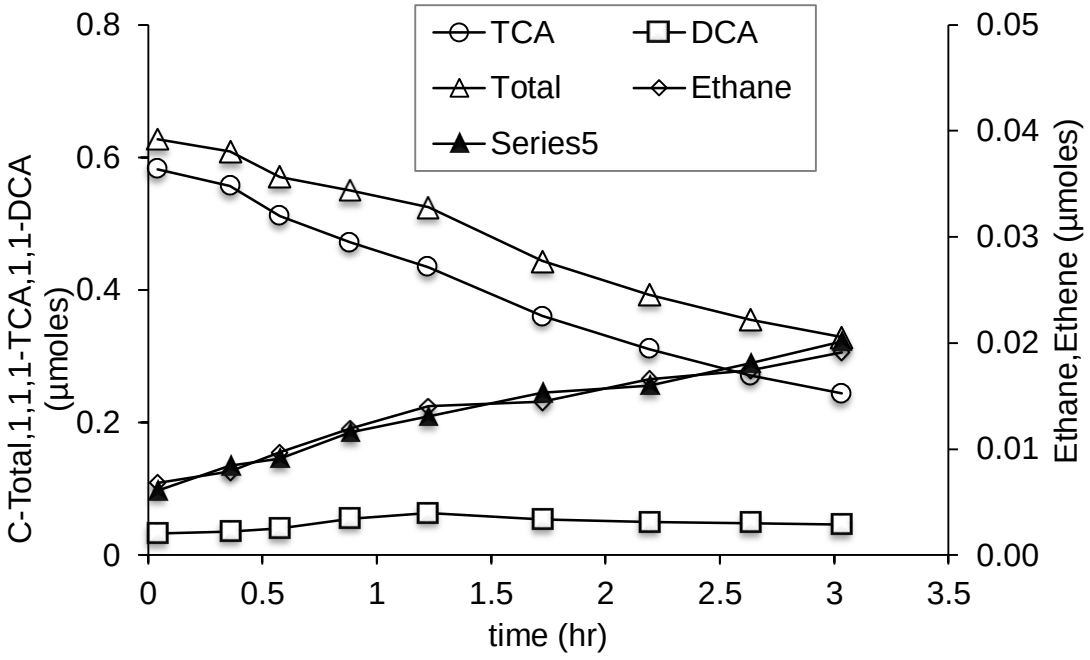

Figure b.20: 1,1,1-TCA degradation and byproducts (µmoles)with fresh 0.1 g/L nZVI modified with 1.5 wt.% sulfide prepared in 4 g/L CMC. Initial 1,1,1-TCA = 0.077 µmoles, or 103 µg/L (50 µL of 206.25 mg/L 1,1,1-TCA stock solution).